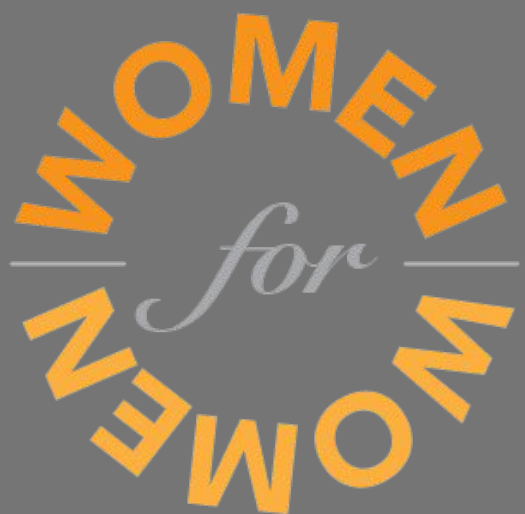


# WOMEN FOR WOMEN

## A safe space for women in Zaatari Refugee Camp

Group 7:

Amelia Tapia  
Iro Stefanaki  
Grammatiki Dasopoulou  
Nayan Herath  
Ioannis Tsionis



AR3B011 EARTHY | GROUP 07

Amelia Tapia	4939123
Iro Stefanaki	4950402
Grammatiki Dasopoulou	4950399
Nayanthara Herath	4758390
Ioannis Tsionis	4873440

EARTHY  
MSC.3 Q1 2019  
Dr. Pirouz Nourian

Master of Architecture, Urbanism, and Building Sciences  
Building Technology Track  
Faculty of Architecture and the Built Environment  
TU Delft  
October 2019

# CONTENTS

<b>Introduction</b>	<b>3</b>
<b>Design process</b>	<b>4</b>
<b>Location</b>	<b>9</b>
<b>Configuration</b>	<b>15</b>
<b>Form finding</b>	<b>27</b>
<b>Adobe brick testing</b>	<b>36</b>
<b>Structural analysis</b>	<b>44</b>
<b>Brick patterning</b>	<b>53</b>
<b>Constructability</b>	<b>63</b>
<b>Conclusion</b>	<b>71</b>
<b>References</b>	<b>74</b>
<b>Appendix</b>	<b>75</b>
<b>Brick report</b>	<b>76</b>

# Introduction

Women for women is a safe communal center for the female population of Za'atari camp. This facility intends to secure, accommodate and protect women against gender-based violence, provide help with maternity issues or educate them socially. The building program consists of a medical clinic sector, workshop and classroom facilities, a large recreation space, as well as a protected housing area for women in need of immediate help or temporary isolation.

This center is designed to function in the most populated district inside the refugee camp. However, it is considered to be a prototype design process, which would fit in different needs and locations that lack facilities dedicated for women's health and safety.

Due to the building's purpose, safety and privacy became two of the most important aspects in the configuration of internal spaces and movements. Women of this culture gather in groups for communal

purposes and acceptance. We aim to give them a more comfortable space which fulfills their needs.



Figure 1: 3D Visual representation of Women for Women safe center.

---

# Design process

## First phase

The first phase of the design process was to identify the problem based on criteria set by the team. A specific piece of land was to be identified and basic idea generation was carried out.

(The flow chart will be shown more zoomed in before each specified part)

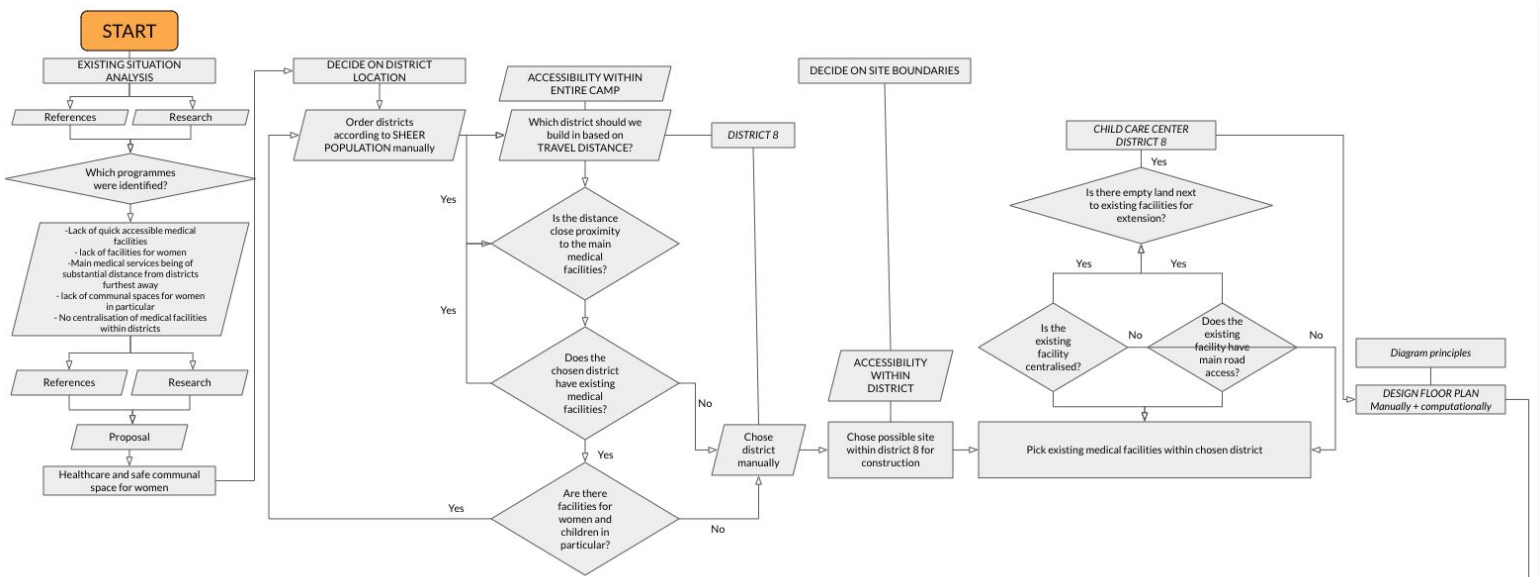


Figure 2: First phase flowchart.

## Phase 2

## Second phase

Phase two was carried out to design the building through manually designing the plan for the women's center because of specific needs the team set out from the start. Computational form finding and finalising the dynamically relaxed shape according to necessary aesthetics was the final process of Phase 2.

(The flow chart will be shown more zoomed in before each specified part)

### Phase 1

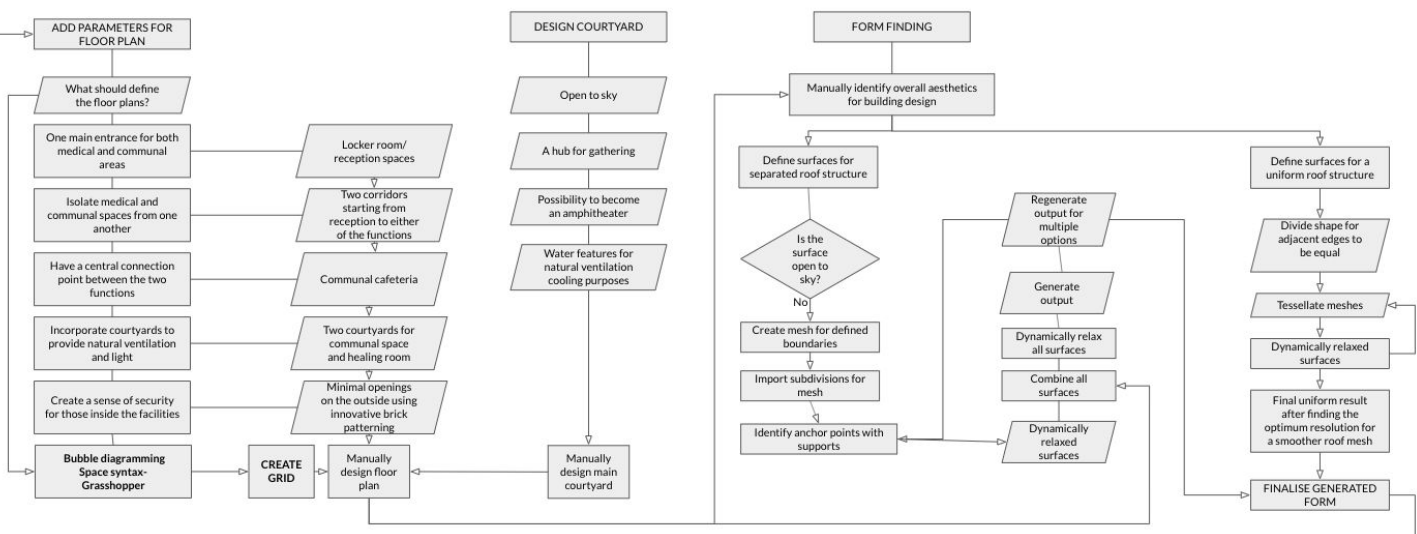


Figure 3: Second phase flowchart.

### Phase 3

## Third phase

Phase 3 had a strong focus on structural analysis and incorporating adobe bricks into the forms generated computationally. Most of the work happened parallel to one another informing each process from results derived from each other along the way.

(The flow chart will be shown more zoomed in before each specified part)

### Phase 2

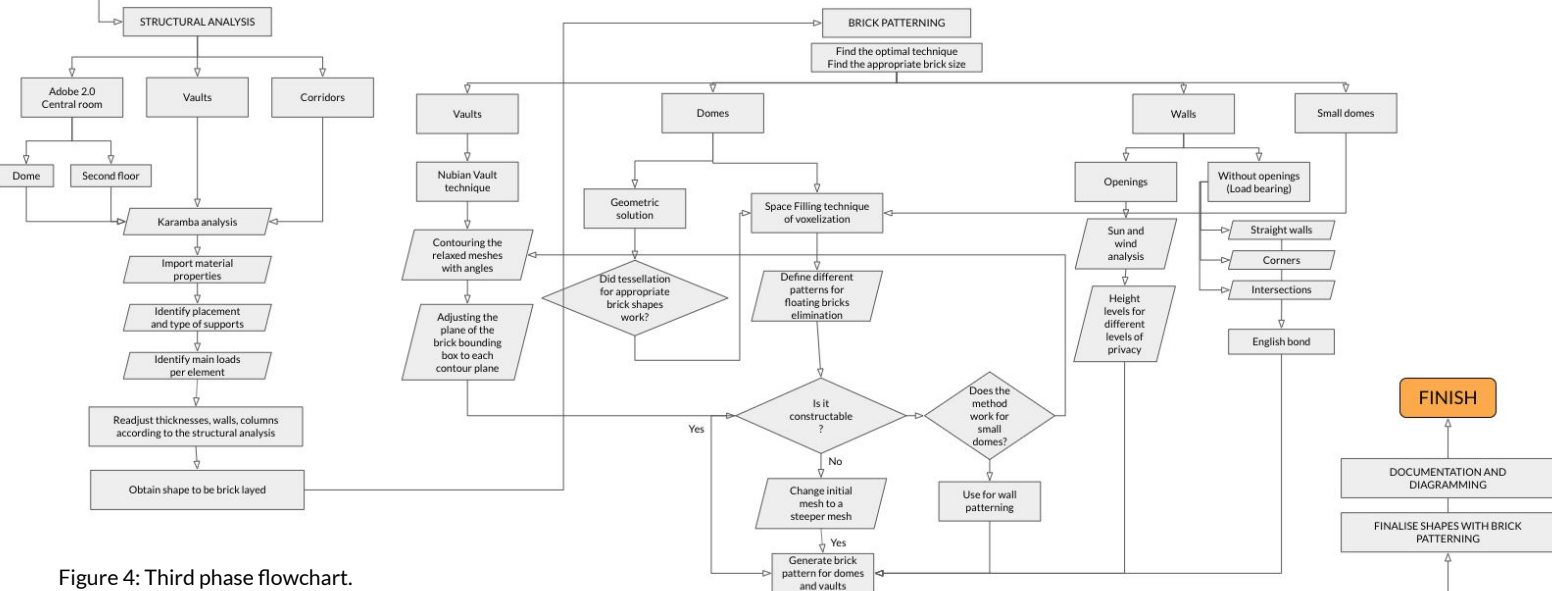


Figure 4: Third phase flowchart.



Figure 5: 3D Visualisation of the main entrance and the south facade.

---

# Location

---

## Phase 2

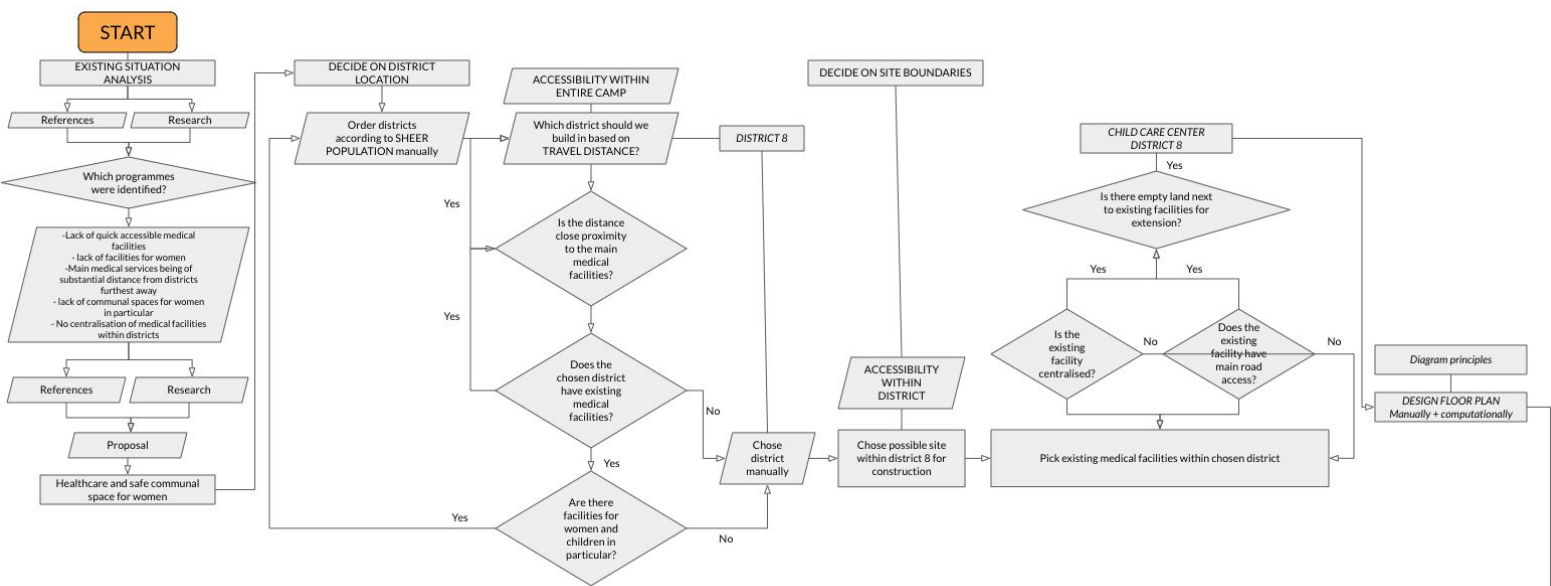


Figure 6: Choice of district 8 flowchart.

## Why women's health in district 8?

- Long-distance from the existing maternity clinic, general hospital, mother & child clinic
- 15,489 women in the entire Zaatari refugee Camp (20% of the population)
- 4.145 women in district 8
- 1.000 women from 12-39 years old<sup>5</sup>
- Lack of Facilities dedicated for women's health and safety
- Women already gather in groups for communal purposes, we wanted to give them a more comfortable space dedicated for communal gatherings, cooking, workshops, classes etc.
- 20% of the refugees are in female-headed households.<sup>5</sup>



Figures 7,8,9,10: Women's and children's life in Za'atari Refugee camp. Source: <https://www.pri.org>

# Location

## Zaatari refugee camp

Women for Women center is located in district 8 as a solution which can be replicated in the other districts.

- Most populated district
- Long-distance from the existing maternity
- Existing facilities for youth and children.

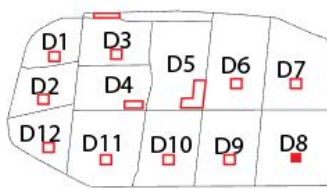


Figures 11: Za'atari refugee camp with existing facilities and District 8 (left).

# Principles

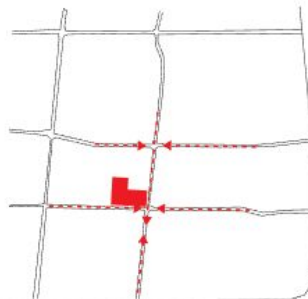
The following principles were based off the existing needs identified. Research and references by authorised publications allowed for parameters based on needs. Safety and privacy became two of the most important aspects of the configuration of internal spaces and movement.

Ventilation strategies via wind studies and natural light using sun analysis was considered when planning for external walls and internal division walls.



DECENTRALIZATION

Figure 12



ACCESIBLE  
PUBLIC SPACE

Figure 13



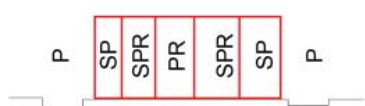
CLEAR ENTRANCE

Figure 14



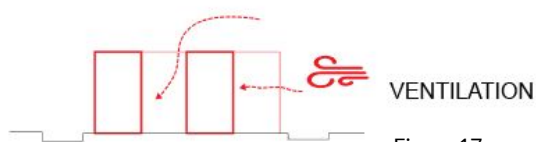
SAFETY

Figure 15



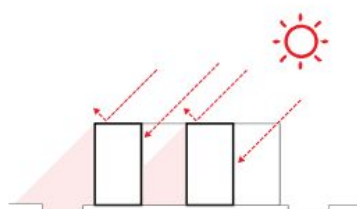
PRIVACY  
public  
semipublic  
semiprivate  
private

Figure 16



VENTILATION

Figure 17



SHADE/  
NATURAL LIGHT

Figures 18

Figures  
12,13,14,15,16,17,18:  
Design principles.

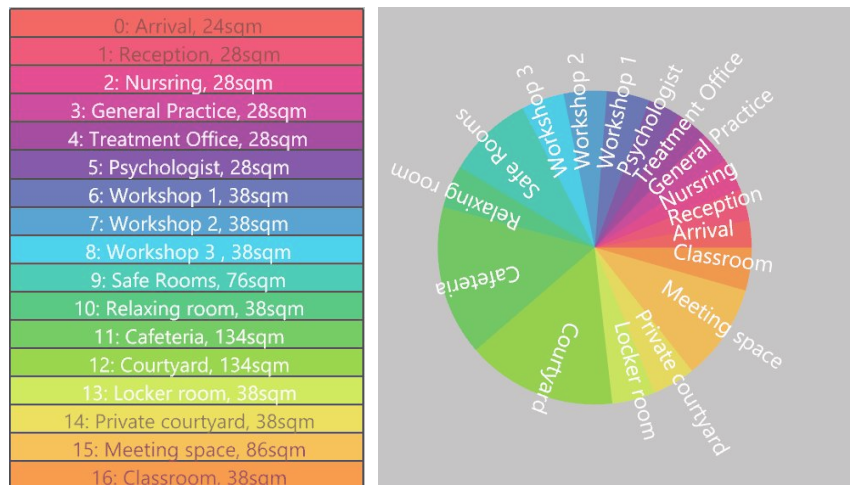


Figure 19: Program with areas

## Space syntax

The first steps for the spatial configuration was to define the spaces and the requirements of each space that a building like this needs. After completing the program of the building, a REL chart was developed to illustrate the closeness and the connections

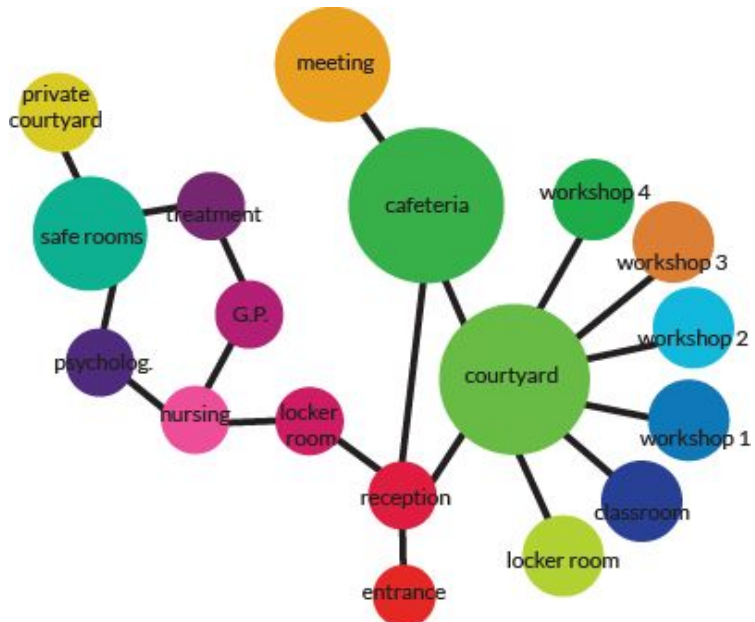


Figure 20: Space syntax

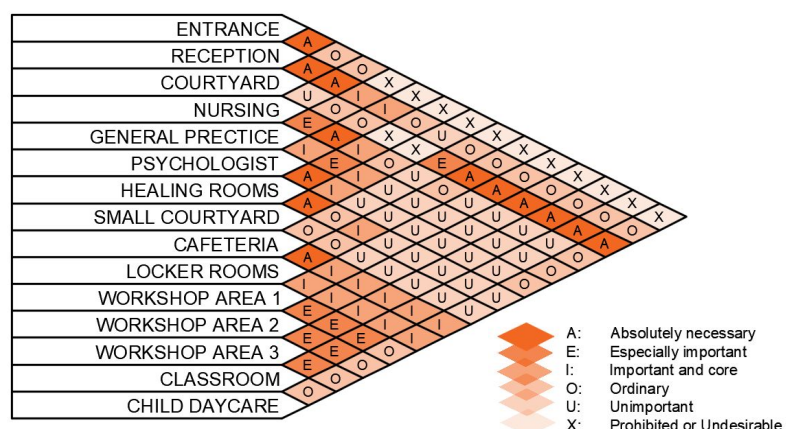


Figure 21: REL chart

---

# Configuration

## PHASE 1

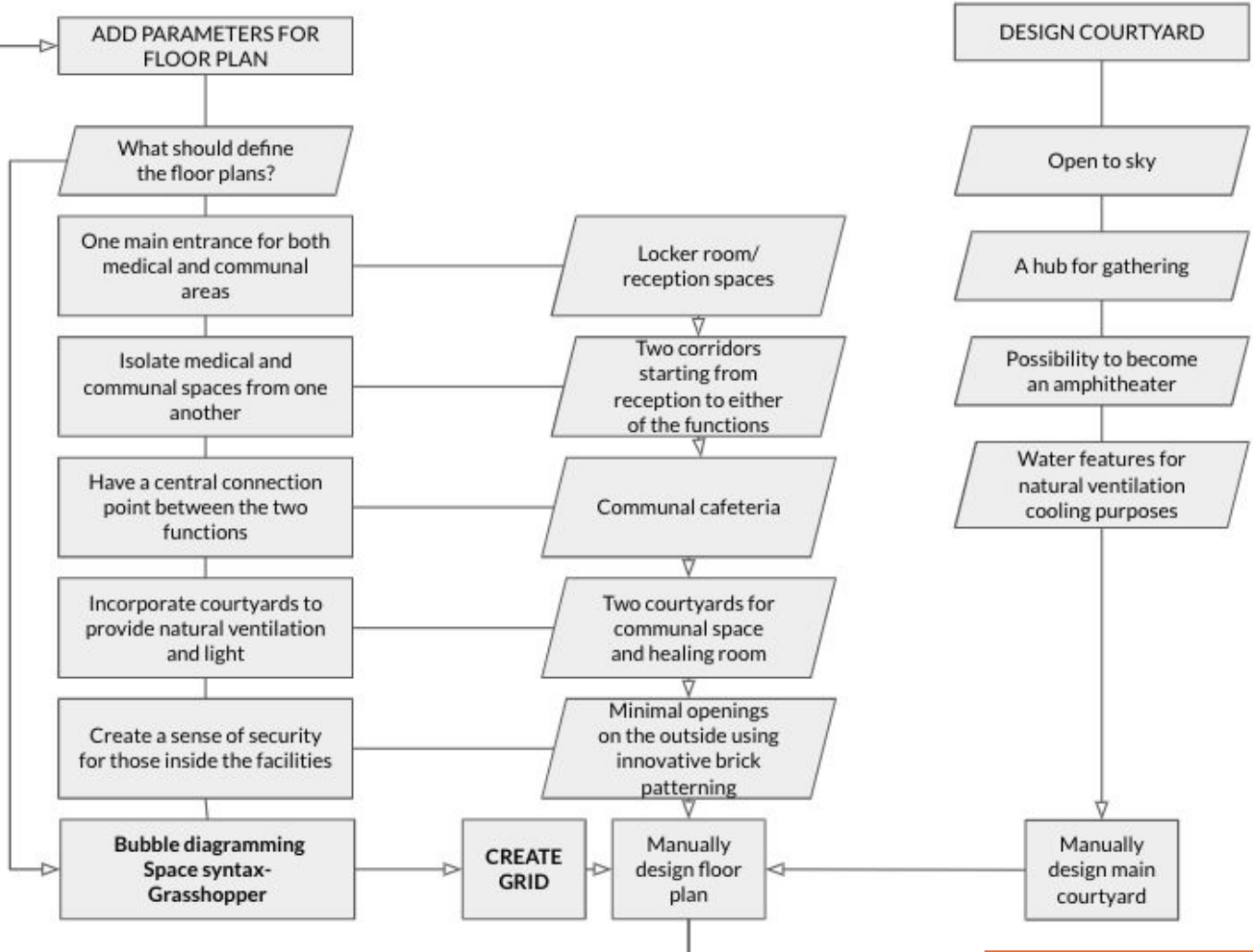


Figure 22: Configuration flowchart

**PHASE 2  
CONTINUED**

# Configuring Programme

Figure 23 presents the 1.50 m by 1.50 m grid that is used as a first reference to configure the spaces.

Figure 24 shows the result from Space syntax (plugin for grasshopper), the areas and square meters are placed depending on their connections, privacy type and size.

As a third step, the main configuration shows 4 main divisions (figure 25): Health department, community department, connection space and main entrance.

Figure 26 shows the main connections between the two departments and the connections area with the main entrance.

In figure 27, all spaces with its size, name and connections are placed according to the Space syntax distributions and the grid.

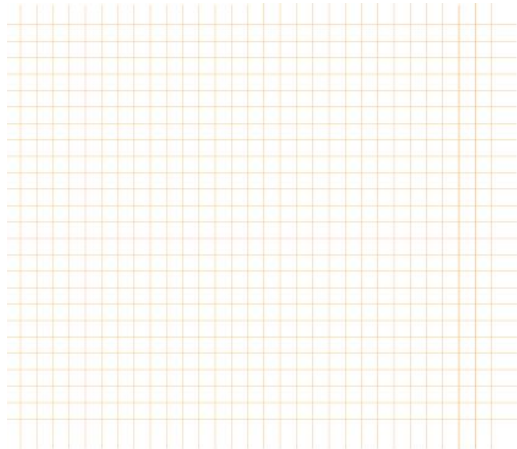


Figure 23: Grid

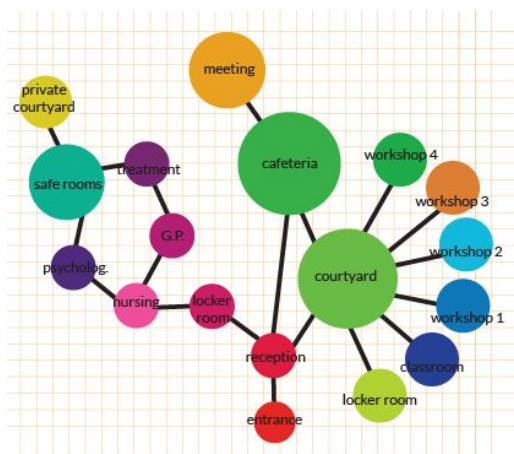


Figure 24: Space syntax on the grid

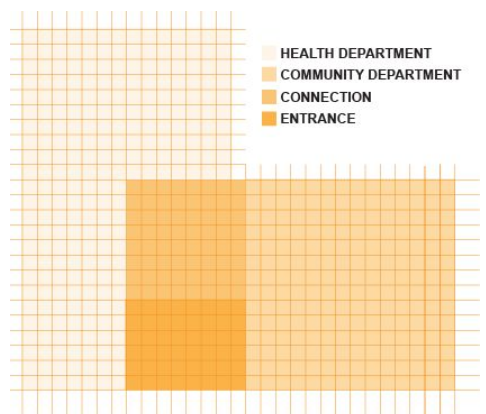


Figure 25: Main configuration

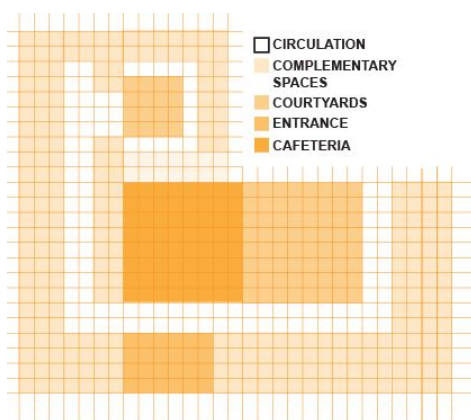


Figure 26: Spaces configuration

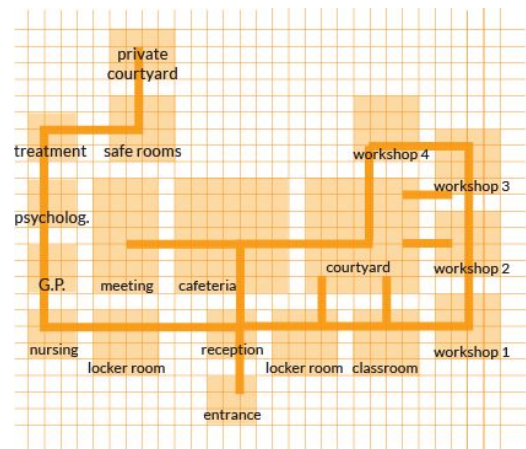
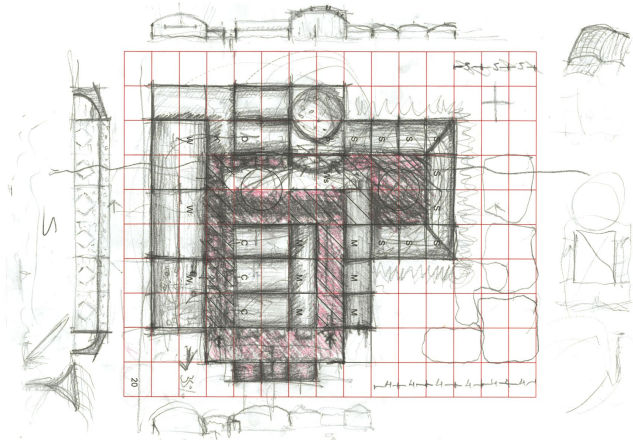


Figure 27: Connecting spaces

Figure 28: Grid exploration



## Sketching process

The basic configuration process bounced off the REL chart which allowed for dividing area according to need and the bubble diagram showing a basic suggestive configuration.

After obtaining the two diagrams, other criteria such as user behaviour and general design aesthetics were manual inputs to the configuration process. Many sketches and iterations were made specially for the plan in order to hero the principles we set out to achieve. Overall design of the floor plan was manually configured.

Figure 29: Programme according to grid exploration

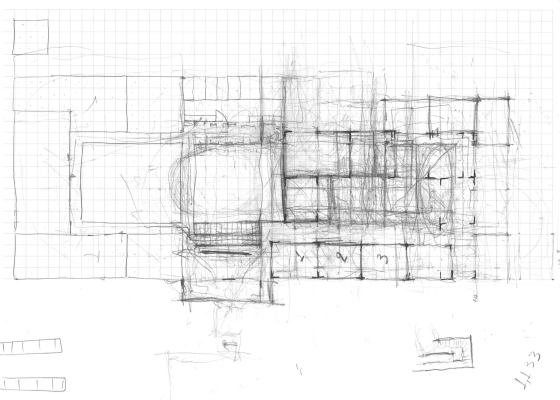


Figure 30: Programme

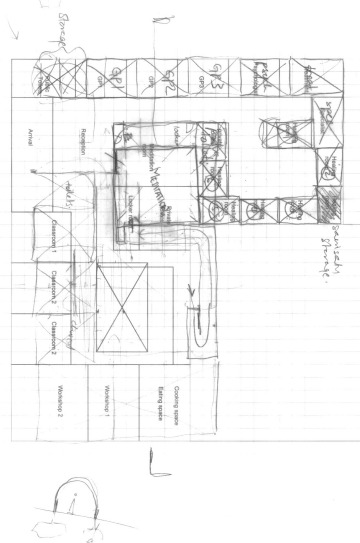


Figure 31: Programme in section

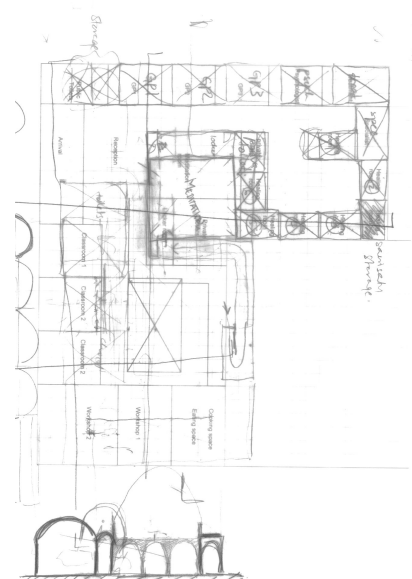
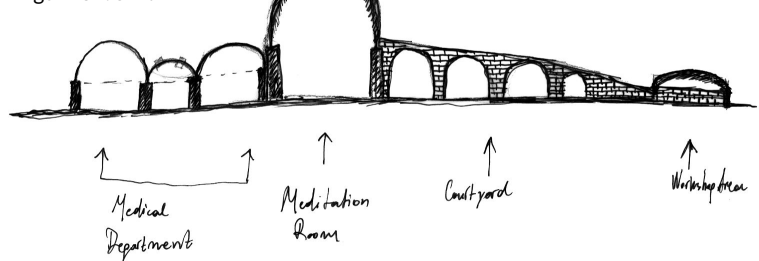


Figure 32: Section



## Sun/wind movement

Sun and wind movements were taken into consideration in the early design stages of the project. Sun analysis was an important aspect in designing openings and wall patternings to achieve maximum sunlight through winter and minimum sunlight through the hot summer days.

Wind was yet another important factor in designing openings and when considering possible roof shapes according to predominant wind movements.

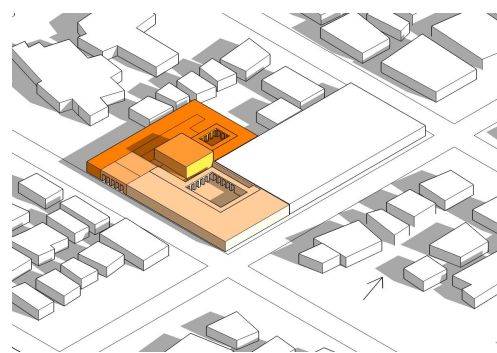


Figure 33: Summer sun at 10 AM



Figure 34: Summer sun at 6 PM

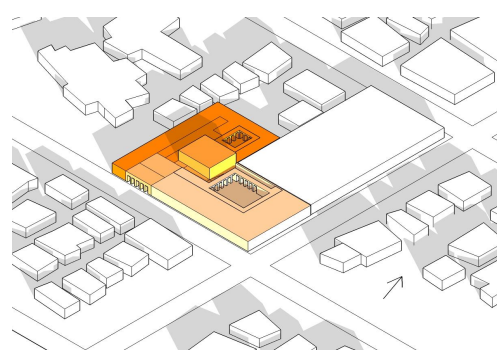


Figure 35: Winter sun at 10 AM

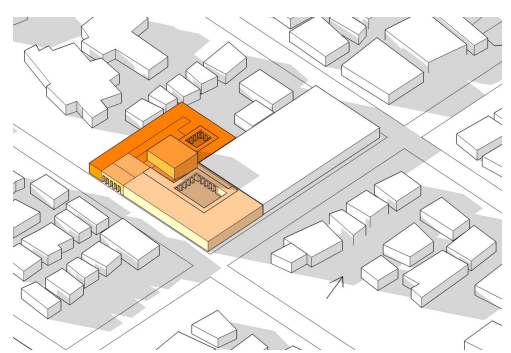


Figure 36: Winter sun at 6 PM



Figure 37: Predominant wind direction (West)

# Internal programming

The internal programming is shown in the following diagrams. Each activity, connections, size and privacy type were considered to configure the floor plan, according to the Space syntax and the grid (page 18).

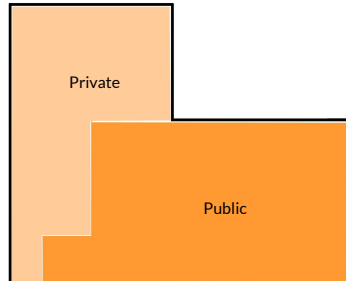


Figure 38: Zoning

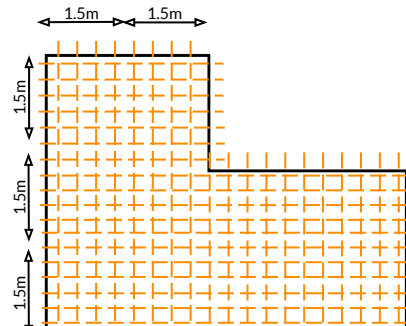


Figure 39: Grid

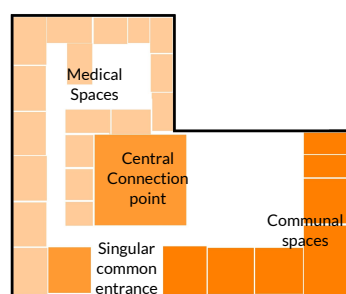


Figure 40: Configuring

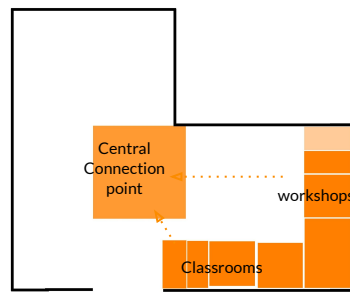


Figure 41: Communal Configuring

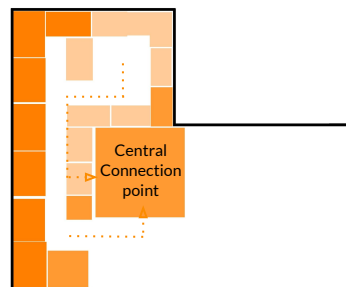


Figure 42: Medical Configuring

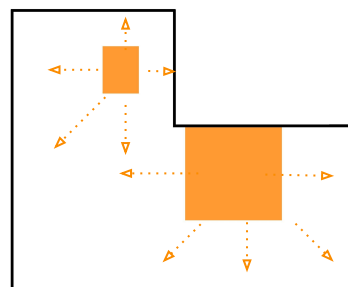


Figure 43: Courtyard connections

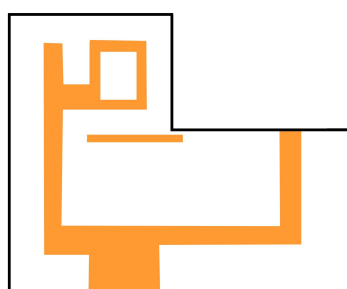


Figure 44: Internal Movement corridors

## User experiences and privacy

It was of utmost importance for the configuration of the plan to be done manually because of how different users would experience the different functionalities of the Center. Three main users were taken into consideration, a woman of 18 years old entering the facility for the first time (Figure 45), a woman with a child needing medical attention in secret (Figure 46), a female medical staff (Figure 47).

The configuration was heavily influenced by the movement and thought process of the users we chose as profiles. We believe this process of thinking allowed for a more easy circulation inside the building.

Figure 45: INTERNAL MOVEMENTS: Single woman with no children

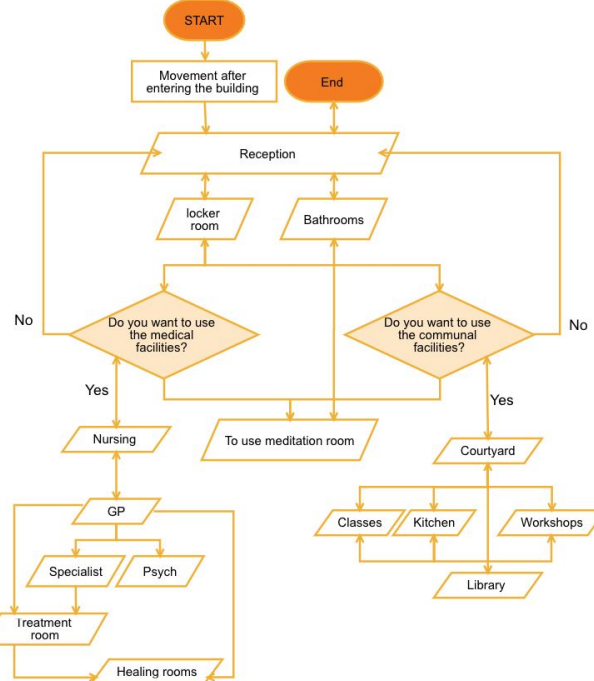


Figure 46:

INTERNAL MOVEMENTS: Woman with child needing special help

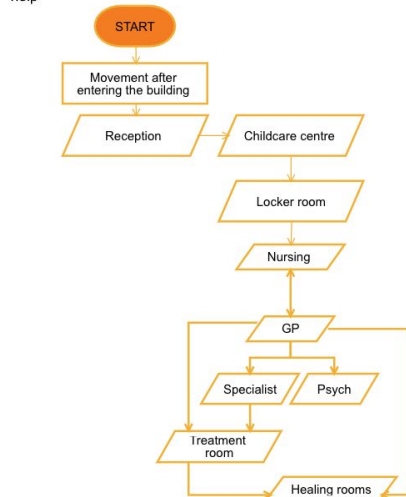
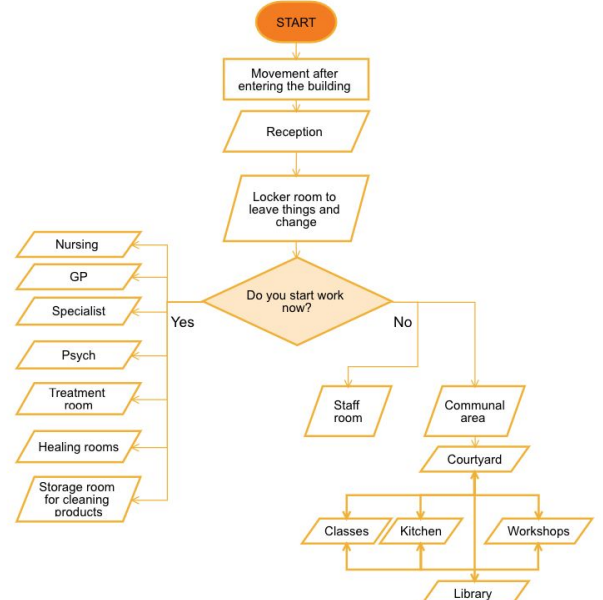


Figure 47:

INTERNAL MOVEMENTS: Medical staff



## Privacy configuration

As shown in Figure 49, four different types of privacy levels were used to configure the florplaan according to the grids, functions, connections and sizes.

The main entrance will be the most public area of the building, providing a clear and open connection point to the surrounding areas.

The complementary spaces for each department, such as staff/locker rooms, public toilets, nursing and storage are part of the SEMI-PUBLIC privacy type. The cafeteria will be the connection between all spaces, therefore, it will be art of SEMI-PUBLIC type as well.

Spaces that need more privacy than the previous ones, such as the Specialist, psychology and treatment offices will be the SEMI-PRIVATE area of the Health Department. The workshops and class room areas will represent the SEMI-PRIVATE are of the Community department. The big courtyard will also be part of this type, been connected to the workshops and cafeteria but not directly to the main entrance.

The most private spaces of the entire building are the healing rooms, with its own storage, toilets, showers and private courtyard. The meeting space above the Cafeteria will be also private to provide a calm and relaxing space for users to sit and meet, while eating or drinking something from the cafeteria.



Figure 48: Privacy zoning

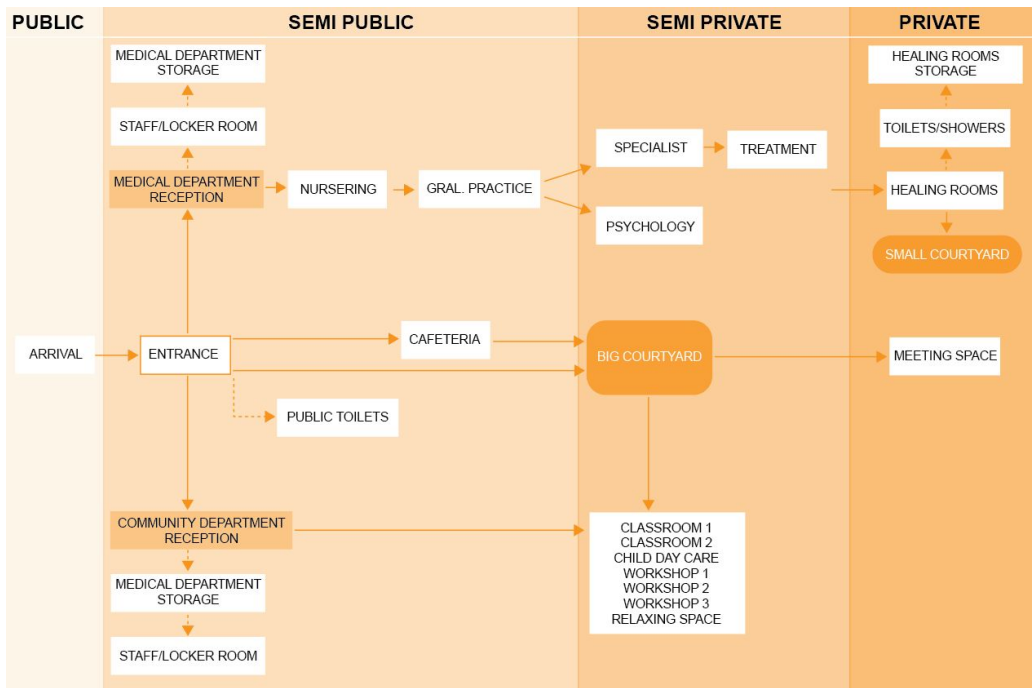


Figure 49: Types of privacy diagram

## Floorplan

The floorplan, with spaces, structure and grid is shown on this page. Here, it is clear the difference between load bearing walls, divisions and columns.

The different types of user experiences are shown in page 22.



Figure 50: Types of privacy diagram

## Sections

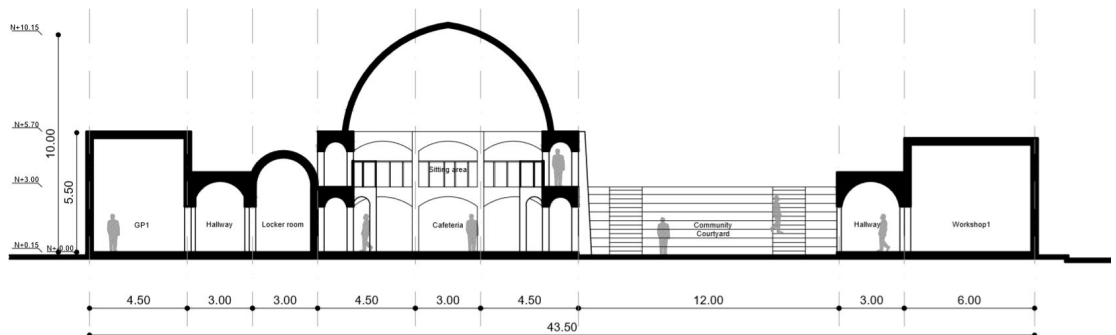


Figure 51: Section A-A'

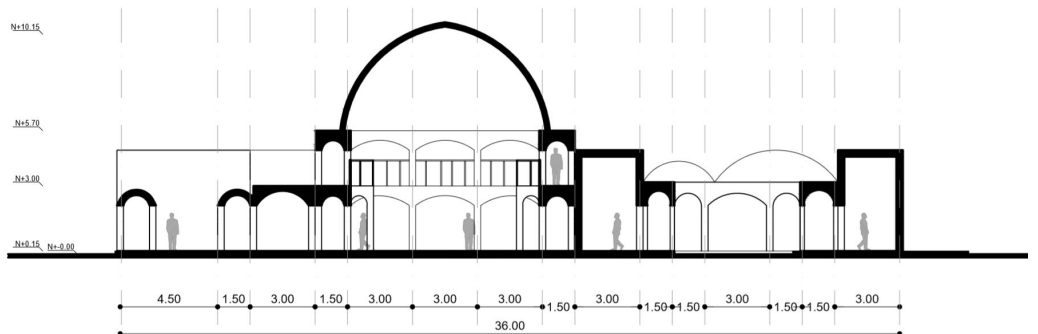


Figure 52: Section B-B'

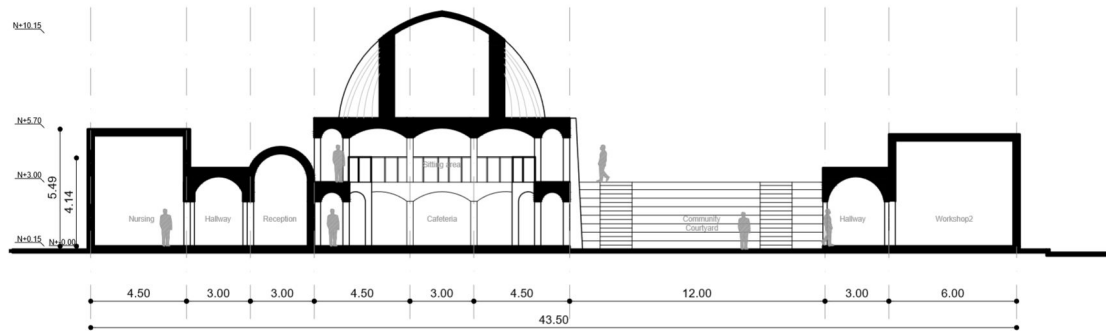


Figure 53: Section 1-1'

## Rooftop typologies configuration

The rooftops were configured depending on each space location, structural grid, predominant grid and sun path.

Figure 54 shows the different roof typologies on a plan.

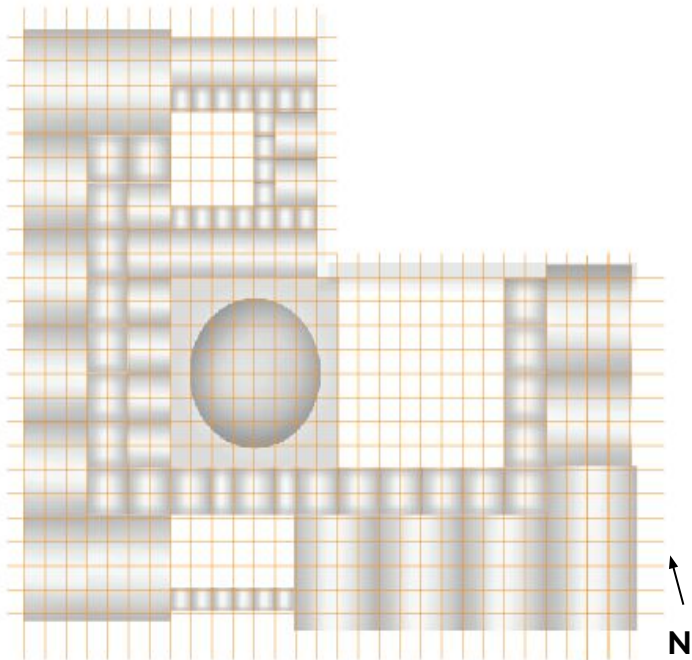


Figure 54: Roofs configuration

Figure 55 shows de the different thickness of the structure, depending if it's a internal or external load bearing wall, a division or columns.

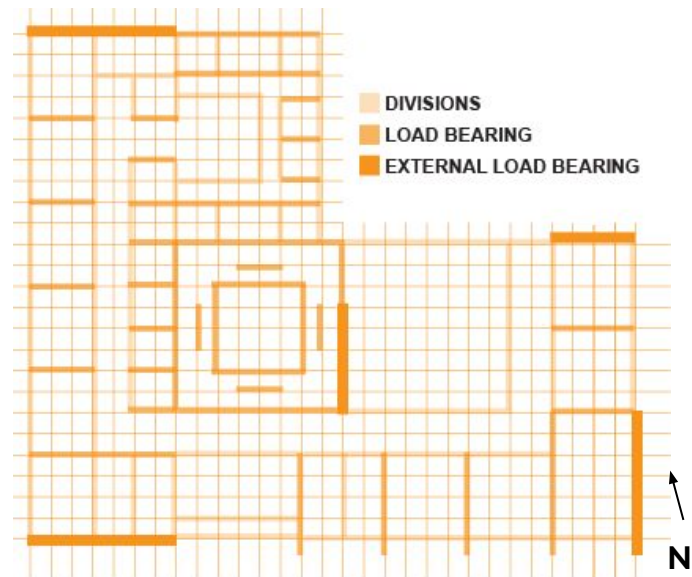


Figure 55: Structure

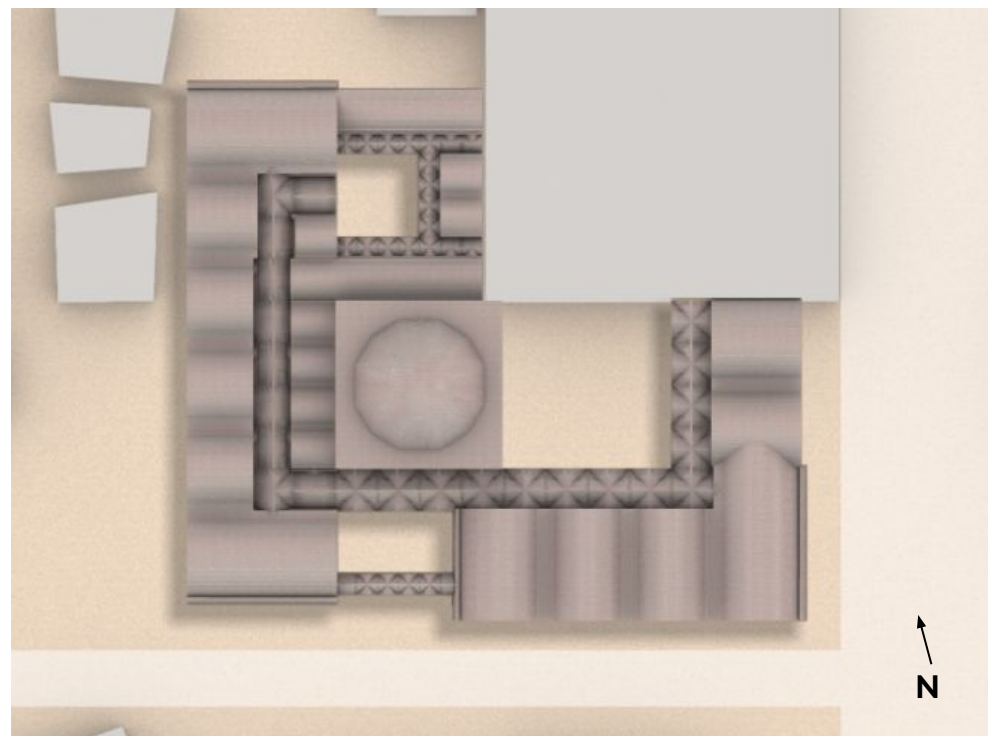


Figure 56: Roofs configuration, plan

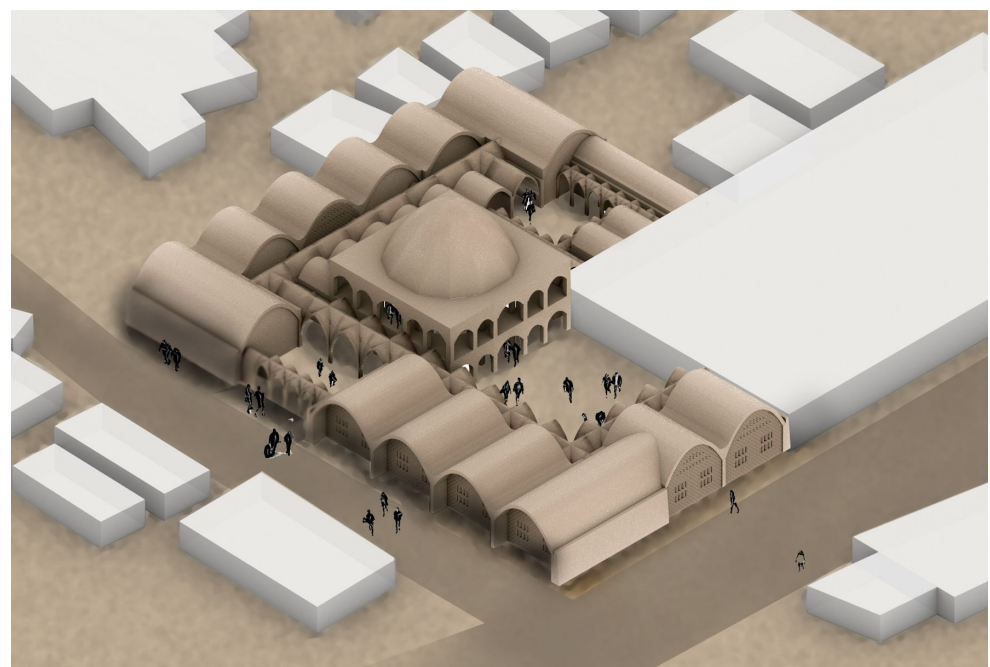


Figure 57: Roofs configuration, 3D model

---

# Form finding

---

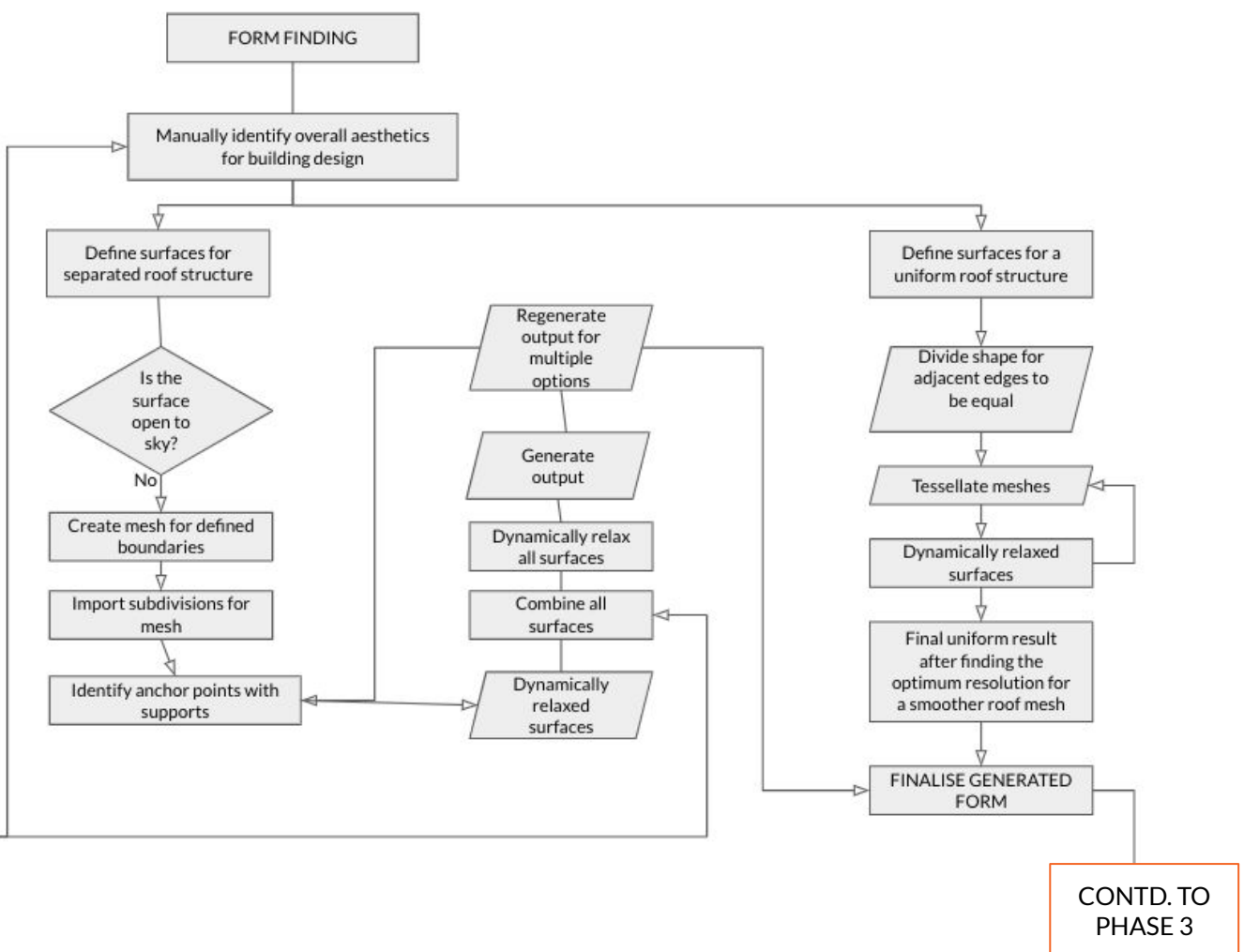


Figure 58: Form finding-flowchart

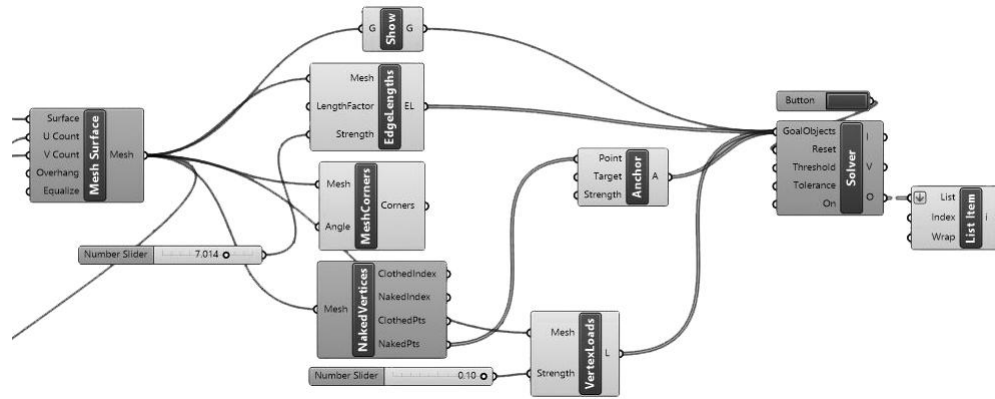


Figure 59: Script in Grasshopper

## Form finding for roofs in community and medical spaces

Most rooms in the building, both in communal and medical department, were decided to be roofed under two-sided vaults. The first step for the form finding of these roofs was to define the direction of the vaults. That decision was taken according to architectural preferences as well as structural purposes.

Therefore, in order to avoid very thick walls to carry the loads, the vaults were chosen to span the short side of the rooms, as it is presented in the image below.

The surfaces of different shaped rooms or different direction were imported separately in Kangaroo and tessellated with a regular grid to provide the straightforward geometry of a vault. The tessellated meshes were anchored in the walls and after applying the appropriate load, they were dynamically relaxed. The value of the load was adapted in order to provide a reasonable height for the roof shape.

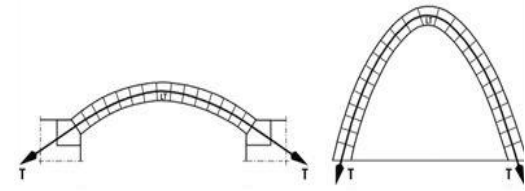


Figure 62: Source: Kılıç Demircan, R. & Ozturk Kardogan, P.. (2018). Studying the Historical Structure Damage Due to Soil Hazards and Examination of Applied Repairment-Strengthening Techniques. 10.1007/978-3-319-64349-6\_44.

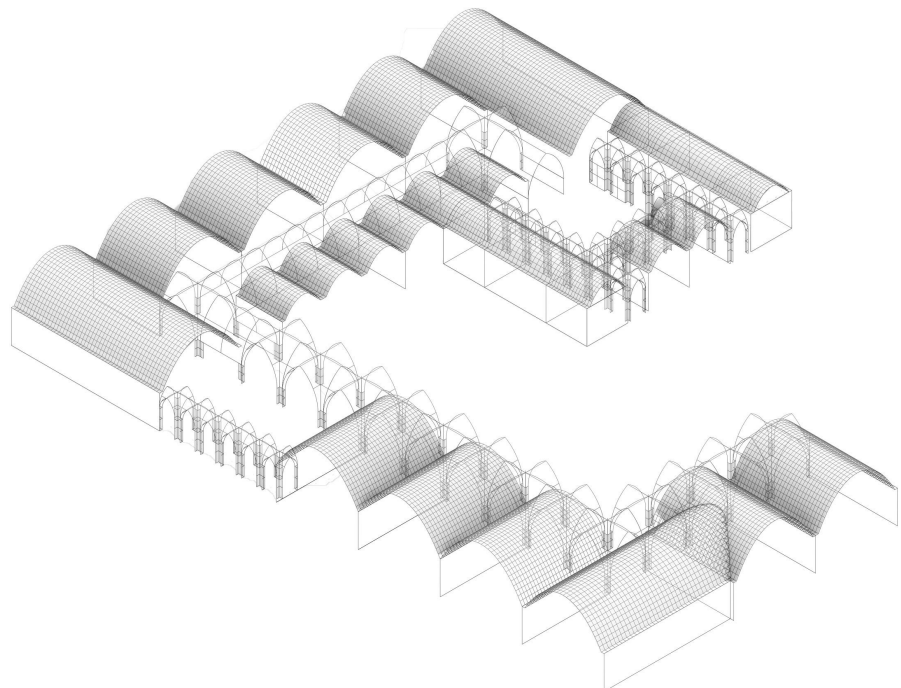
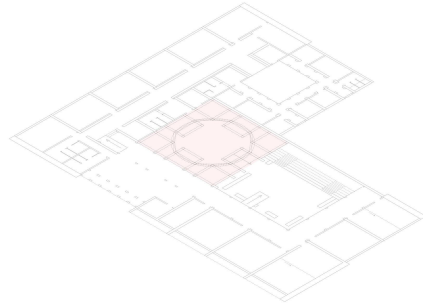


Figure 60: Roof division areas

Figure 61: Support lines of the roof meshes

Figure 63: Final outcome after the dynamic relaxation



## Further form finding\_Central Room

### Different tessellations and forms of the small domes

The central room was decided to be developed in two floors. The ceiling of both floors was open in the center according to the polygon dome above it. The irregular shape of the arches supporting the filling for second floor and the dome is illustrated in the bottom left image. Several attempts were developed regarding the shape and the tessellation of the meshes which after relaxation provided with the final result. The final form was preferred for aesthetical and structural reasons.

From the failed trials some conclusions occurred. First of all, in order to have welded relaxed meshes, it is important the initial shapes to share equal adjacent edges. Otherwise, even if the tessellation is the same, it is not able to continue to the next mesh and the relaxed elements are unwelded.

Another deduction that came from the different attempts, was that the triangular tessellation did not work well in a four-points supported vaults. The relaxed mesh was too flatten, which would emerge difficulties in the construction. A quadrilateral tessellation provided the final smoother welded relaxed form.

Finally, the irregular shape of the arches was anchored in the area of the whole cross section of columns underneath them, to provide a realistic form.

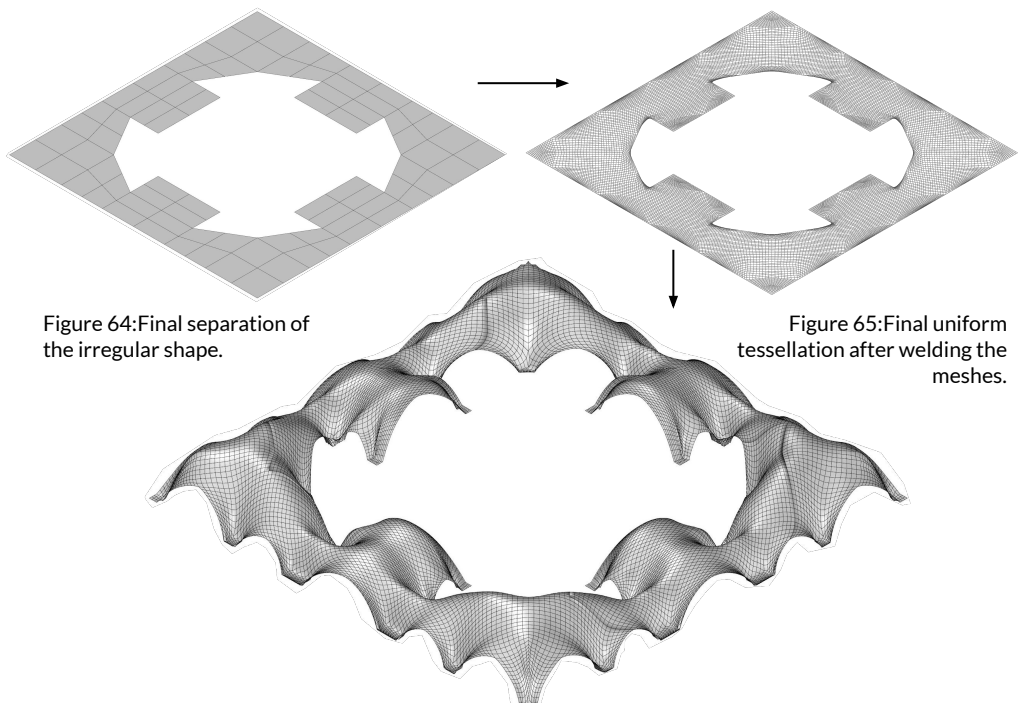
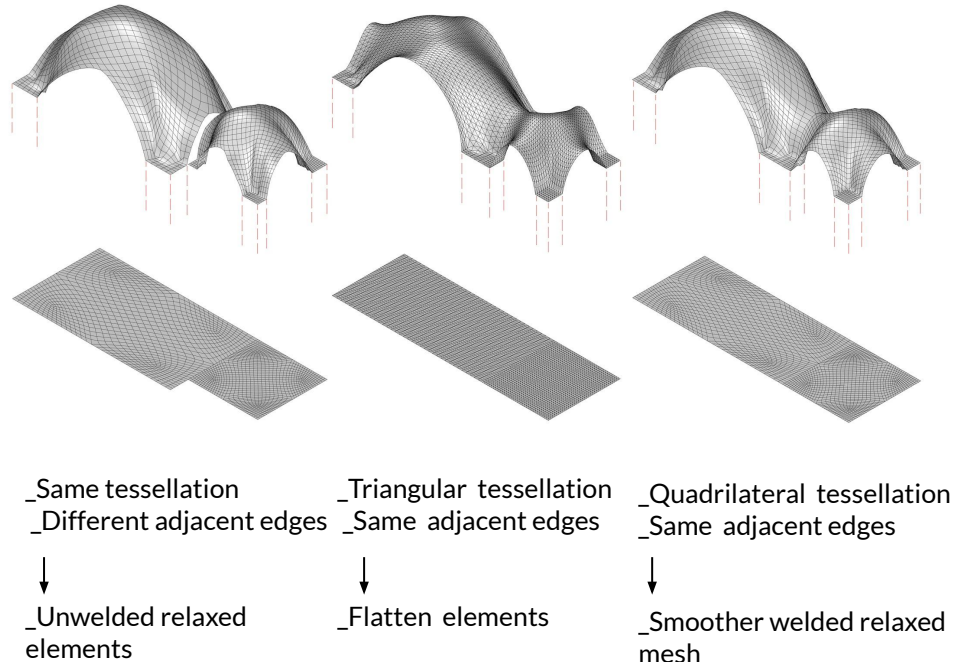
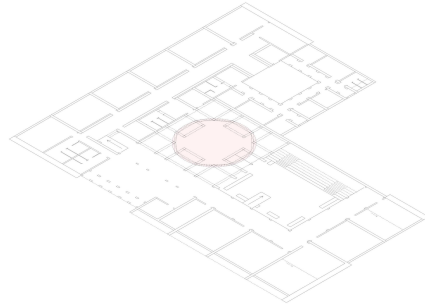


Figure 64: Final separation of the irregular shape.

Figure 65: Final uniform tessellation after welding the meshes.

Figure 66: Final uniform free-form roof shape.



## Further form finding\_Central Room

Tessellation and form of the dome

On top of the central room, a majestic dome highlights the important function of solidarity that the recreation space provides. For that reason great effort was spended to generate the form of it.

Firstly, following the initial plan, the base of the dome was translated as a square-based dome, anchored in all sides. Later for structural reasons the base of the dome had to be transferred in the inner columns and four extra columns were added to support it. The shape of the base became circle and the hemisphere shape was analyzed.

After the brick laying procedure, the circular base converted to a polygon one in order to allow filling that space with regular shaped bricks. The dome is supported by 12 columns, with almost equal distances, therefore the base is a dodecahedron.

For the tessellation of the mesh, it was realized that the most dense tessellation, the smoother the final result. In addition, the triangular tessellation provided us with a steeper dome than the quadrilateral one.

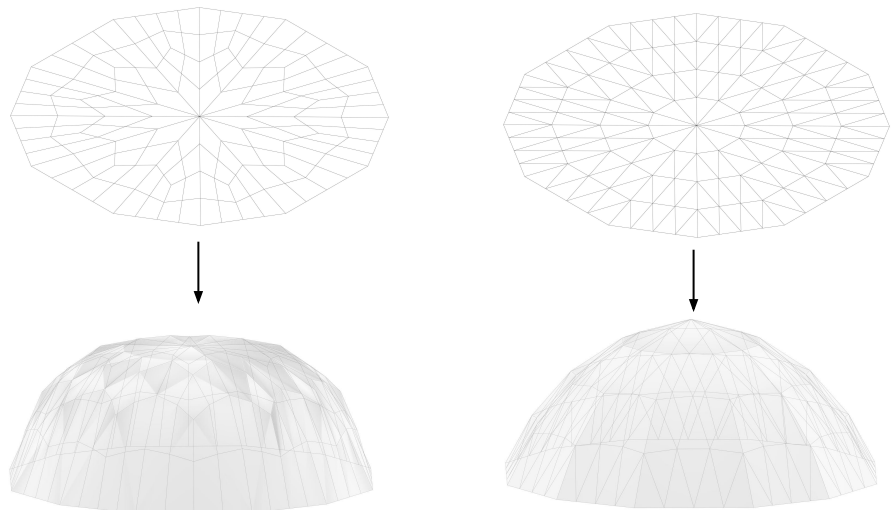


Figure 67: Rare quadrilateral and triangular tessellation.

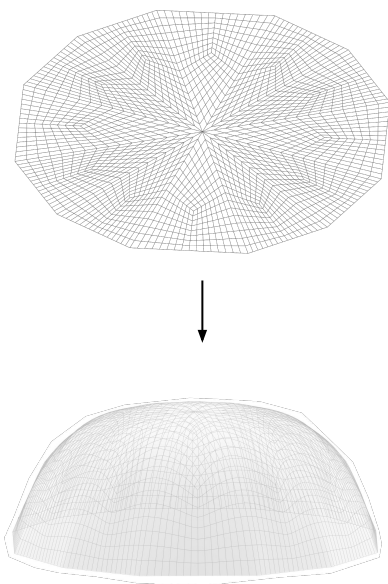


Figure 68: Quadrilateral dense tessellation..

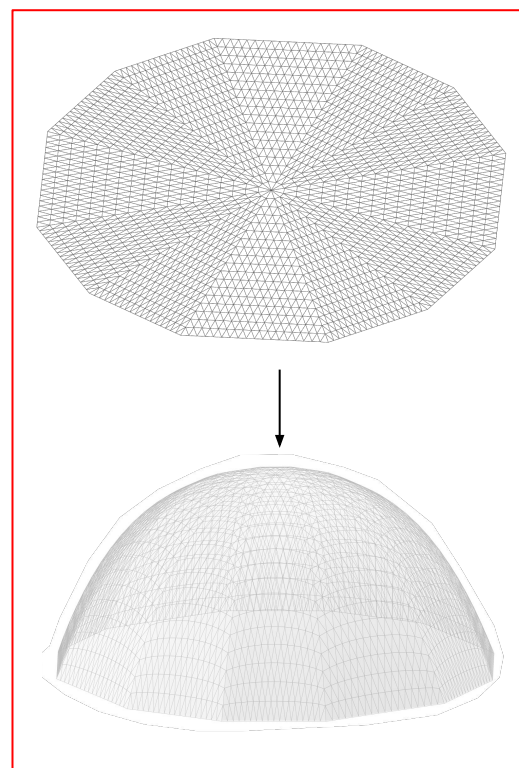


Figure 69: Triangular dense tessellation. Chosen final form

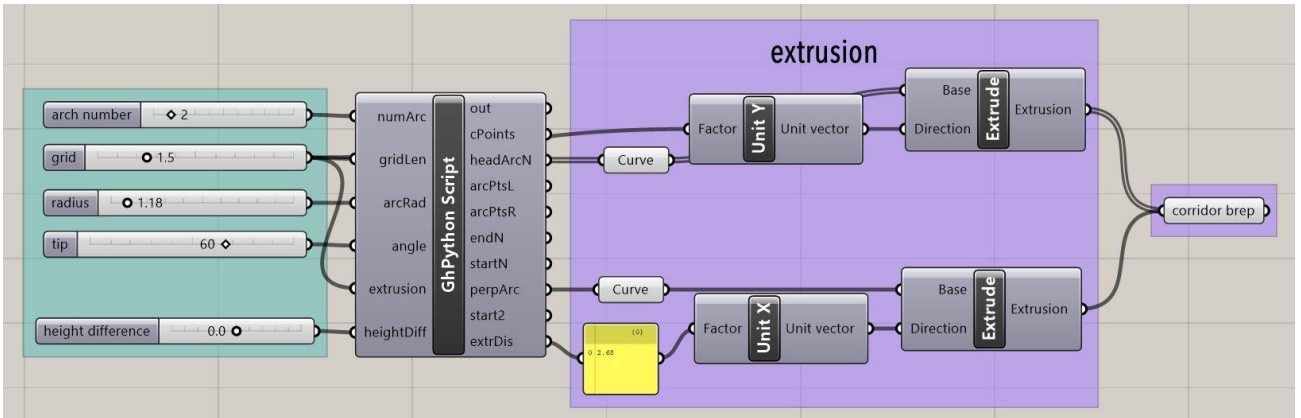


Figure 70: Grasshopper script

## Python scripting component

One other important element of this design is the corridor system, which intends to connect the different function sectors of the whole building program. For a number of reasons, it was necessary to have modularity in this element, due to varying volumes and structural requirements around their position. Therefore, a script that instantly generates the required shapes would vitally help in exploring various planning decisions.

Since the planning phase, the space of the pathways was reserved for a separate modular structure that would fit inside the selected grid dimensions. Subsequently, it was necessary that this system would be able to adapt different grids, as well as changes in planning. The precision in dimensions for this component was also an input that would have to be adjusted, depending on the final outcome of the brick layering, structural thickness and constructability findings.

Variations in the aesthetics of this component could provide a distinct character for this repetitive element. Consequently, its final form was depending on decisions made for the rest of the building, intersections with other structures or entrance openings, and thus, making it appropriate to use scripting methods for its forming.

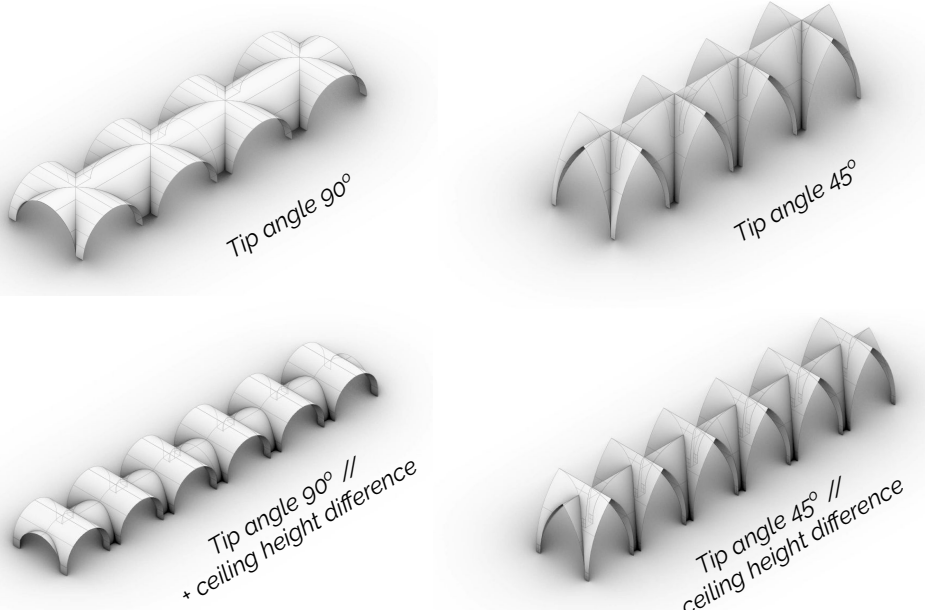


Figure 71: Different angle exploration

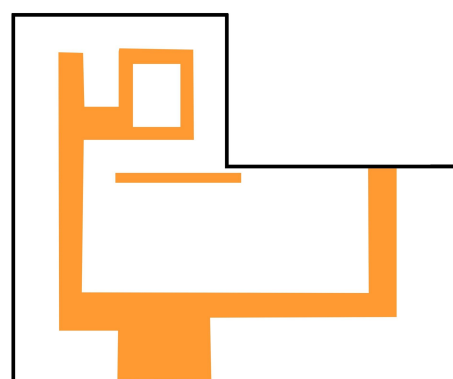


Figure 72 : modular components designed with python script are placed on corridors and entrance of the building to provide shade and rain protection

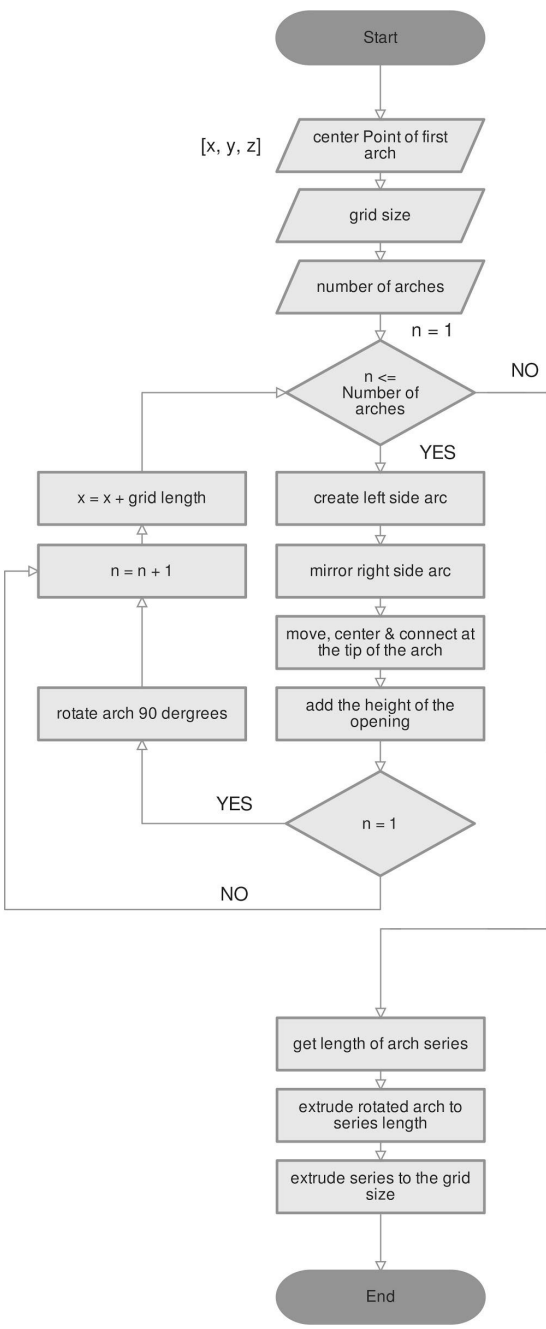
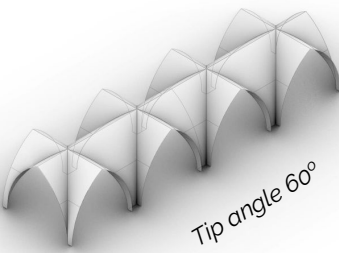


Figure 73: Python flowchart (left)  
Figure 74: Python script (right)

```

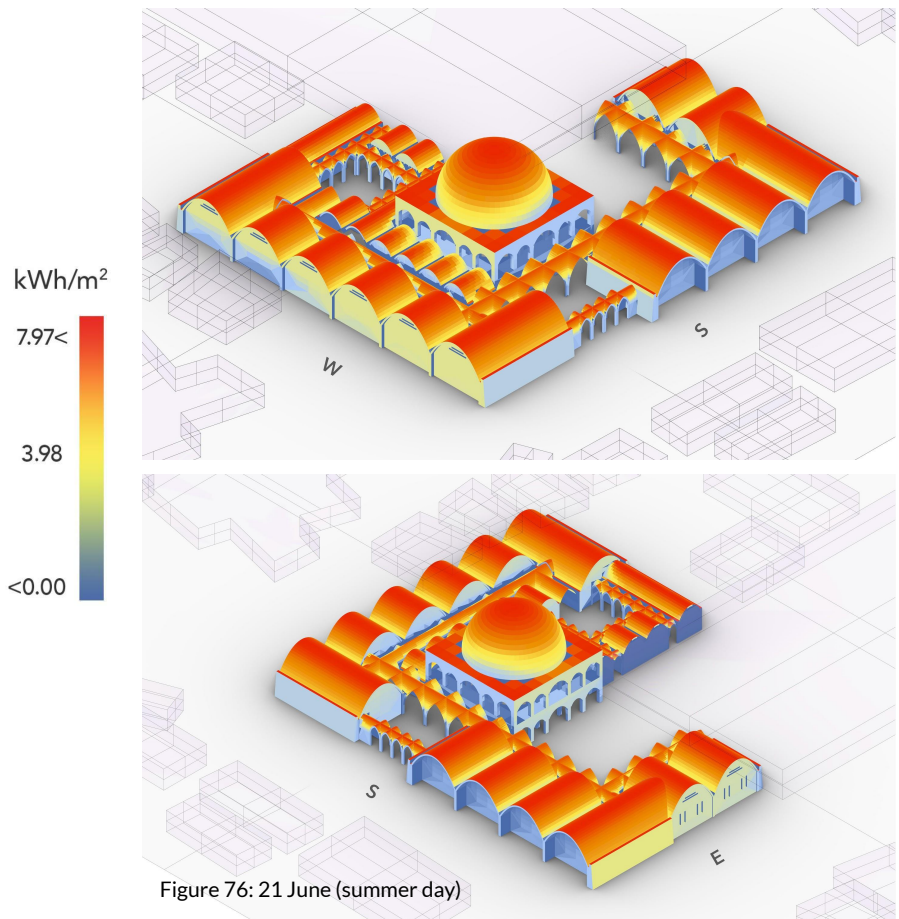
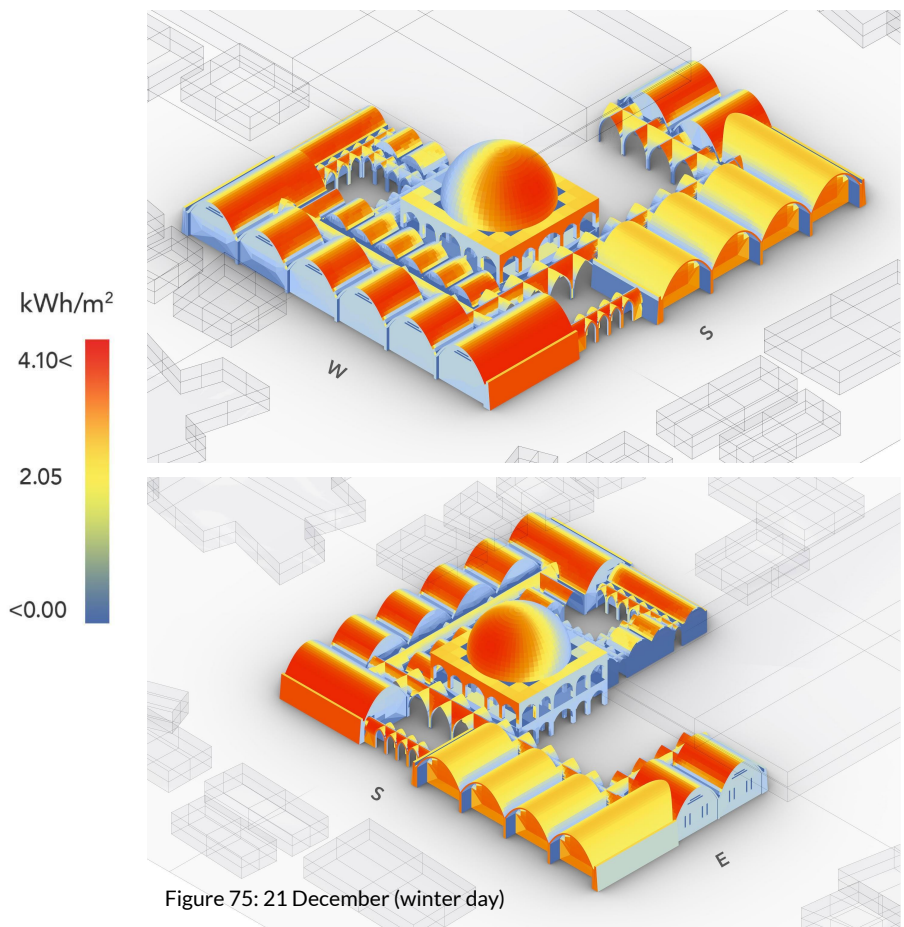
1 __author__ = "Ioannis_Tsionis"
2 __version__ = "2019.09.30"
3
4 #This script creates the surface geometry of a groined vault
5 #depending on the grid length and a number of openings.
6 #By changing the arc radius and the angle,
7 #different sizes of semicircular or pointed vaults can be produced.
8
9
10
11 import rhinoscriptsyntax as rs
12 import Rhino.Geometry as rg
13
14 cPoints = []
15 headArcN = []
16 arcPtsL = []
17 arcPtsR = []
18 startN = []
19 endN = []
20 planeN = []
21
22 #The script runs with a single point as an input.
23 #For the specific script [ x=0 ,0,0] is considered for the base point
24 x = 0
25 #This point will be the middle point
26 #of the length of the first arch opening in the array
27
28 #For the number of arcs input,
29 #a series of components is generated linearly through a loop
30
31 for i in range(0,numArc):
32     ....cPoint = rs.AddPoint(x,0,0)
33     ....
34     ....#The first arc is created
35     ....
36     ....arcPtL = rs.PointAdd(cPoint, [-arcRad, 0, 0])
37     ....arcPtsL.append(arcPtL)
38     ....arcPtR = rs.PointAdd(cPoint, [arcRad, 0, 0])
39     ....arcPtsR.append(arcPtR)
40     ....
41     ....uPoint = rs.PointAdd(cPoint, [0, 0, arcRad])
42     ....plane = rs.WorldZXPlane()
43     ....plane = rs.RotatePlane(plane, -90, axis=(0,1,0))
44     ....headArcL = rs.AddArc(plane, arcRad, angle)
45     ....rs.MoveObject(headArcL, [x,0,0])
46     ....headArcR = rs.RotateObject(headArcL, cPoint, 180, axis=(0,0,1), copy=True)
47     ....
48     ....endL = rs.CurveEndPoint(headArcL)
49     ....endR = rs.CurveEndPoint(headArcR)
50     ....endN.append(endL)
51     ....endN.append(endR)
52     ....
53     ....#If a different than 90 degrees angle is selected as the arc radius,
54     ....#the arch sides have to reconnect and form the tip of the arch.
55     ....
56     ....gap = rs.DistanceToPlane(rs.WorldYZPlane(), endL)
57     ....rs.MoveObject(headArcL, [-gap + x, 0, 0])
58     ....rs.MoveObject(headArcR, [gap - x, 0, 0])
59     ....
60     ....#The arch perpendicular to the linear array (corridor pathway) is created
61     ....
62     ....if i == 0:
63         ....start1 = rs.CurveStartPoint(headArcL)
64         ....perpArc = rs.JoinCurves([headArcL, headArcR], delete_input=False)
65         ....perpArc = rs.RotateObject(perpArc, start1, 90, axis=(0,0,1), copy=True)
66         ....start2 = rs.CurveEndPoint(perpArc)
67         ....dis = start1.DistanceTo(start2)
68         ....gapPerp = abs(gridLen-dis)/2
69         ....perpArc = rs.MoveObject(perpArc, [0,gapPerp,-heightDiff])
70         ....
71         ....cPoints.append(cPoint)
72         ....headArcN.append(headArcL)
73         ....headArcN.append(headArcR)
74         ....
75         ....startL = rs.CurveStartPoint(headArcL)
76         ....startR = rs.CurveStartPoint(headArcR)
77         ....startN.append(startL)
78         ....startN.append(startR)
79         ....
80         ....x = x + gridLen
81         ....
82         ....extrDis = start1.DistanceTo(startN[-1])
83         ....print(extrDis)
84

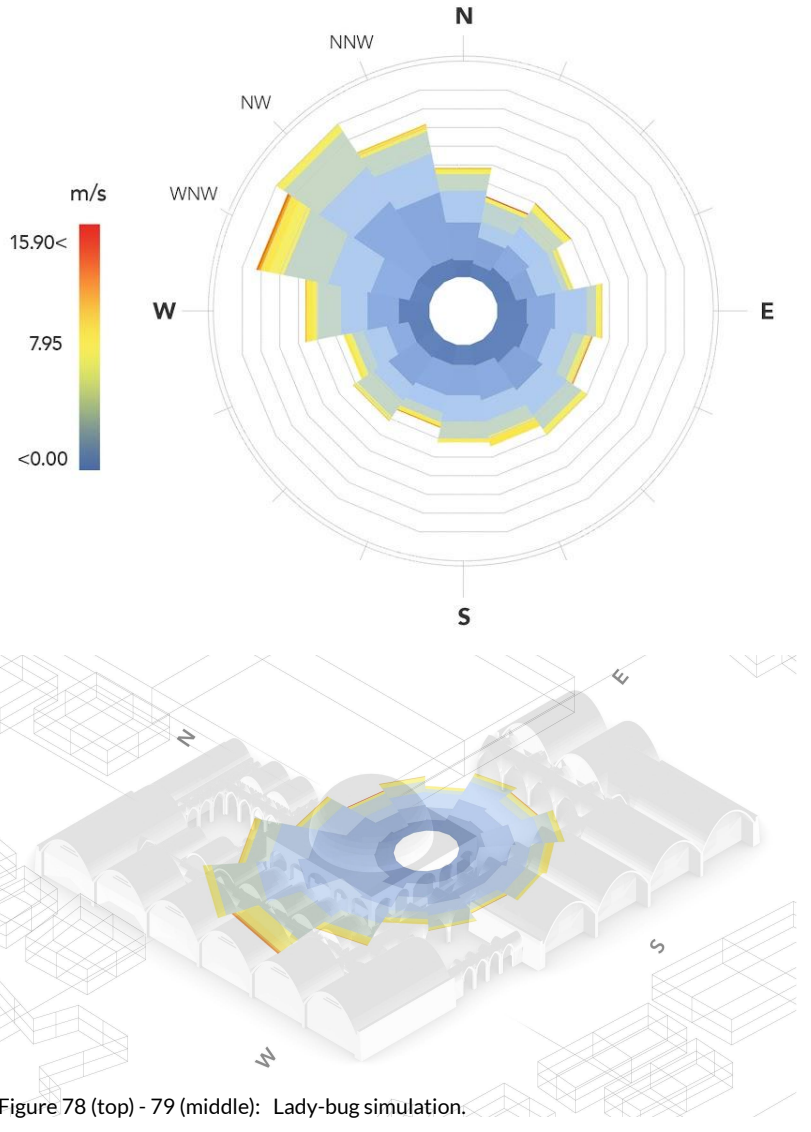
```

## Solar radiation analysis

Following the forming of the design volumes, a solar radiation analysis was conducted. This study was archived, in order to evaluate and adjust the different spaces through shadings and ventilation openings regarding their potential thermal comfort. The coordinates that were considered, were taken from the closest nearby airport site 10 kilometers to the northwest of the refugee camp, King Hussein Air Base. Also known as Mafraq Air Base, the site is an air base 3 kilometres of the city of Mafraq, in the Mafraq Governorate of Jordan.

The results of the analysis provided us with a brief visualization of the geometry behavior. As can be seen through a comparison between a typical summer (21<sup>st</sup> of December) and winter day (21<sup>st</sup> of June), the curvature of the roofs can heat up the interior volumes in distinct ways. The climate of Jordan can fall to temperatures of 5°C in January, whereas the hottest summer days can sometimes reach 35°C or more. This data demands the provision of a natural cross-ventilation flows, combined with shadings and overhangs for summer days, as well as facade walls able to gain additional amounts of solar heat during a winter day.





## Ventilation strategy

In order to achieve comfortable interior temperatures, the wind breeze direction was taken into account. The wind rose chart shows that throughout the year wind can come from all directions. However, the prevailing flow comes from the northwest-to-west direction.

Since the majority of the building roofs curvature is oriented along the west-east axis, the wind direction favors the possibility of cooling the roofs through natural cross ventilation. In addition, the empty spaces of around 2 meters high below the vault ceilings provide sufficient height to allow the cooling process of heated inclined surfaces. Walls that face west and east obtain ventilation openings at the roof's height, with larger opening areas facing the prevailing breezes, in order to create wind pressure and get rid of standing waves inside the building.

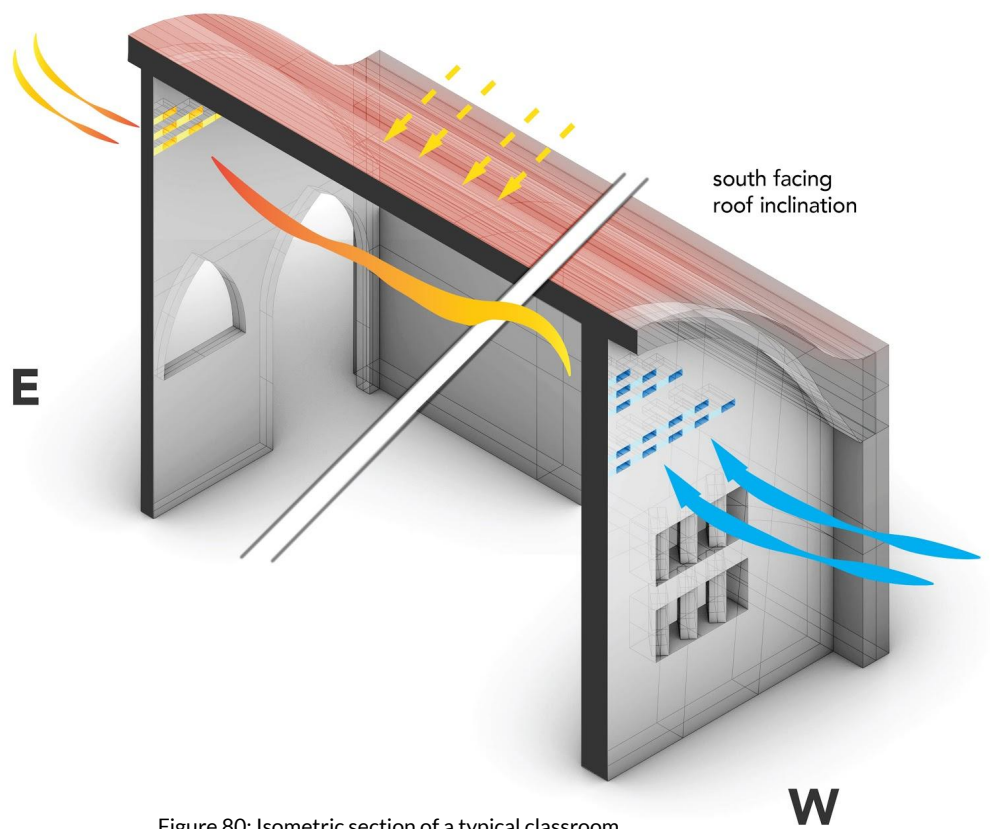


Figure 80: Isometric section of a typical classroom.

---

# Adobe brick testing

# Introduction

The following section is a study of the making and testing of adobe earth bricks for the “Earthy” design studio with the aim of designing and engineering earthy buildings for betterment of a district of the Al Zaatri Refugee Camp in Jordan.

Different types of adobe bricks will be tested by its individual material strength and dimensions. Bricks will be hand made according to one mould with pure adobe mix and more with the addition of extra materials to the mix.

The mixture of adobe and the additional materials used were chosen according to the site specific nature of Zaatri Refugee Camp in Jordan. It is of dry arid desert climate with a maximum of 34°C in summer (2019 August warmest) to a minimum of 7°C in winter (2019 January coolest) (1). In order for the following bricks to be made in Zaatri Refugee Camp, the additional materials used need to be sourced locally. Therefore all materials chosen for use, will be similar or the same material readily available in the region of Mafraq, Jordan.



Figure 81: Jordan's local adobe  
Source: <http://ap.buffalo.edu/>



Figure 82: Local waste with potential for adobe making  
Source: <https://www.giz.de/>



Figure 83: Adobe mixture for brick testing



Figure 84: Materials preparation for brick testing

# Objectives

The objectives of this study were:

1. Make adobe bricks combined with different types of materials that can be found around the area of the Zaatari Refugee Camp, in Jordan.
2. Test the adobe bricks, with 6 different types of mixtures and 2 different sizes, to determine their compressive strength.
3. Compare between the different mixtures and same size samples to determine the highest compressive strength.



Figure 85, 86 and 87: Brick making, testing and comparing.



Figure 88: Straw



Figure 89: Wood chips



Figure 90: Coconut fibers



Figure 91: Natural leaves



Figure 92: Rope natural fiber

## Methodology

### Brick making procedure

#### **Available Material/ resources for basic brick mixture:**

Clay  
Coarse Sand  
Fine sand  
Water  
Mixing tubs  
Buckets  
Mixer  
Moulds  
Scale

#### **Mixture and samples made:**

**Mixture ratio:**  
30% clay, 30%fine sand, 40% coarse sand,  
10%water for total weight of dry mixture.

#### **Samples to be made:**

1. small compression specimens of adobe only
2. small compression specimens of adobe with additional material mix
3. large compression specimens of adobe only
4. large compression specimens of adobe with additional material mix

### Additional materials used

Additional material chosen to be incorporated into adobe bricks:

1. **Straw**
2. **Wood chips**
3. **Coconut fiber brush fill** (to mimic animal hair)  
Why use coconut fiber brush fill material? Coconut fiber: Stiffer and more durable material with resistance to water up to a certain extent. Coarseness and water resistance gives the material great friction
4. **Natural leaves, partially dried**
5. **Rope natural fiber 10cm**
6. **Rope natural fiber 40cm**  
Type and advantages of natural rope material: **TAMPICO:** Produced in Mexico from the stalk of the Agave plant. It has a soft to medium texture and is off white in color. It is heat, alkali, and acid-resistant. The porous fibers absorb water and work wet or dry. Heat distortion temperature is 283° F.



Figure 93: Small specimens-adobe only + additional mix



Figure 94: Big specimens-adobe only + additional mix

## Results

A Zwick z100 machine, was used in order to determine the compressive strength of the different samples of the hand-made adobe bricks. The machine is able to do static tensile tests of any materials at room temperature. It was set with a maximum elongation of 12 mm for the small samples and 15 mm for large samples. Below shows results for small sized compression bricks :

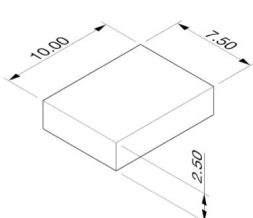


Figure 95: Size of small compression brick (cm)

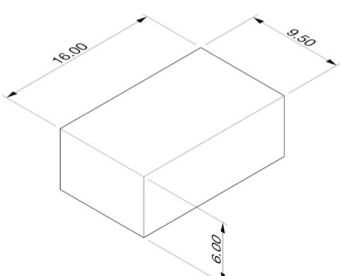


Figure 96: Size of large compression brick (cm)

Sample	Length (mm)	Width (mm)	Height (mm)	Force (N)	Elongation (mm)	Compressive strength (N/mm <sup>2</sup> )	Average value
<b>Adobe only</b>							
1S1	100	75	25	38700	12	5,2	4,9
1S2	100	75	25	84000	12	11,2	
1S3	100	75	25	15700	12	2,1	
1S4	100	75	25	13700	9,5	1,8	
1S5	100	75	25	52000	12	6,9	
1S6	100	75	25	15000	12	2,0	
<b>Adobe + wood chips</b>							
2S1	100	75	25	56700	12	7,6	6,6
2S2	100	75	25	38300	12	5,1	
2S3	100	75	25	52500	12	7,0	
<b>Adobe + straw</b>							
3S1	100	75	25	78600	12	10,5	8,6
3S2	100	75	25	47600	12	6,3	
3S3	100	75	25	66700	12	8,9	
<b>Adobe + coco fibres</b>							
4S1	100	75	25	67800	12	9,0	11,1
4S2	100	75	25	92400	12	12,3	
4S3	100	75	25	89900	12	12,0	
<b>Adobe + leaves</b>							
5S1	100	75	25	36300	12	4,8	5,7
5S2	100	75	25	51100	12	6,8	
5S3	100	75	25	40100	12	5,3	
<b>Adobe + rope fiber 10cm</b>							
6S1	100	75	25	97600	12	13,0	12,2
6S2	100	75	25	89000	12	11,9	
6S3	100	75	25	89000	12	11,9	
<b>Adobe + rope fiber 40cm</b>							
7S1	100	75	25	91000	12	12,1	10,3
7S2	100	75	25	52700	12	7,0	
7S3	100	75	25	89000	12	11,9	
<b>Adobe + coco fibres + wood chips</b>							
8S	100	75	25	24400	6	3,3	

Large samples							
1L (40cm rope fiber)	160	95	60	58800	15	3,9	2,3
2L (adobe only)	160	95	60	11100	15	0,7	
3L (adobe + coco fibres)	160	95	60	40600	15	2,7	
4L (adobe + straw)	160	95	60	27500	15	1,8	

Table 1: Results after compression strength test.

## Summary brick tests

	Average Maximum compression strength (N/mm <sup>2</sup> )
Adobe only	4.9 N/mm <sup>2</sup>
Straw	8.6 N/mm <sup>2</sup>
Wood chips	6.6 N/mm <sup>2</sup>
Coconut fiber	11.1 N/mm <sup>2</sup>
Leaves	5.7 N/mm <sup>2</sup>
Rope fiber 10cm	12.2 N/mm <sup>2</sup>
Rope fiber 40mm	10.3 N/mm <sup>2</sup>

Figure 97: Small compression brick (cm)

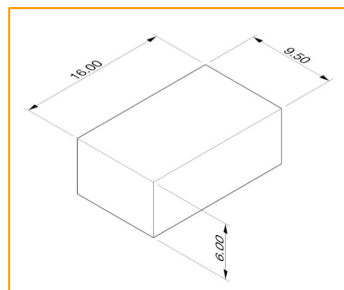


Figure 98: Large compression brick size (cm)

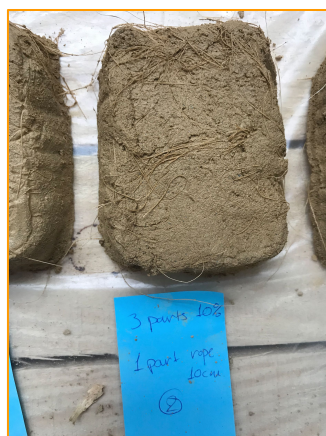


Figure 99: Small brick with natural  
rope fiber 10cm mixture with the  
highest average maximum  
compression strength (12.2  
N/mm<sup>2</sup>)

## Analysis and conclusion

According to the above information, with regards to the results of ultimate strength per category, it is evident that the average Compressive strength endured by the adobe only bricks were a low 4.9 N/mm<sup>2</sup> compared to the average of Adobe+rope fiber of 12.2 N/mm<sup>2</sup>. Safe design strength per category was defined under earthy construction of a parametrically designed building for site specifically, Jordan. Due to the absence of regulatory building codes for Adobe bricks in Jordaan itself, standard codes from Peru was used. Peru has experience with adobe brick constructions and is based on similar conditions as the Zaatari camp (climate and earthquakes possibility).

According to the technical construction standard in Peru (Adobe Code E.080) (3), the standard compressive strength of the unit must be minimum 1.2 N/mm<sup>2</sup>. Given, that all small samples tested had the lowest average value of 4.9 N/mm<sup>2</sup>, we presume all small adobe only bricks and adobe+material bricks pass necessary standard and also exceed expectations. Cumulative ultimate compressive strength for the smaller compression adobe bricks were of much higher value comparative to the larger sized adobe bricks. The lowest average being for adobe only of 0.7 N/mm<sup>2</sup> with the highest Adobe+rope fiber 3.9 N/mm<sup>2</sup>. Overall the large adobe bricks with rope fiber had a much higher compressive strength compared to the large plain Adobe brick with 3.9 N/mm<sup>2</sup> above necessary for standard codes. In terms of mixture with adobe and an external material, Adobe+rope fiber 10cm had an exceptionally high compressive strength therefore would be the most ideal to use in the construction phase.

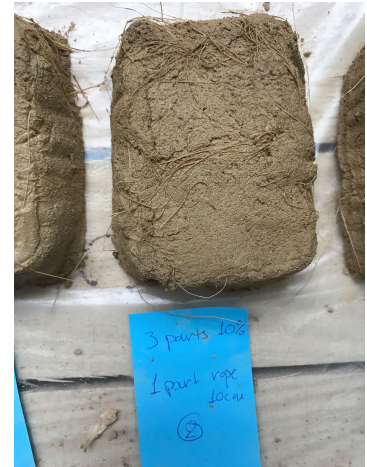


Figure 100: Adobe + rope fiber 10cm. Compression brick, small sample with highest compressive strength



Figure 101: Adobe only Compression brick, small sample with lowest compressive strength



Figure 102: A Zwick z100 machine used for compression testing

## Recommendations

It is important to keep in mind a few limitations to this test compared to the values/ processes we obtain in real life. Firstly, the **material** we have used in the experiments are of the highest quality clay and purest of water. This may not always be the case due to where the material will be sourced from. When building in Jordan, we will be limited to earth manually dug out from the site with water that may be infused with other elements.



Figure 103: mixed used for brick making

Secondly, the **process**, we were given the opportunity to use an electric mixer, which allowed for the adobe mix to be of good/equal consistency. This may not always be the case due to the limited availability of resources in a refugee camp. The drying conditions were quite controlled as it was indoors during temperatures of 20°C-13°C throughout the week. This will definitely not be the case on site because the adobe bricks will be drying outside and influenced by the local temperature and weather conditions. Therefore the conditions will influence properties such as the drying time and drying rate, therefore the overall performance of the bricks.

Thirdly, the **method used for testing**. We have used the A Zwick z100 machine for conducting the above tests. In real time, a load will not be continuously pressed no top of the brick in an even manner over a controlled period of time. They will only fail over time with external influences such as weather wear and tear.

Overall, the brick tests are of good use in a controlled environment to get specific measurements, however will not be the case in real life. It is important to take into consideration the above research. However, also important to keep in mind of how valid they are in real time over a specific time period using slightly different materials. The inability to test the material in its original environment having undergone natural wear and tear would be a limitation to this research process.



Figure 104: Electric mixer



Figure 105: Indoor drying process



Figure 106: Zwick z100 machine

---

# Structural analysis

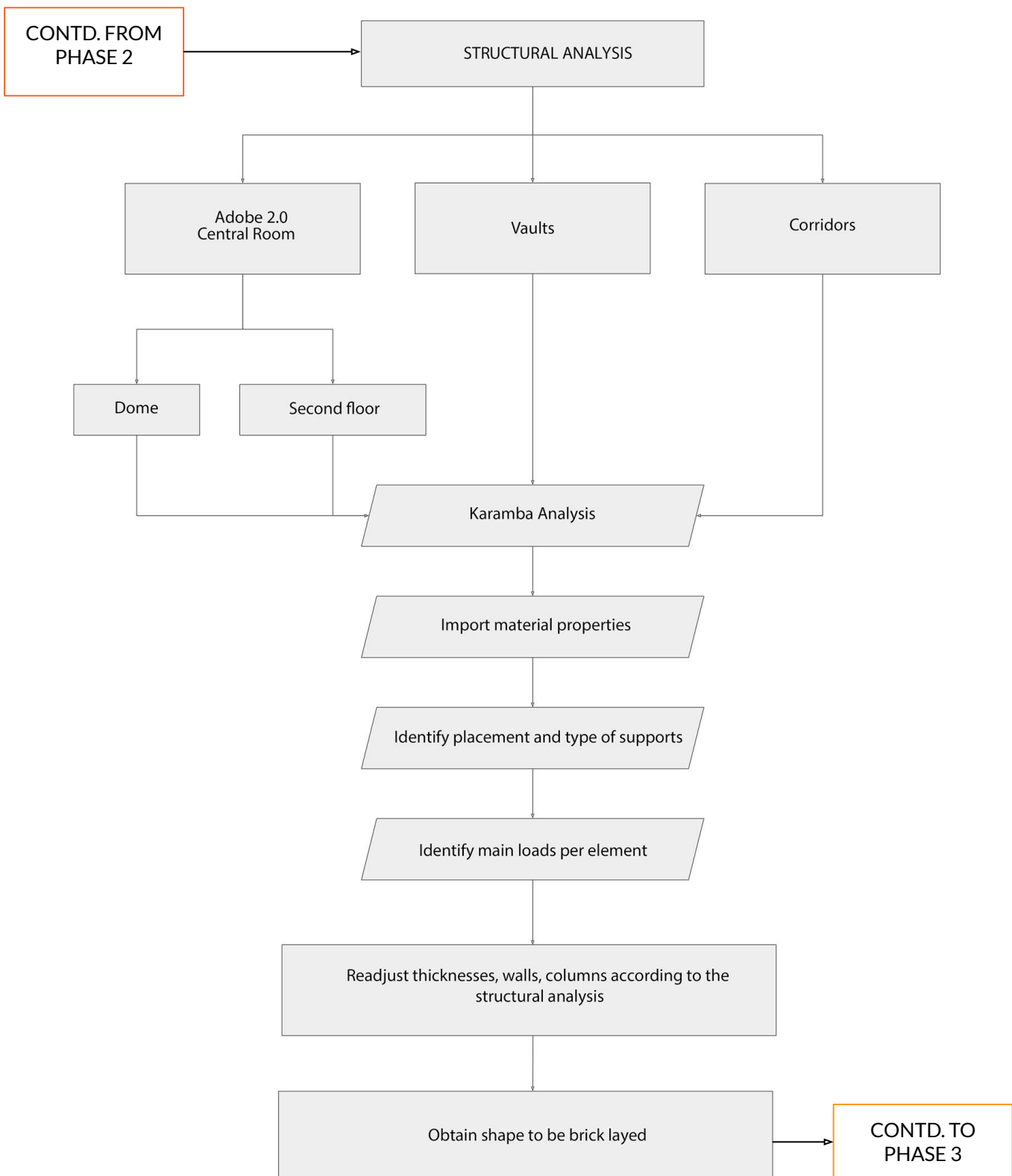


Figure 107: Structural analysis flowchart

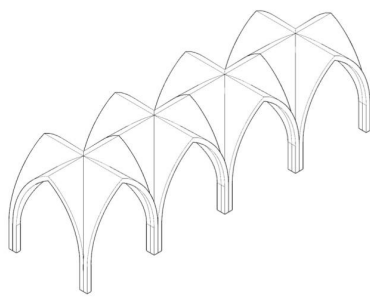


Figure 108: Rib Vault System

## Structural elements

This chapter provides significant information regarding the structural analysis of the building. The structural verification came in several steps as the deformations and the principal stresses have been calculated in each space separately. In order to achieve more accuracy, we designed and simulated three different cases for the corridors, one two-sided vault from the communal department, the dome and the central. The calculations based both in analytical and numerical calculations. For the numerical calculations, Karamba plug-in Rhino Grasshopper has been used. The provided images show explicitly the deformations and the stresses while the kind of the supports is also indicated. An 1.2 safety factor for the gravity and an 1.5 for live loads have been used. Concluding, an optimisation in wall thickness has been achieved.

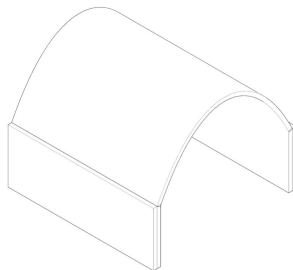


Figure 109: Catenary vault

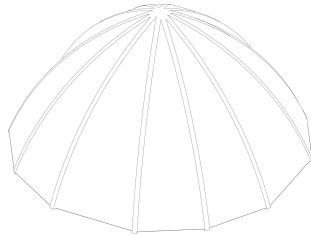


Figure 110: Large Catenary dome

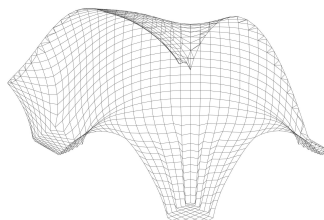


Figure 111:Free form vault structure

## Rib vault openings system

This section presents the three different explorations regarding the corridors in order to achieve the greatest results. The three different cases concern the placement of the openings and in each case the results are presented. As a load combination, the dead load of the structure has been used as the height for wind, sand and snow load is negligible. From the analytical calculations the maximum displacement should not exceed the 1 cm.

More specifically:

$$\text{Deflection limit} = L/250 = 2.6/250 = 1 \text{ cm}$$

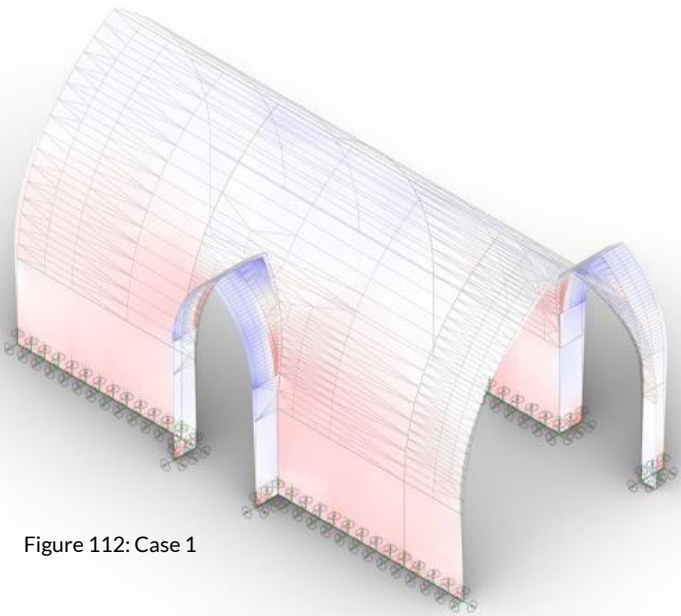


Figure 112: Case 1

### Case 1

The first case concerns the simulated model from the initial plan. The openings of the doors are placed without any structural investigation. Despite this the maximum displacement is **0.52 cm**, below the limit of the 1cm. The blue color presents the achieved tensile stresses while the red the compression ones. The structure is supported with fixed connections to the ground.

Maximum displacement
0.52 cm
Maximum tensile stress
0.090 MPa
Maximum compression stress
0.049 MPa

# Rib vault openings system Karamba analysis

## Case 2

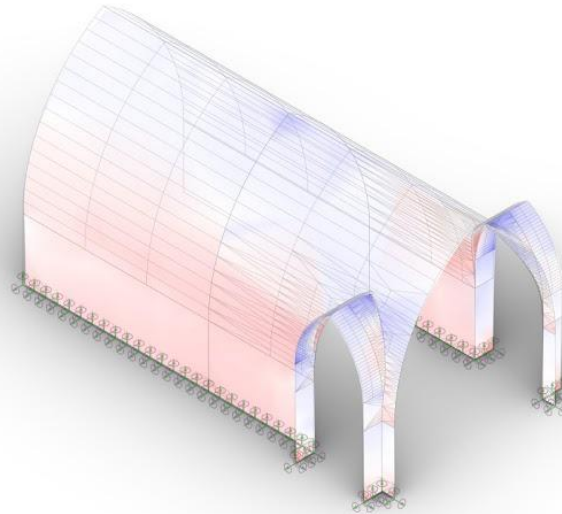


Figure 113: Case 2

The second case concerns the symmetrical placement of the openings. Despite this the maximum displacement is **0.49 cm**, below the limit of the 1cm and slightly better than the first case. Again, the blue color presents the achieved tensile stresses while the red the compression ones. There is no change in the support connections

Maximum displacement
0.49 cm
Maximum tensile stress
0.065 MPa
Maximum compression stress
0.051 MPa

## Case 3

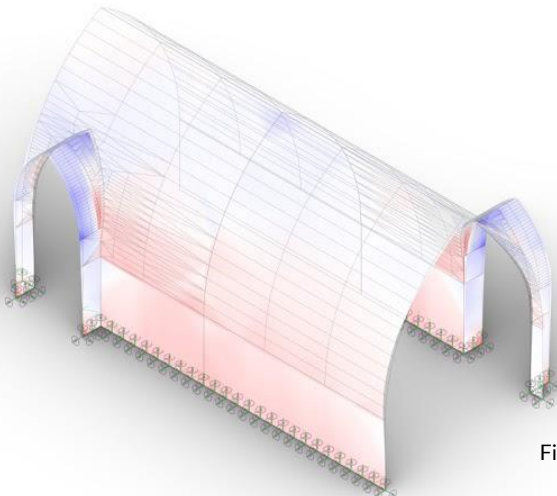


Figure 114: Case 3

The third case and the final chosen one for the building concerns a diagonally opposite placement of the openings. The maximum displacement is **0.47 cm**, below the limit of the 1cm and slightly better than the second case. Again, the blue color presents the achieved tensile stresses while the red the compression ones. There is no change in the support connections.

Maximum displacement
0.47 cm
Maximum tensile stress
0.065 MPa
Maximum compression stress
0.049 MPa

## Numerical calculations

Maximum tensile stress  
0.195 MPa

Maximum compression stress  
0.059 MPa

## Vaults Karamba analysis

This chapter presents the results obtained from Karamba analysis as far as concerned the two-sided vaults both in medical and communal departments. For this reason, two close classrooms from the communal department have been stimulated in Karamba plug-in. From these results, the final thickness of the exterior and interior walls consolidated. As a start the initial thickness of the exterior walls was **0.60m.** and the interior **0.30m.** The plate thickness is considered 0.16cm same as the brick width. Concluding, as a load combination, the dead load of the structure has been used as the height for wind, sand and snow load is negligible.

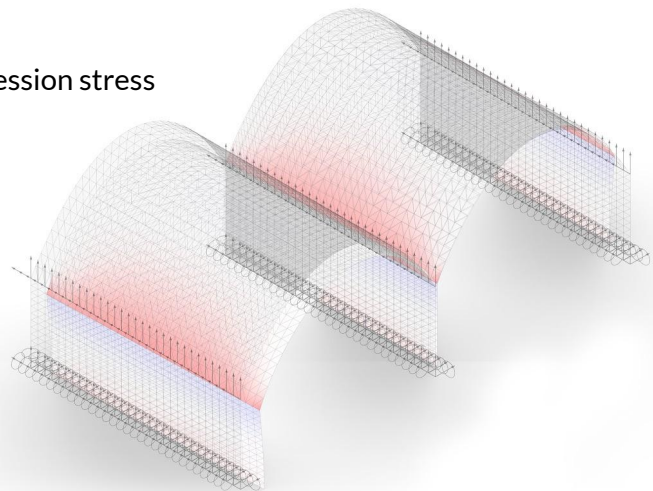


Figure 115: Principal stress representation

Maximum displacement  
1.66 cm

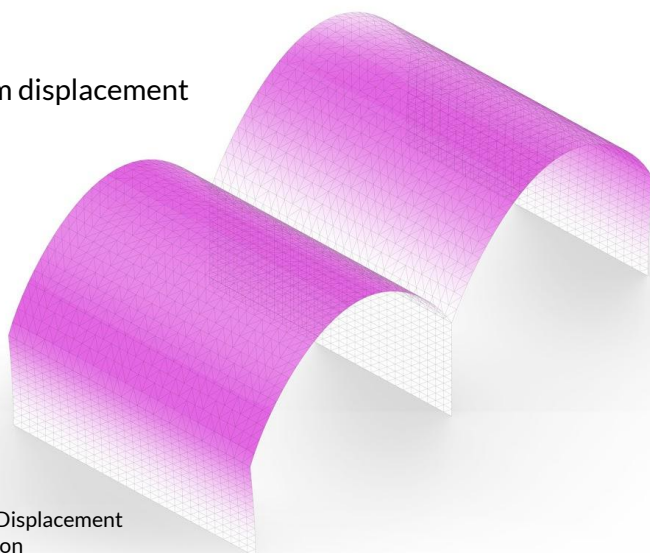
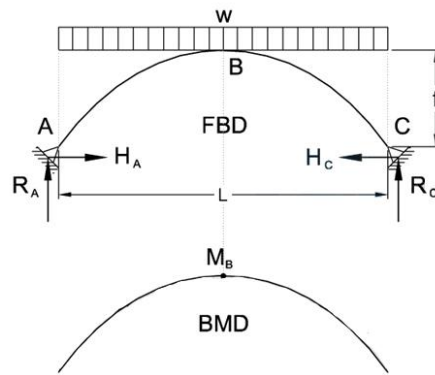


Figure 116: Displacement representation

Walls supports	Tx	Ty	Tz	Rx	Ry	Rz
Vaults-walls connection	-	Ty	Tz	-	-	-

Table 2: Connections and supports used in Karamba analysis



(Figure 116: Two hinged Arch, Source: <http://structx.com/>)

## Dome Karamba analysis

During the analytical calculations the dome has been evaluated as a simple model of two hinged arch with an equally distributed load (weight of the bricks) as it is described in figure 116. The maximum deflection regarding the analytical calculation is 4 cm and more specifically:

In numerical calculations, sand load of 2 kN/m<sup>2</sup> and dead load for the dome have been used. The next table presents the results. The dome is supported on the columns beneath it.

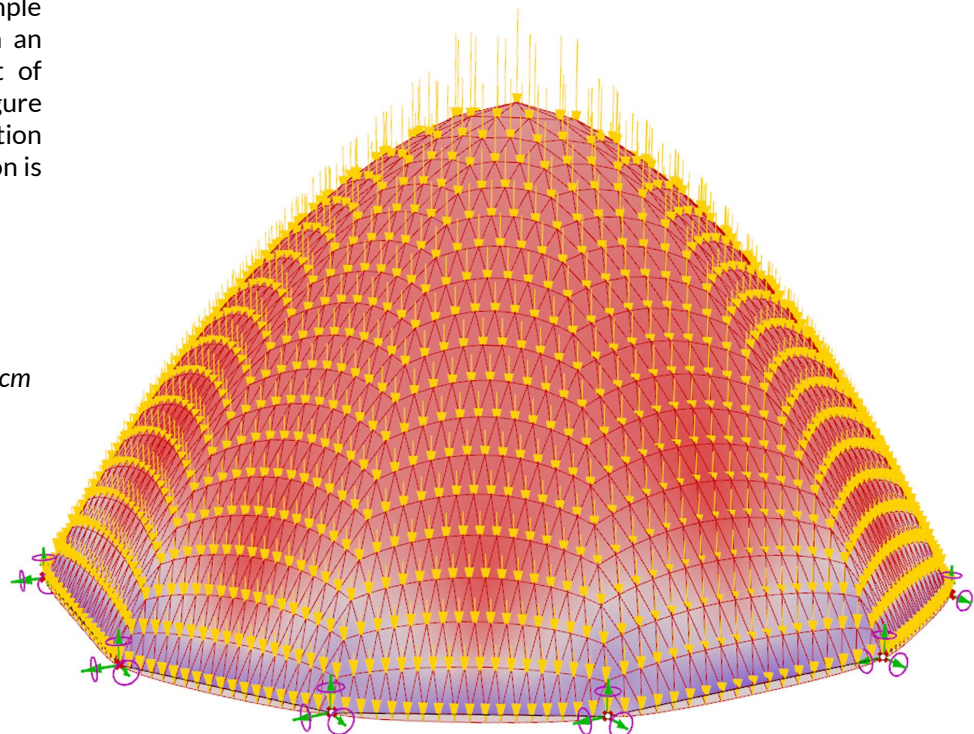


(Figure 117: Forces distribution and displacement in Karamba plug-in)

Maximum displacement LC0: 0.89 cm LC1: 0.47 cm Maximum tensile stress 0.22 MPa Maximum compression stress 0.12 MPa
--------------------------------------------------------------------------------------------------------------------------------------

<b>Load combinations</b> LC0: Gravity LC1: Sand load
------------------------------------------------------------

(Table 3: Results from Karamba analysis)

## Numerical Calculations

Load combinations	Maximum displacement	
LC0: Dead load of dome	LC0: 2.15 cm	
LC1: Dead load of filling	LC1: 0.92 cm	
LC2: Live load	LC2: 0.54 cm	
Maximum tensile stress	Shell	Columns
Maximum compression stress	1.57 MPa	1.02 MPa
	0.91 MPa	2.57 MPa

## Free form vaults (Center room) Karamba analysis

The central building hosting the dome in the middle has been the most challenging part during the structural validation of the building. For this reason, there are three different load combinations used for the final results. The LC0 concerning the dead load of the dome, the LC1 concerning the brick filling between the shell and the ceiling and the LC3 concerning the live load. For the live load a value of 4kN/m<sup>2</sup> was considered. The blue color presents the achieved tensile stresses while the red the compression ones. The maximum tensile and compression stress while also the maximum displacement are indicated in the table below while the range values in Appendix.

Columns supports (ground level)	Tx	Ty	Tz	Rx	Ry	Rz
Shell to column connection	Tx	Ty	Tz	-	-	-
Column to column connection	Tx	Ty	Tz	-	-	-

(Table 4: Support and connection types in the central building)

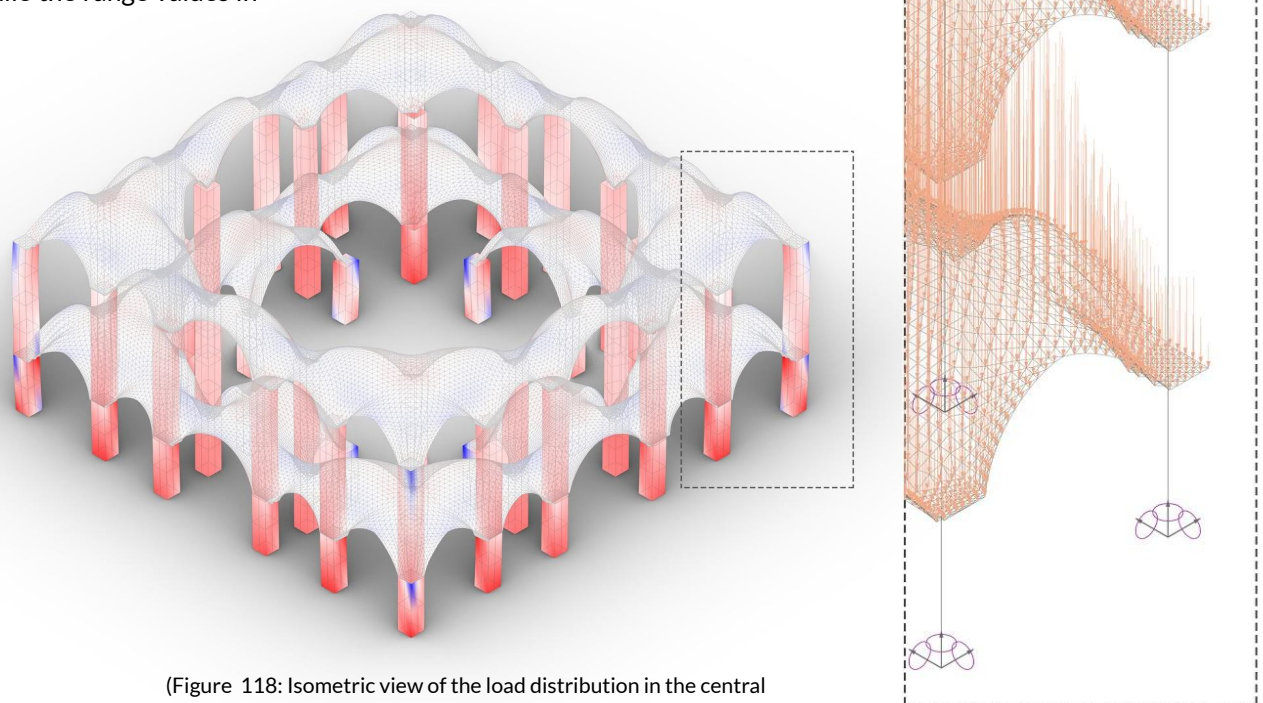
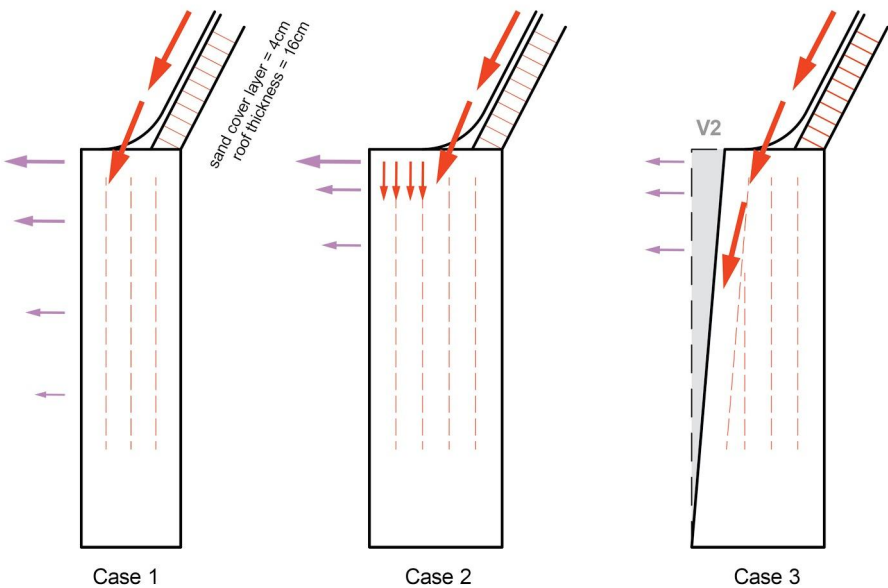


(Figure 118: Isometric view of the load distribution in the central room)



## Load-bearing side walls, optimization

This section presents an attempt to optimise the width of the exterior walls in terms of better distribution of the forces. The Karamba simulation indicated that the exterior walls was necessary to be thicker. The initial width was set as 60cm and the maximum displacement was **2.10 cm**. Case 2 presents the the exterior walls with a thickness of 80cm. From an architectural point of view, so to create a better connection between the walls and the roofs, while the forces will be better distributed, a piece from a mass (Case 3) is formed and placed on the wall (Figure 119).

Thickness **60cm**

Max displacement  
**2.10cm**

Thickness **80cm**

Max displacement  
**1.00cm**

Thickness **60-80cm**

Max displacement  
**~1.70cm**

**V1 > V2**

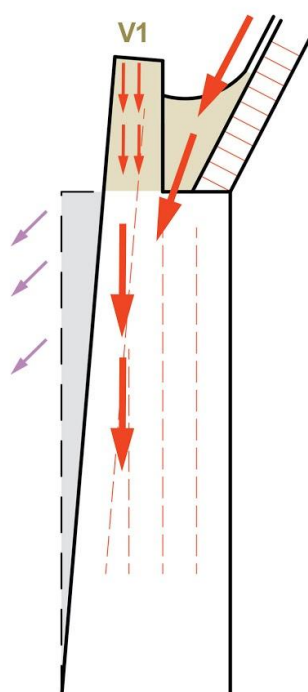


(Figure 119: Optimised exterior wall).

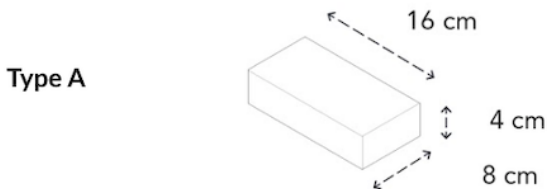
---

# Brick patterning

---

Brick patterning for the dome and free form structures

---



Type A: bricks on the free form vaults of the central room

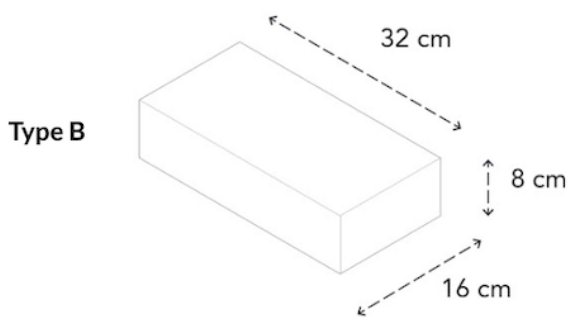
## Brick types

This building is designed to be built only from adobe bricks. For construction, structural and architectural reasons there have been used three different types of bricks in terms of dimensions and patterns. The three types followed the 1-2-4 common proportions.

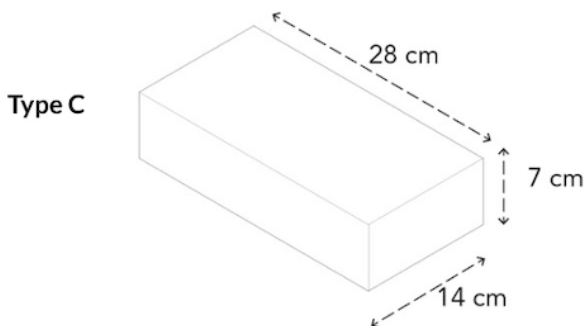
The first type is a 8x16x32 cm brick, predominant in the whole building.

The second type is used to build the vaults in the center room: 4x8x16 cm. This size enables a more accurate form following of the predetermine shapes.

The third type is used to build the columns: 7x14x28 cm. This type's dimensions were adjusted after the Karamba simulation, where the minimum column size was defined.



Type B: bricks on every room (community and medical department)



Type C: bricks in the columns of the central room

## Dome brick pattern

### *Regular geometric mesh*

The first computational approach to determine the brick patterning on the dome shape on top of the central room is made up of regular geometric meshes created with Grasshopper. The aim of this approach was to find one single shape for the bricks.

As a result, it was found that it is not possible to have one single size and shape for all the bricks, therefore this method was eliminated as a methodology to find the pattern.

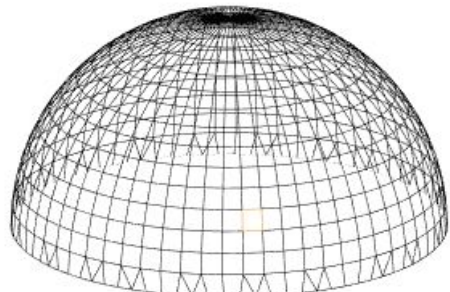


Figure 120 Cuadricular mesh

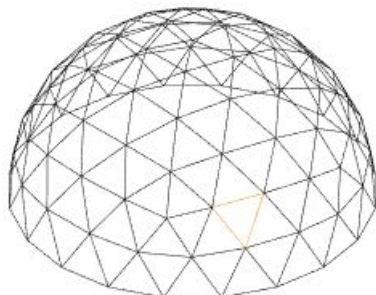


Figure 121: triangular mesh

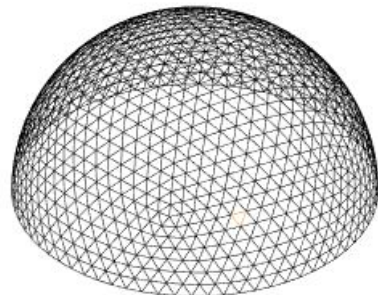


Figure 123: smaller divisions for a triangular mesh

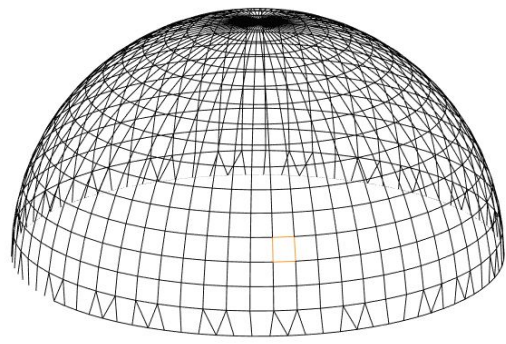


Figure 124: Semi-sphere shape

## Dome brick pattern

### Semi-sphere shape

The second computational approach to determine the brick patterning on the dome is the voxelization method, which converts geometric objects from their continuous geometric representation into a set of voxels that best approximates the continuous object.

With the use of grasshopper, the semi-sphere shape, with a diameter of 10 m, is filled with pixels that have the geometry and dimensions of the bricks that will be used to build the dome.

The first brick pattern used for this method is shown in figure 125 and 126. The final voxelized shape is shown in figure 127 and 128.

As a result, it was found that the brick pattern obtained with this method does not work in the top part of the shape, because the top brick do not have support and float on the air. Therefore, improvements had to be made in order to provide support to every brick that conforms the dome.

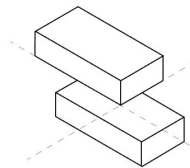


Figure 125: Brick pattern

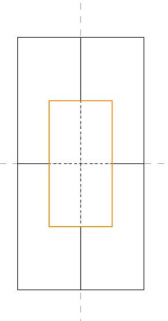


Figure 126: Top view of brick pattern

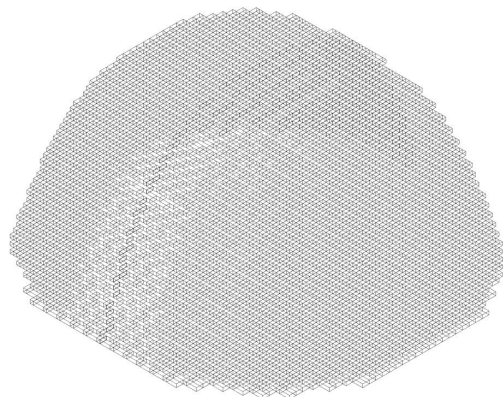


Figure 127: Voxelized shape  
isometric view

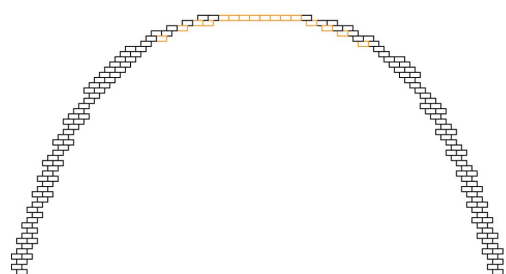


Figure 128: Brick pattern section

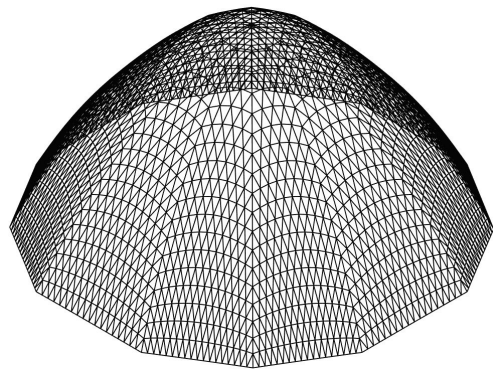


Figure 129: Pointed semi-sphere shape

## Dome brick pattern

### Pointy semi-sphere shape

The shape of the dome is converted into a pointed one to reduce the flattened area on the top part of the dome.

The first brick pattern used for this method is shown in figure 130. The final voxelized shape is shown in figure 132 and 133.

As a result, it was found that the brick pattern obtained with this method has less unsupported bricks on the tip of the dome.

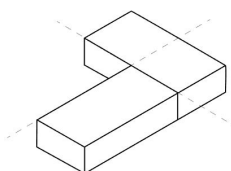


Figure 130: Brick pattern

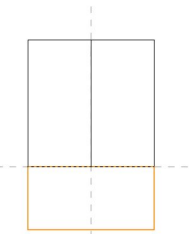


Figure 131: Top view of brick pattern

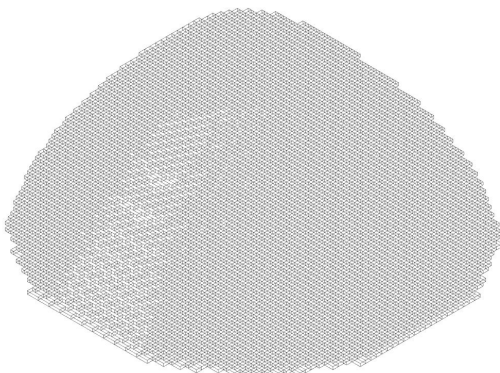


Figure 132: Voxelized shape isometric view

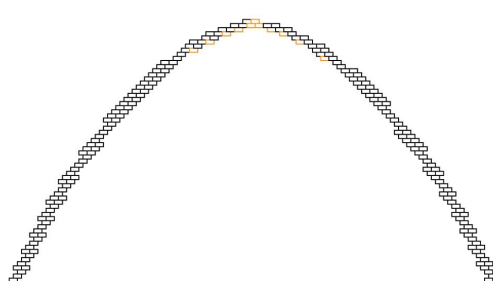


Figure 133: Brick pattern section

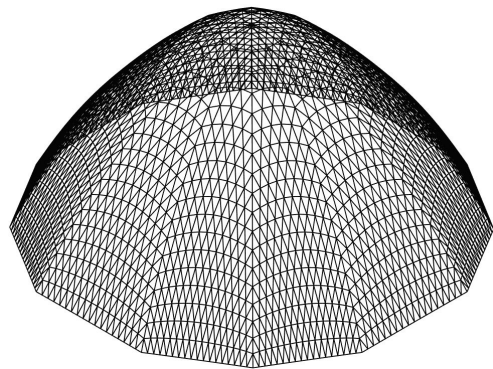


Figure 134: Pointed semi-sphere shape

## Dome brick pattern

### Pointy semi-sphere shape

With the same shape of the dome a second brick pattern is tested to improve the brick layering process to the top of the shape.

The second brick pattern used for this method is shown in figure 135. The final voxelized shape is shown in figure 137 and 138.

As a result, it was found that this brick pattern provides less unsupported bricks on the tip of the dome. This problem can be solved with form-work for only the last five rows of bricks.

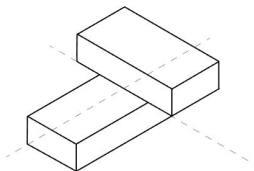


Figure 135: Brick pattern

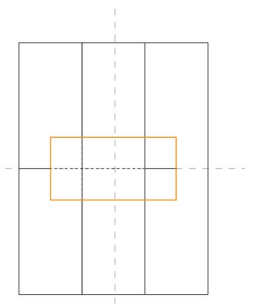


Figure 136: Top view of brick pattern

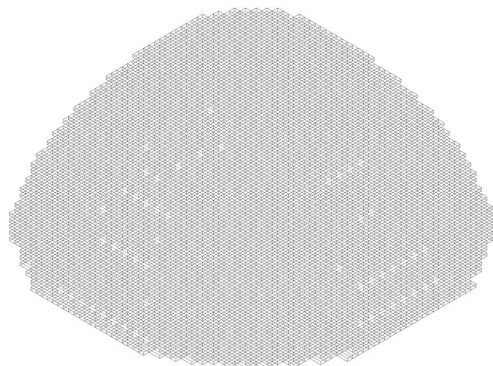


Figure 137: Voxelized shape isometric view

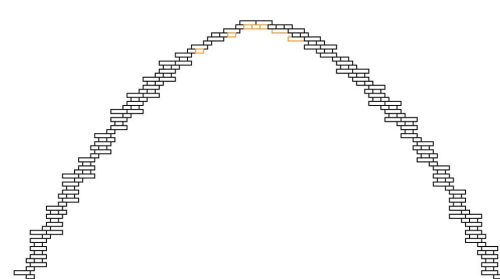


Diagram 5: Brick pattern section

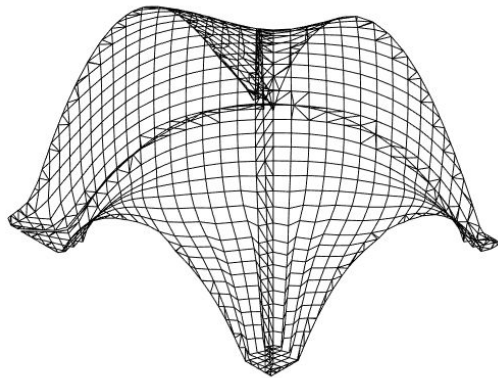


Figure 139: Free form shape

## Free form shape brick pattern 2 directional vaults

The same voxelization method is used to determine the brick pattern on the two directional vaults that support the second floor and dome above the cafeteria space.

The first brick pattern used for this method is shown in figure 140 and 141. The final voxelized shape is shown in figure 142 and 143.

As a result, it was found that the brick pattern obtained with this method does not follow the expected shape of the two directional vaults. Therefore, further tests were made with different patterns to improve this shape.

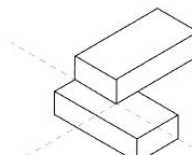


Figure 140: Brick pattern

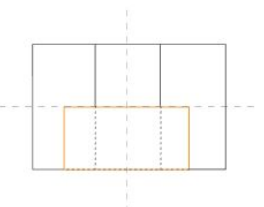


Figure 141: Top view of brick pattern

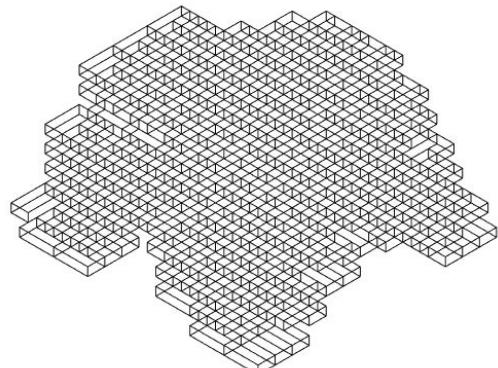


Figure 142: Voxelized shape  
isometric view

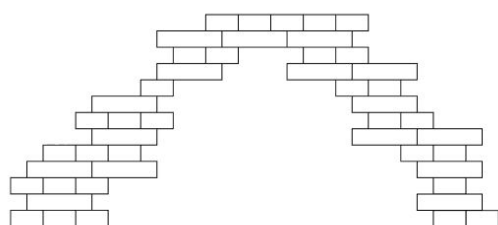


Figure 143: Brick pattern section

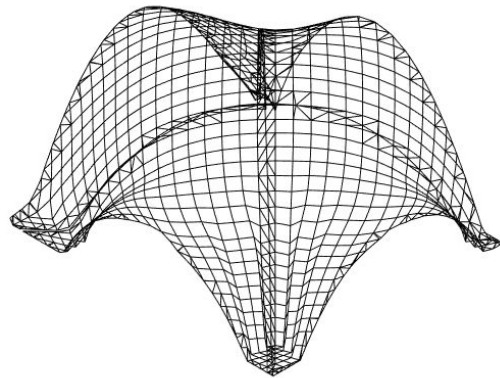


Figure 144: Free form shape

## Free form shape brick pattern 2 directional vaults

The second brick pattern used for this method is shown in figure 145 and 146. The final voxelized shape is shown in figure 147 and figure 148.

As a result, it was found that the brick pattern obtained with brick pattern follows better the wanted shape but in terms of constructability, this method provides more problems than solutions. This will be further discussed in the next section: Constructability.

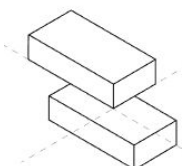


Figure 145: Brick pattern

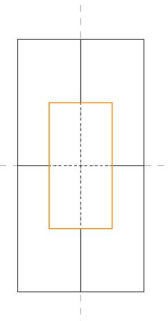


Figure 146: Top view of brick pattern

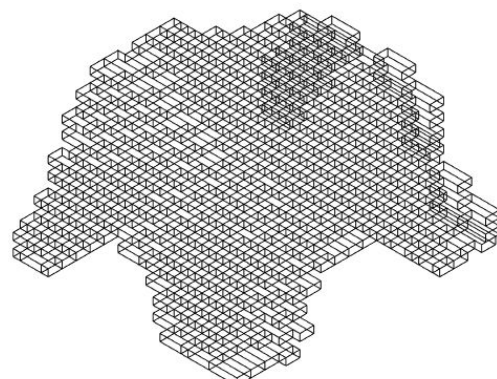


Figure 147: Voxelized shape  
isometric view

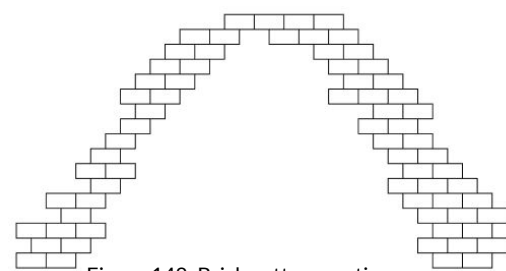


Figure 148: Brick pattern section

## Central room columns

The Karamba analysis indicated that the columns needed to be approximately  $0.40 \times 0.40$  m, so the forces be better distributed.. For this purpose, the brick type used is **Type C**, with an adjusted pattern and dimensions. Diagrams 3 and 4 illustrate the first and the second layer of the pattern which are replicate in vertical direction and attribute the final pattern.

Figure 149, presents an exploded view of the columns and the shell, reflecting the final brick laying in the central room. For the construction of the shell, there is an excessive description in the next chapter.

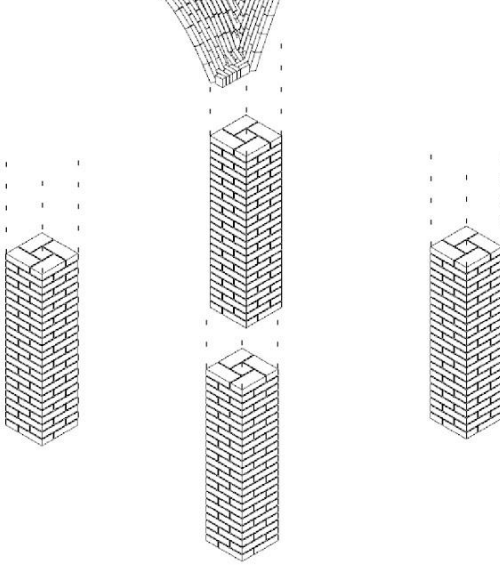
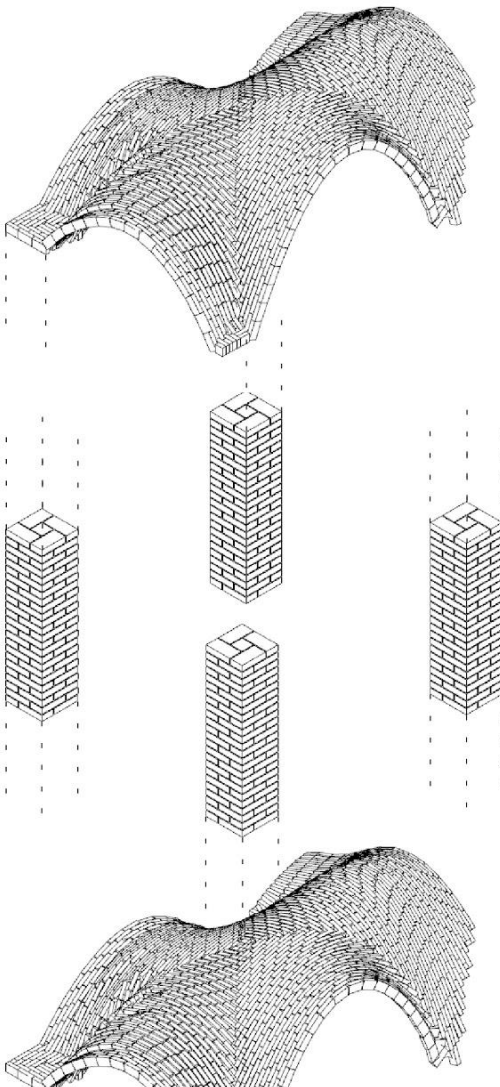


Figure 149: Brick patterning exploded view

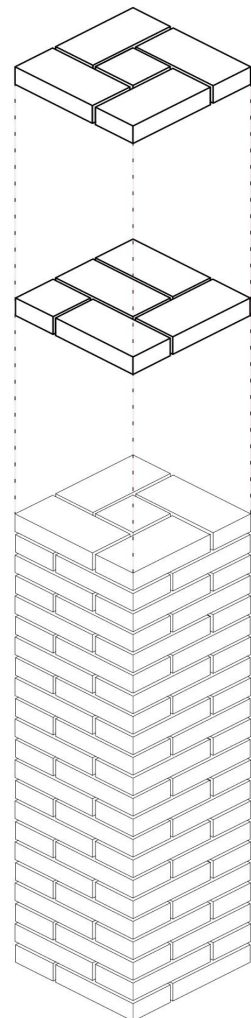


Figure 150: Brick pattern layers

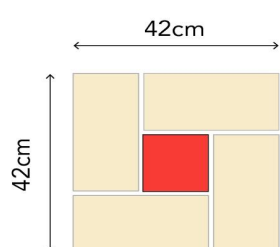


Figure 151: Second layer pattern

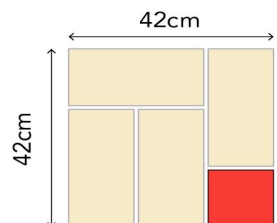


Figure 152: First layer pattern

## Wall patterning

### English bond

The walls in the medical and the communal spaces are constructed with an english bond brick pattern. This specific type was chosen due to its convenience having in mind that the building will be constructed from local people.

These diagrams illustrate the intersection solution in the interior walls and the corner solution.

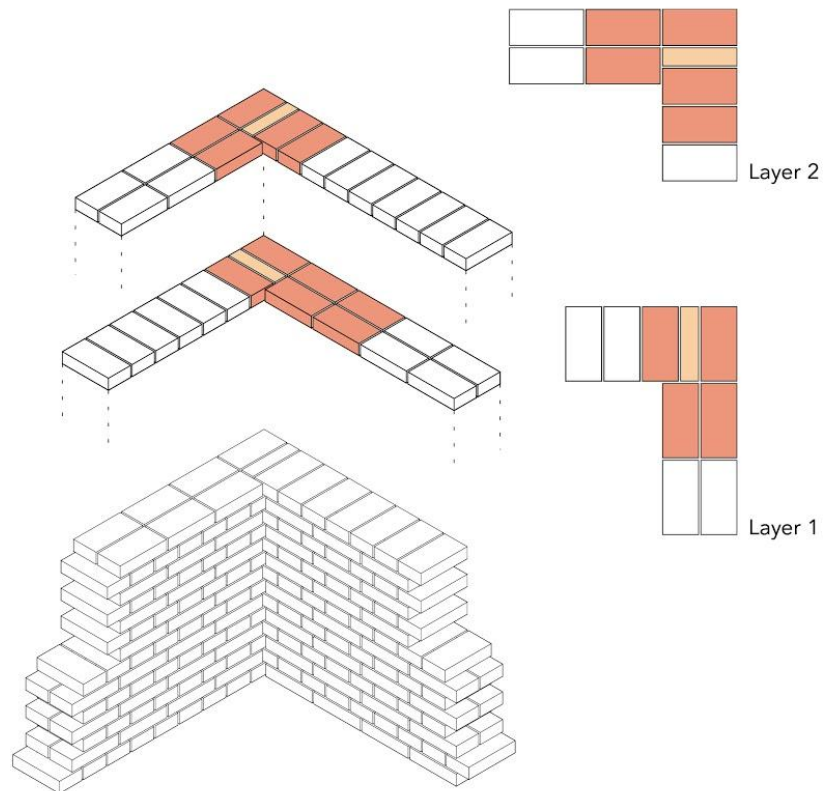


Figure 153: Corner Solution  
Brick dimensions: 08x16x32 cm

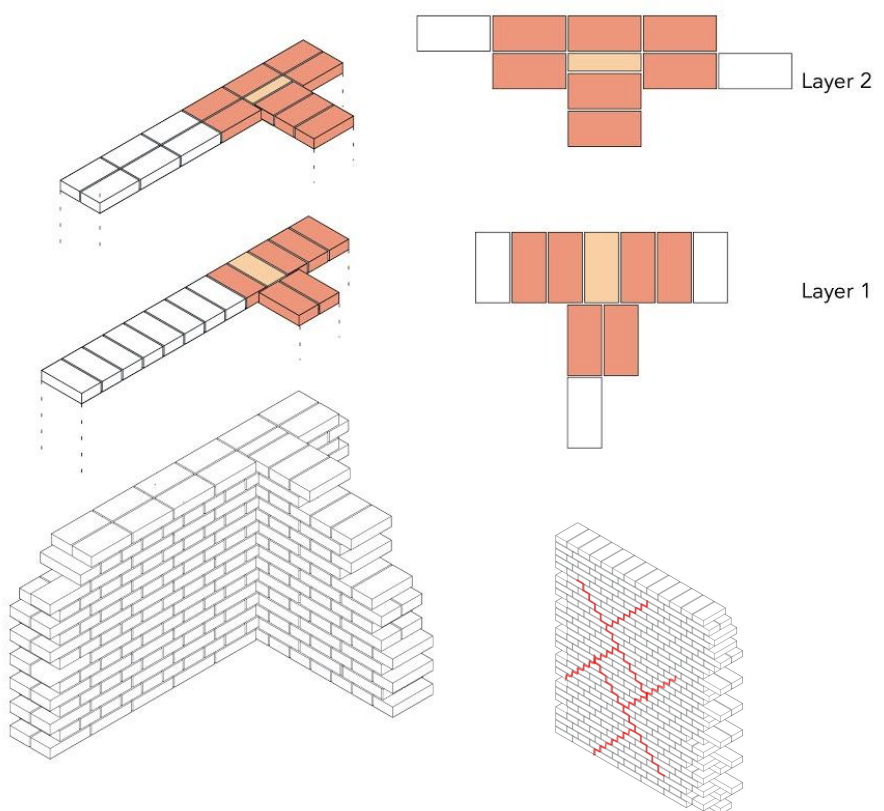


Figure 154: Intersection solution  
Brick dimensions: 08x16x32 cm

Figure 155: Case of failure due to shear stress. Diagonal Cracking.

---

# Constructability

---

Constructability for the dome, vaults and free form  
vaults

---

## Inspiration for construction process

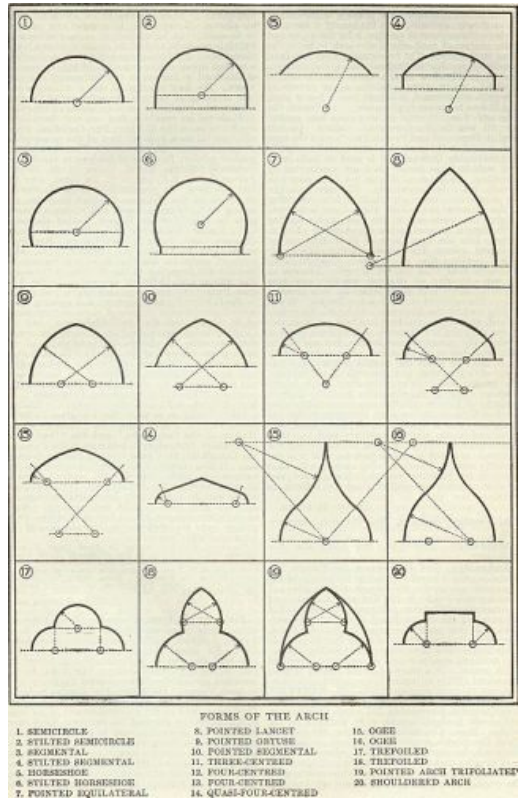


Figure 156: Arch formations

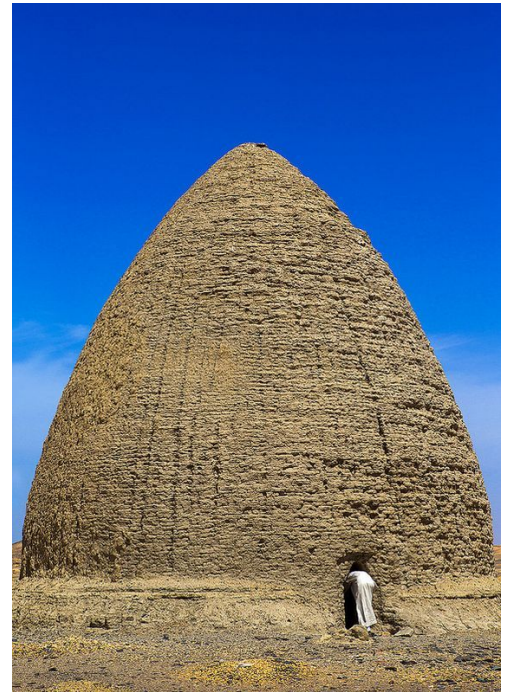


Figure 156: Beehive tombs, Old Dongola, Sudan

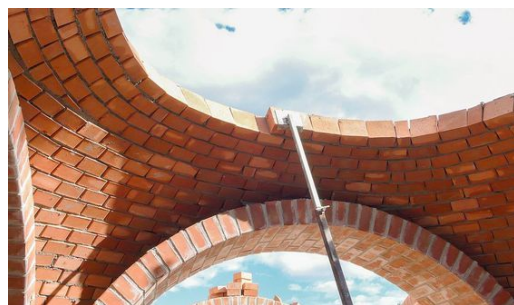


Figure 157: Brick dome construction using compass method



Figure 158: Dome Cupole per Arbitare

## Constructability for computationally generated dome and vault

The first step to devising a construction system for the healthcare and communal center was to derive the initial shaped of the domes and vaults from the form finding process.

Once the forms were finalised via the dynamic relaxation process, the domes and vaults were defined.

Using the dome as a primary example; the initial shape derived from the structural analysis process suggested a dodecagon shape. The shape was then voxelized in order to find patterning for the bricklaying which resulted in a patterning as shown to the left (figure 160 and figure 161). It is evident in the two images that the brick laying after voxelization had little resemblance to a real life construction process. This was mainly due to the bricks being overlapped unevenly, the overlapping of the bricks were not geometric, some bricks in the bottom had less structural integrity because of the way it was selected in the voxelization process and mostly because there was no logical way of expressing the voxelized dome in a construction site in Jordaan.

Due to these obvious limitations it was inevitable that a more logical construction approach was to be adapted into the dodecagon dome realized from the form finding and structural analysis phases.

It was important to the project for all the dome and vault systems to have a logical building approach. This would not only allow for the domes and vaults to be built in an ease, but also for the health and communal facilities to be replicated with ease if this model satisfies the necessary needs of the District 8 as an example.

It was also made necessary that Zaatari refugee camp has very little resources that could help in the building process. Therefore formwork was to be kept to a minimum, and no additional material other than hand made adobe bricks were to be incorporated into the building design and construction itself.

The next few pages of the constructability phase of this report will look into construction methods for the domes and vaults using the compass method shown in figure 162 and geodesic dome design shown in figure 163. These two methods will be used in all the dome and vault structures due to its ease of understanding, minimal use of resources and excellent structural properties.



Figure 159: Dodecagon dome as a result of structural optimisation using Karamba

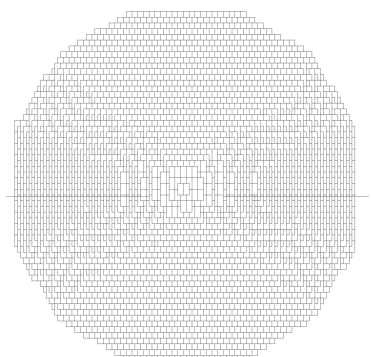


Figure 160: Plan of dodecagon dome after voxelization process



Figure 161: Left view and middle section of voxelized dodecagon dome overlapped with circular geometry

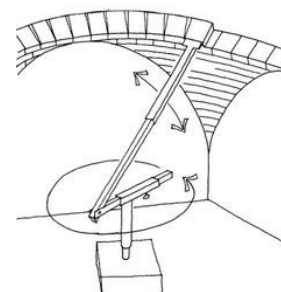


Figure 162: Compass method of constructing geodesic domes

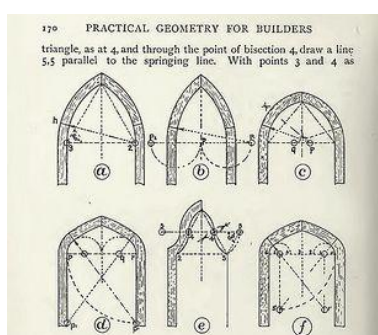


Figure 163: Geodesic dome construction geometry illustrations

## Vault construction systems

Nubian vault systems have been used for vault construction for many years. Mostly because of its structural stability but in this case, mostly because of its construction method that requires little to no formwork. As the bricks are slanted at an angle and supported against the brick wall in the background.

Rib vault systems have been used since the beginning of the 8th century in Islamic architecture. The arches reinforced by a network of adobe ribs filled in with adobe bricks of smaller sizing.

It was of utmost importance that both the systems only required basic support for the catenary arches and the rest to be guided using minimal to no additional material in terms of formwork. Therefore both the vaults have a simple method of construction;

1. Measure and mark point gives as in the geometric diagram (figure 164 & 165).

2. Cut piece of wood according to heights given, to mark the center point of the arches.

3. Build the catenary arches using the compass method and used wood scaffold\*. (figure 167).

4. Build the dome using a filling method and the vault using the nubian system (figure 165 & 166).

5. Plaster over the bricks from the exterior for more bonding.

\*The used wood scaffold would be made out of pieces of wood found on site or provided by an organization for the construction of the women's center.

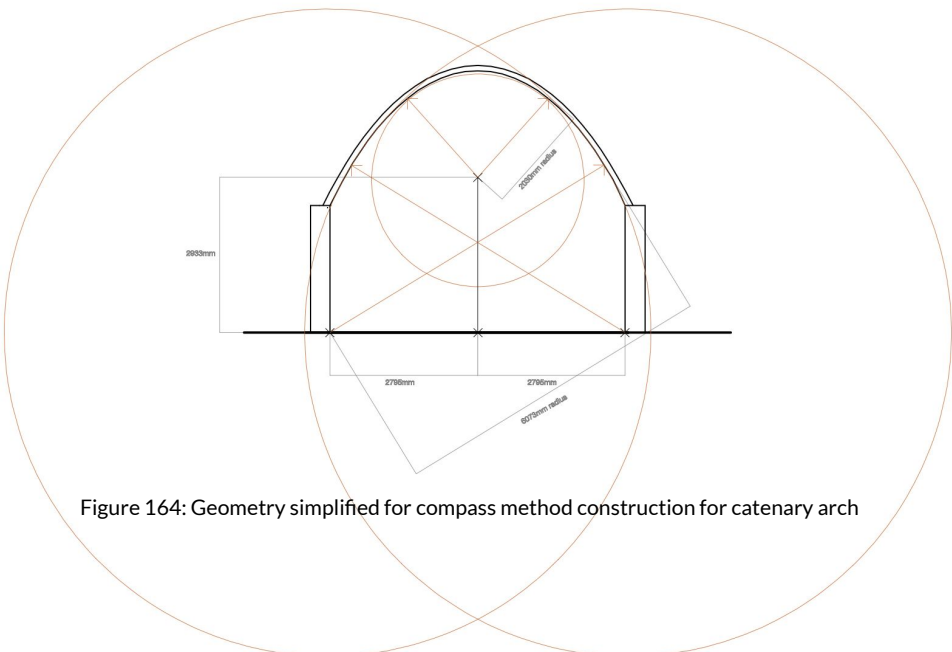


Figure 164: Geometry simplified for compass method construction for catenary arch

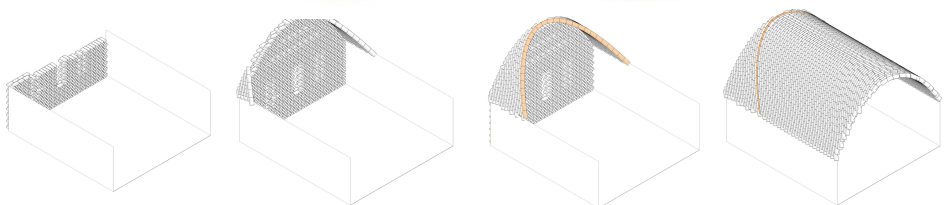


Figure 165: Construction steps for catenary arch with a Nubian vault system

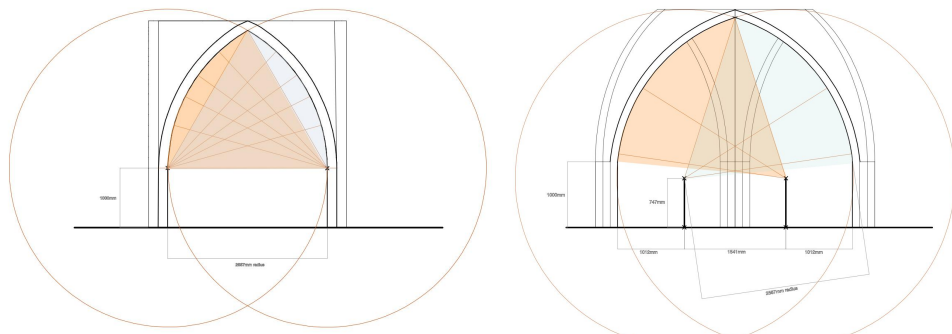


Figure 166: Construction steps for catenary arch for rib vault system

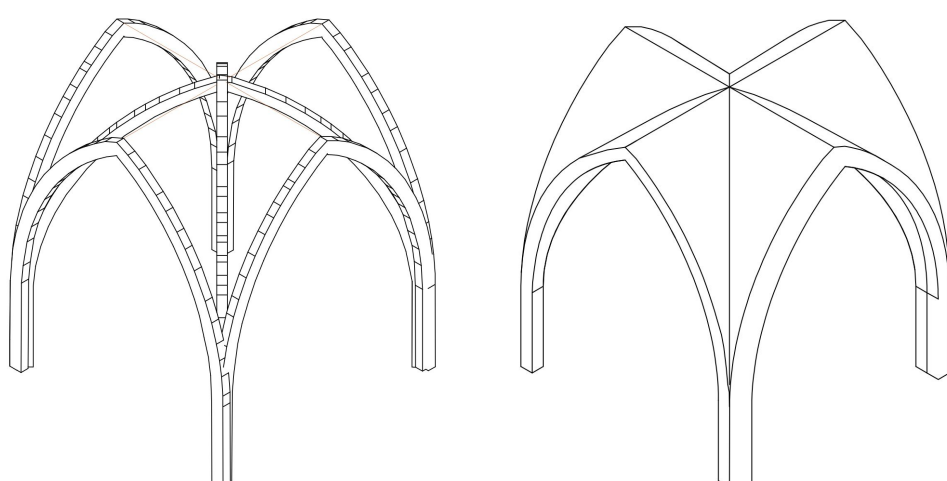


Figure 167: Catenary arch rib system for rib vault

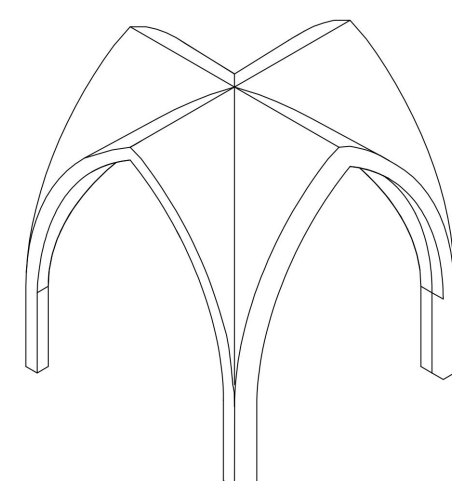
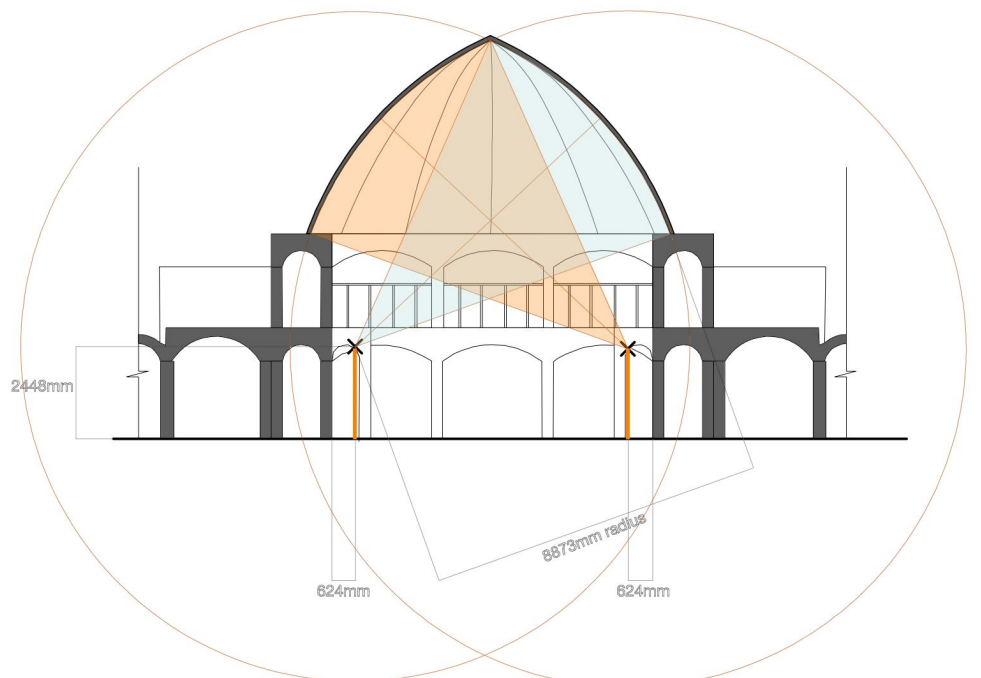


Figure 168: Rib vault with brick filling



## Dodecagon dome construction system

The dodecagon dome was formed as a result of structural analysis and the voxelization method used to figure out the brick organization method. Due to the limitations of the brick laying method as shown in the voxelization process (page 46), a new construction method was to be identified. The following illustrated process is a overlaying of bricks using the aid of the compass system, used since the early times of dome construction.

Steps:

1. Mark and set up the center points.
2. Cut 12 pieces of wood to the given height of the radius posts. Place them on top of the 'X' (measurements given in figure 169 cross section geometry drawing)
3. Start from the bottom and build upwards. Stack the bricks on side 'Z' guided by the compass 'Y' placed opposite to the flat surface. (figure 170)
4. Continue building upwards until center is reached and use dodecagon key stone to hold the dome in place.

Figure 169: Construction steps for catenary arch for dome structure

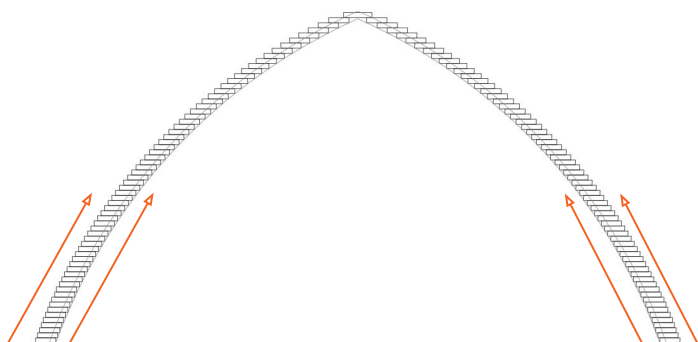


Figure 170 : Section of brick placement for either side of dodecagon wedges

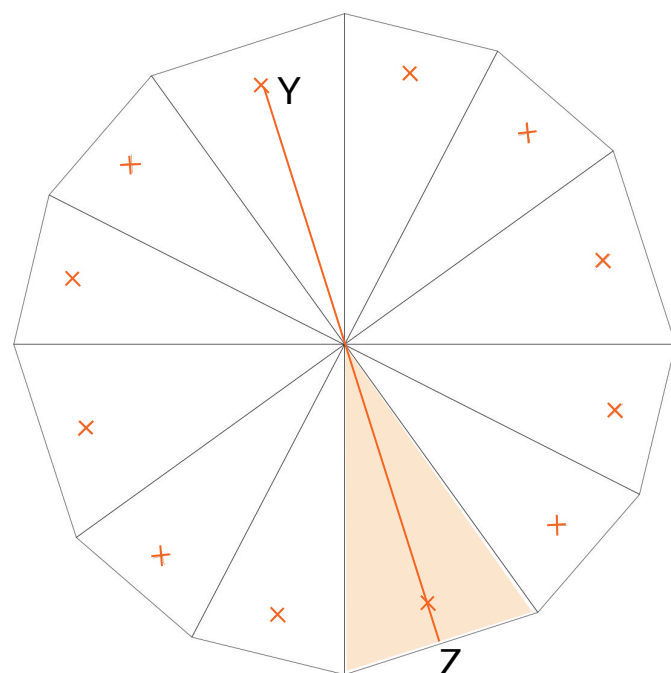


Figure 171 : Placement of compass system 'X' for the opposite wedge of the dodecahedron

# ADOBE 2.0

## Free form vaults

Due to the complexity of the form found using computational methods, it was unrealistic to build the entire structure at once without using scaffolding and formwork for the entirety.

Due to the set out limitations of NO EXTRA MATERIAL AVAILABILITY, the following method tries to construct/mimic the computationally generated shape by dividing the entire form into parts. When looking into detail, the entire structure consists of 4 parts as shown via colour coding. Once a section of the parts are built they will then be replicated in a mirrored form as you may see in figure 172.

Basic form work for the arches will have to be built using available pieces of scrap wood purely to achieve shape until key stone is added.

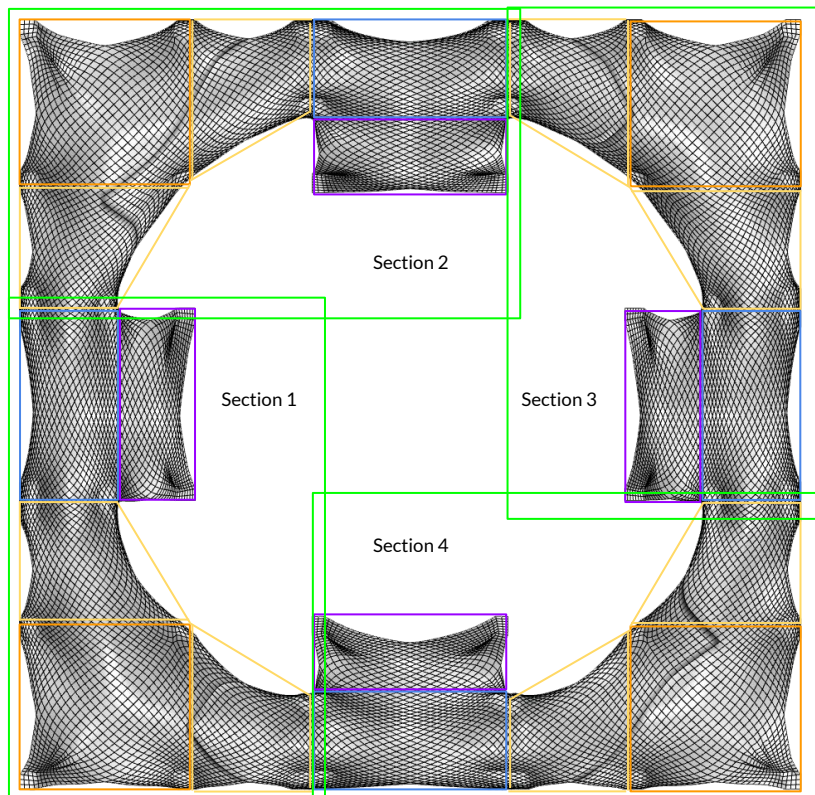
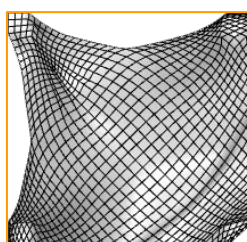
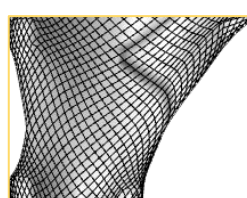


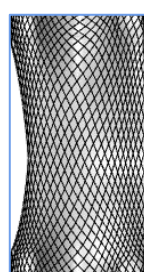
Figure 172: Top view of free form dome structure divided into 4 repeatable shapes and 4 repeatable sections



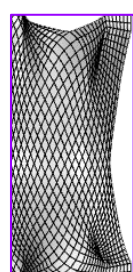
**PART 1**  
Corner dome



**PART 2**  
Joining dome



**PART 3**  
Central dome



**PART 4**  
Balcony support dome

**STEP 1: build arches using a string drawn from the center of the marked circular geometries**

## PART 1 construction process

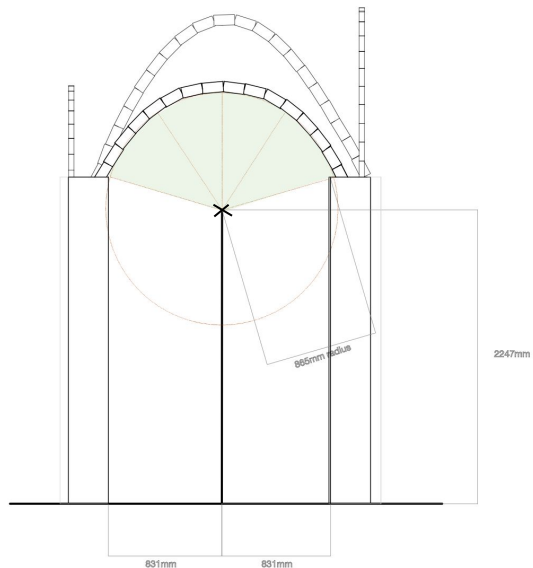


Figure 173:: build 2 main semi-sphere arches using a string drawn from the center of the marked circular geometries

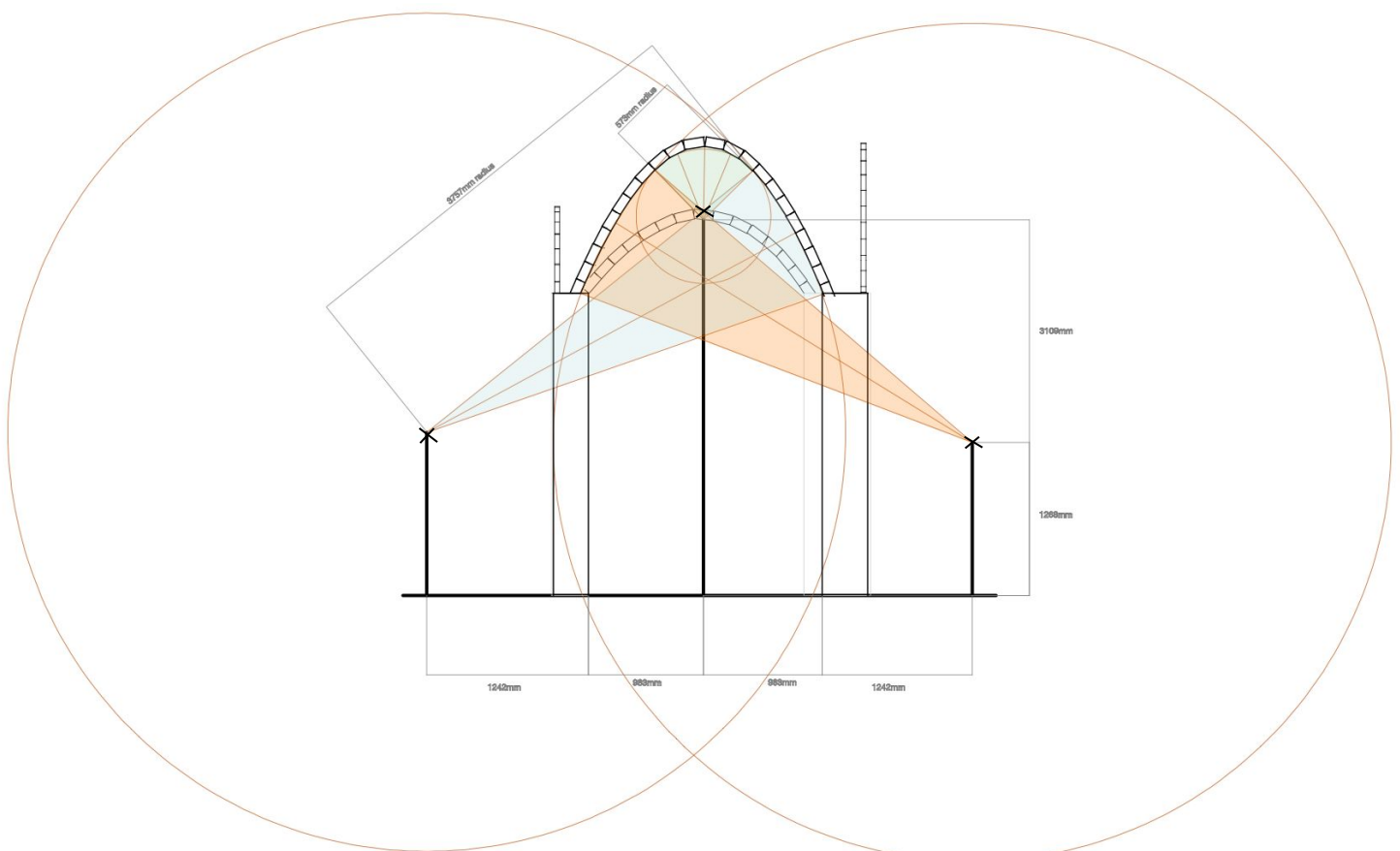


Figure 174: build main 2 catenary arches using a string drawn from the center of the marked circular geometries

**STEP 2: build extruded vaults with direction to the marked mid point at 3 m height**

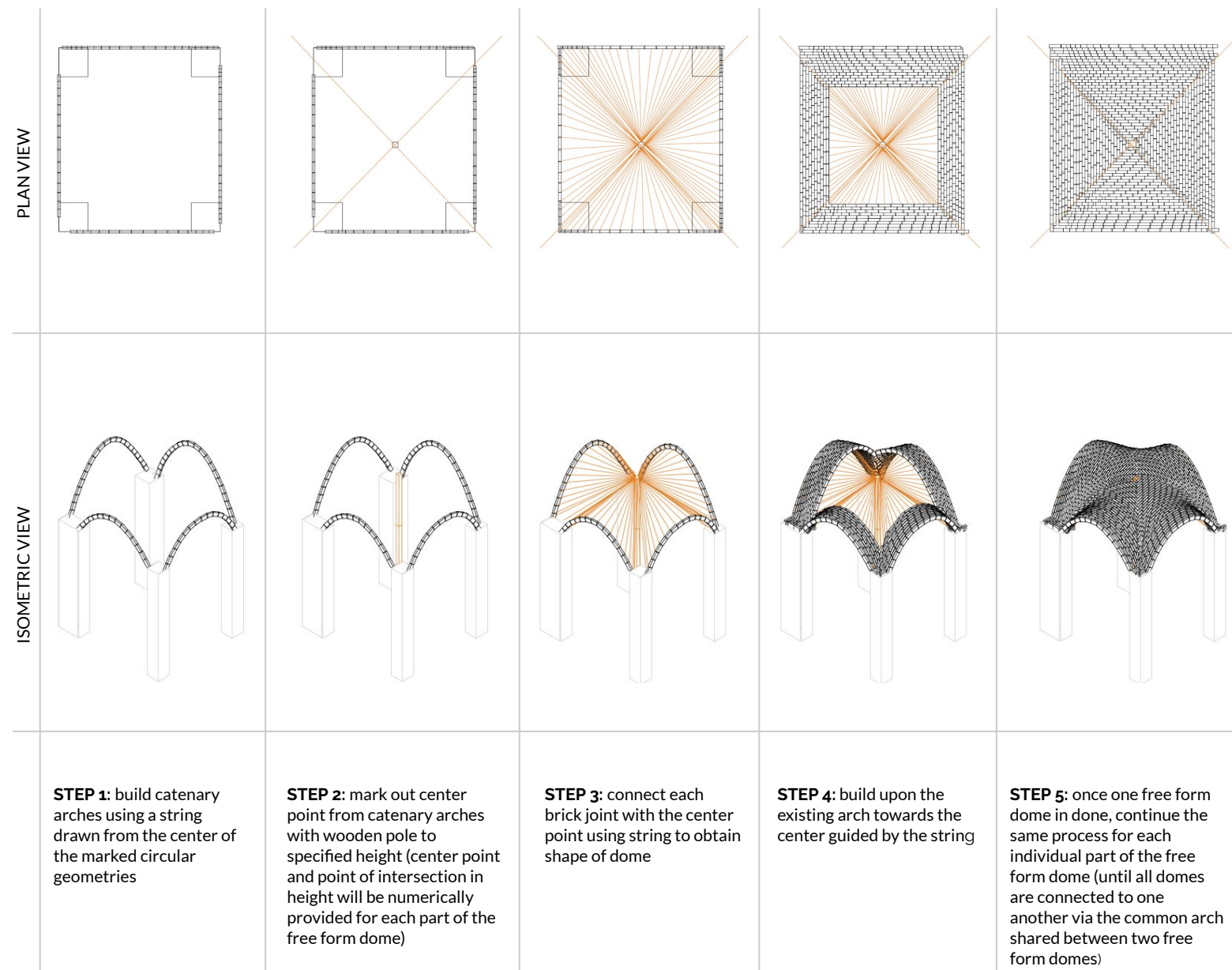


Figure 175: Elevations showing mid point for free from vault

# Conclusions

History has proven that designing and constructing an adobe building with traditional means and materials has always been feasible. Although, designing and predicting the construction of a safe space for women in Za'atari refugee camp through computational designing and coding constitute a quite challenging procedure. During Earthy course, a first configuration regarding the location and the required spaces achieved while the general form finding of the building was developed through computational methods.

## CONFIGURATION

Computational methods were used to study all different types of connections, privacy types and size for each space. After the Space Syntax results, the configuration was made manually considering all different aspects that the computational method was not able to. For example, a grid that would trace the main axes for the structure and space limits; a sun and wind study that provides information for placing different activities with different requirements on a specific location to provide comfort conditions for users; different types of users experiences throughout the building. One of the main purposes of this project is to provide a safe space for women in the Za'atari refugee camp, therefore, privacy and safety were extremely important for the configuration and general design of the building. By doing this, all activities were placed according to a specific private/public condition. For the rooftop typologies configuration, the same grid and space configuration were the main guides to find the best shape according to structural and design requirements.

## FORM FINDING

The form finding of the roofs was completely solved with computational methods, always along with common sense and architectural decisions. During the form finding procedure great outputs emerged regarding the initial tessellation of a mesh. The tessellation has always to follow the form that one desires to achieve as well as the anchored points. A combination of different shapes need to be treated carefully, by being re-divided into shapes sharing equal adjacent edges. In this way the tessellation can easily continue to both shapes generating one welded relaxed mesh.

## ADOBE BRICK TESTING

Cumulative ultimate compressive strength for the smaller compression adobe bricks were of much higher value comparative to the larger sized adobe bricks. The lowest average being for adobe only of 0.7 N/mm<sup>2</sup> with the highest Adobe+rope fiber 3.9 N/mm<sup>2</sup>. Overall the large adobe bricks with rope fiber had a much higher compressive strength compared to the large plain Adobe brick with 3.9 N/mm<sup>2</sup> above necessary for standard codes. In terms of mixture with adobe and an external material, Adobe+rope fiber 10cm had an exceptionally high compressive strength therefore would be the most ideal to use in the construction phase.



## STRUCTURAL ANALYSIS

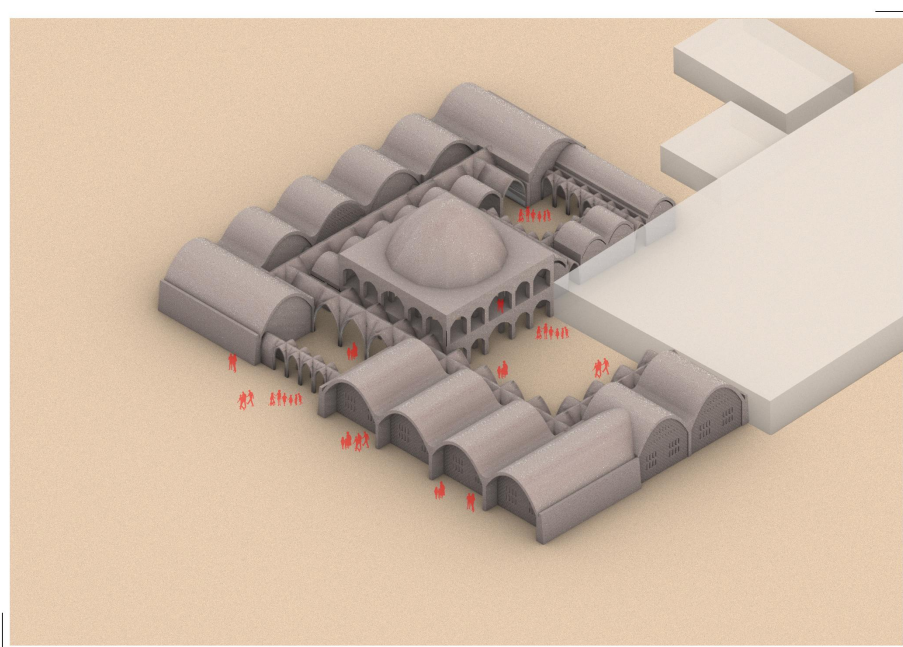
The central room with the dome supporting was quite an intriguing part both in terms of structuring and designing, responding to Adobe 2.0 deservedly. The entire building was structurally analyzed with analytical and mostly numerical calculations, proving with its under the limits from the literature values that adobe is a trustworthy material even in more complex geometries. For the structural analysis, the brick properties of the tested bricks were used in order to analyze in realistic terms.

## BRICK PATTERNING

This project has 4 main shapes to be built as shown in page 46. Each shape presents different conditions and requirements for brick patterning, therefore several computational scripts were made in order to study the best way to find a pattern that follows each shape and provides a better understanding for constructability. The best computational option for the dome shape was the voxelization method. With this option, the final shape was similar to the expected, but for constructability terms, this was not the best option, therefore, in page 67, the construction steps to achieve that form in a more traditional way are shown in detail. For the free form vaults in the center room of the building, the same situation happened. But in this case the voxelization method did not provide a clean shape as the designed one. Thus, a new method of construction, based on a traditional arch and vault construction is shown in detail in page 70.

## CONSTRUCTABILITY

All forms generated computationally were within reasoning and manual inputs throughout the course of design. Because of the consistency in geometry the construction of the basic vaults and dome systems were straight forward and proven by methods used in the past. As a challenge to methods proven since the early 8th Century, the domes supporting the central room were designed as a free form dome system. Designing for material limitation on site other than those for adobe bricks was indeed a very big challenge we accepted to design around. Therefore all domes and vaults were designed to be built using minimal foam work, a pole to mark the center of each radius guiding the shape of the dome using string. The challenge being addressed, it is important to remember the limited material strength of adobe bricks itself, if or when a structure such as this will be built on site at Zaatari Refugee camp in Jordan.



# references

1. M. Gernot (2006), *Building with Earth, Design and Technology of a Sustainable Architecture*.
2. Nourian P, Rezvani S, Sariyildiz S. *Designing with Space Syntax, A configurative approach to architectural layout, proposing a computational methodology*.
3. Nourian P. (2019), *Configurative Design Computational Space Planning, Layout, and Form-Finding in Architecture*, DOI: 10.13140/RG.2.2.26063.94880/
4. Image, page 32 of constructability, *Practical Geometry for Builders and Architects*. (2019). Flickr. Retrieved 30 October 2019, from <https://www.flickr.com/photos/revivaling/4998479748/>
5. UNHCR (March 2019), Jordaan Zaatri Refugee camp fact sheet, Retrieved 15 October 2019, <http://data.unhcr.org/syrianrefugees/regional.php>

# Appendix

## **AR3B0II EARTHY (2019/20 Q1)**

### **Brick Testing Report**

**Group 7:**  
**Amelia Tapia**  
**Iro Stefanaki**  
**Grammatiki Dasopoulou**  
**Nayan Herath**  
**Ioannis Tsionis**

**October 2019**

**Table of contents**

- 1. Introduction**
- 2. Objectives**
- 3. Methodology**
  - 3.1. Brick making procedure
  - 3.2. Additional material
    - 3.2.1. Sample small compression specimens
    - 3.2.2. Sample large compression specimens
  - 3.3. Method of strength test
  - 3.4. Equipment and software used
- 4. Results for each category**
  - 4.1. Estimation of ultimate strength per category
  - 4.2. Estimation of safe design strength per category
  - 4.3. Cumulative ultimate strength for different compositions and dimensions
  - 4.4. Young's modulus
- 5. Discussion of reliability of the data**
  - 5.1. Analysis of the data
  - 5.2. Compare with standard/ other source strength values
- 6. Conclusions**
- 7. Recommendations.**
- 8. References**

# 1. INTRODUCTION

The following report is a study of the making and testing of adobe earth bricks for the "Earthy" design studio with the aim of designing and engineering earthy buildings for betterment of a district of the Al Zaatri Refugee Camp in Jordan.

Different types of adobe bricks will be tested by its individual material strength and dimensions. Bricks will be hand made according to one mould with pure adobe mix and more with the addition of extra materials to the mix.

The mixture of adobe and the additional materials used were chosen according to the site specific nature of Zaatari Refugee Camp in Jordan. It is of dry arid desert climate with a maximum of 34°C in summer (2019 August warmest) to a minimum of 7°C in winter (2019 January coolest) (1). In order for the following bricks to be made in Zaatari Refugee Camp, the additional materials used need to be sourced locally. Therefore all materials chosen for use, will be similar or the same material readily available in the region of Mafraq, Jordan.

# 2. OBJECTIVES

The objectives of this study were:

1. Make adobe bricks combined with different types of materials that can be found around the area of the Zaatari Refugee Camp, in Jordan.
2. Test the adobe bricks, with 6 different types of mixtures and 2 different sizes, to determine their compressive strength.
3. Compare between the different mixtures and same size samples to determine the highest compressive strength.

# 3. METHODOLOGY

## 3.1 Brick making procedure

Available Material/ resources for basic brick mixture:



Clay  
Coarse Sand  
Fine sand  
Water  
Mixing tubs  
Buckets  
Mixer  
Moulds  
Scale

## Mixture and samples made:

Mixture ratio:

30% clay, 30% fine sand, 40% coarse sand, 10% water for total weight of dry mixture.

Samples to be made:

1. small compression specimens of adobe only
2. small compression specimens of adobe with additional material mix
3. large compression specimens of adobe only
4. large compression specimens of adobe with additional material mix

## 3.2 Additional materials used

Additional material chosen to be incorporated into adobe bricks:

1. *Straw*



2. *Wood chips*



3. *Coconut fiber brush fill* (to mimic animal hair)

Why use coconut fiber brush fill material? Coconut fiber: Stiffer and more durable material with resistance to water up to a certain extent. Coarseness and water resistance gives the material great friction



4. **Natural leaves, partially dried**



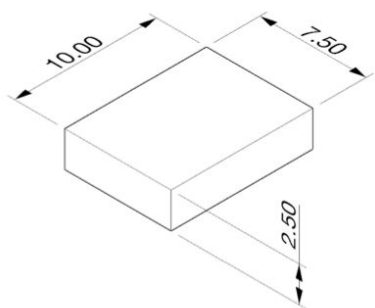
5. **Rope natural fiber 10cm**

6. **Rope natural fiber 40cm**

Type and advantages of natural rope material: TAMPICO: Produced in Mexico from the stalk of the Agave plant. It has a soft to medium texture and is off white in color. It is heat, alkali, and acid-resistant. The porous fibers absorb water and work wet or dry. Heat distortion temperature is 283° F.

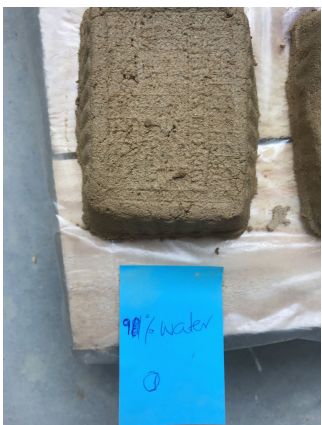


### 3.2.1 Compression specimens, small samples



Sizing in cm for small compression brick

**Sample 1S:** Adobe only, small compression



Mixture:

1st batch

30% fine sand

30% coarse sand

40% clay

10% water

**Sample 2S:** Adobe + wood chips



Mixture:

1st batch

30% fine sand

30% coarse sand

40% clay

10% water

To make 1 part;

Use 1 part wood chips

**Sample 3S:** Adobe + straw



Mixture:

1st batch

30% fine sand

30% coarse sand

40% clay

10% water\*

To make 1 part

Use 1 part straw

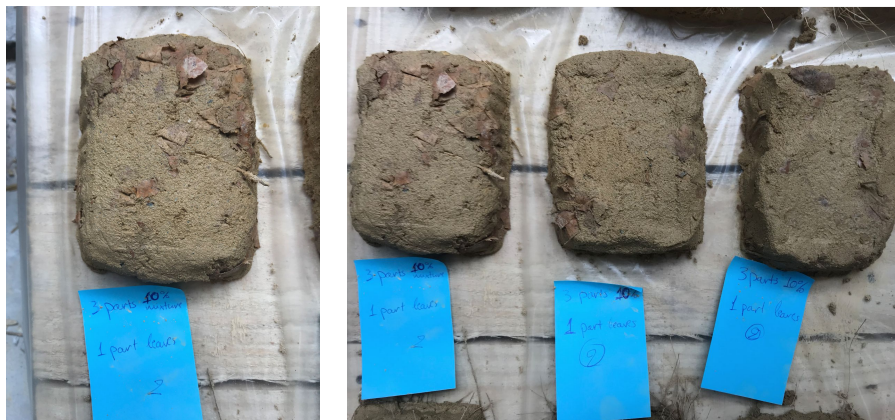
(\*Mixture needed to be slightly more moist compared to the previous tests because of the dry nature of the straw.)

#### Sample 4S: Adobe +natural/vegetable fibre brush fill



Mixture:  
1st batch  
30% fine sand  
30% coarse sand  
40% clay  
10%water  
To make 1 part  
1 part natural fiber

#### Sample 5S: Adobe + Leaves



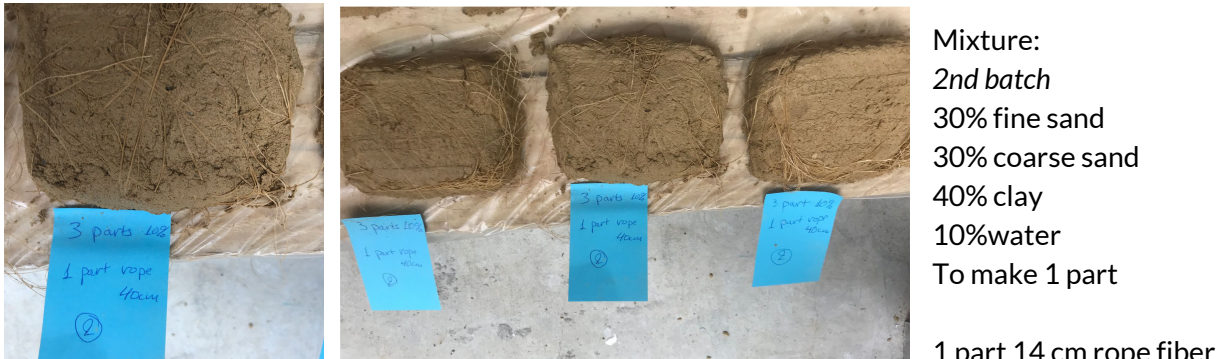
Mixture:  
2nd batch  
30% fine sand  
30% coarse sand  
40% clay  
10%water  
To make 1 part  
Use 1 part leaves

#### Sample 6S: Adobe + rope fiber 10 cm

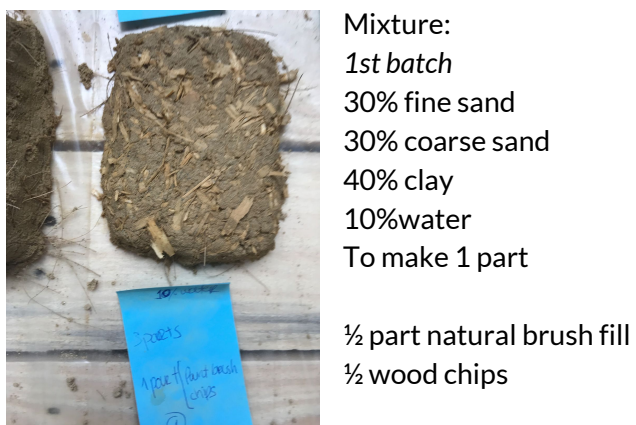


Mixture:  
2nd batch  
30% fine sand  
30% coarse sand  
40% clay  
10%water  
To make 1 part  
1 part 10 cm rope fiber

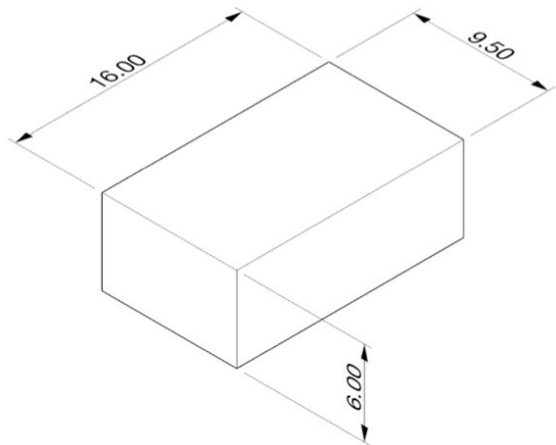
**Sample 7S: Adobe + Rope fiber 40 cm**



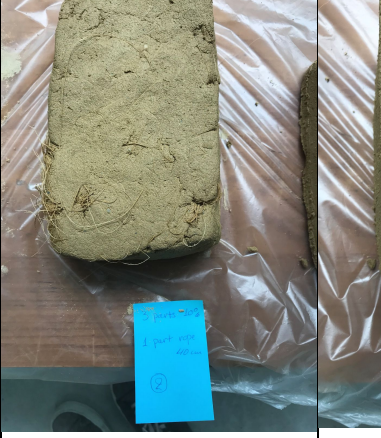
**Sample 8S: Adobe + natural brush fill + wood chips**



### 3.2.2 Compression specimens, large samples



Sizing in cm for large compression brick

Sample 1L	Sample 2L	Sample 3L	Sample 4L
			
3 px 1 part 40cm rope fiber	3 parts only adobe mix	3 parts adobe mix 1 part natural paint brush fill	3 parts adobe mix 1 part straw

### 3.3 Equipment used

Adobe brick making:

Adobe bricks were made using an industrial-strength mixer while all the raw material was measured manually using a floor scale. After mixing all the material using an industrial mixer, the adobe was filled into the moulds manually and compressed manually then removed from the mould and placed on a flat surface to dry.

#### **Adobe brick compression testing:**



A Zwick z100 machine, as shown to the left, was used in order to determine the compressive strength of the different samples of the hand-made adobe bricks. The machine is able to do static tensile tests of any materials at room temperature. It was set with a maximum elongation of 12 mm for the small samples and 15 mm for large samples.

## **3.4 Method of strength test**

Using the A Zwick Z 100 machine, each brick was individually tested for its compression, to determine how a product or material reacts when it is compressed, crushed or flattened by measuring fundamental parameters that determine the specimen behavior under a compressive load. Because adobe bricks (without the use of other reinforcement material) will have mainly compression, maximum force until breaking point (N), elongation (mm), compression strength (N/mm<sup>2</sup>) were recorded.

Each brick was tested individually under a maximum of 100000N compression machine until breaking point, removed, and the next placed.

# 4. Results and comparison

## 4.1 Results of ultimate strength per category

The following table shows the results of compression test conducted using the A Zwick Z 100 machine. The results are grouped according to the type of mixture and added material in it. Minimum of 3 tests of each material mix was tested. From the tests averages were identified.

Sample	Length h (mm)	Width (mm)	Height (mm)	Force (N)	Elongation (mm)	Compressive strength (N/mm <sup>2</sup> )	Average value
Adobe only							
1S1	100	75	25	38700	12	5,2	4,9
1S2	100	75	25	84000	12	11,2	
1S3	100	75	25	15700	12	2,1	
1S4	100	75	25	13700	9,5	1,8	
1S5	100	75	25	52000	12	6,9	
1S6	100	75	25	15000	12	2,0	
Adobe + wood chips							
2S1	100	75	25	56700	12	7,6	6,6
2S2	100	75	25	38300	12	5,1	
2S3	100	75	25	52500	12	7,0	
Adobe + straw							
3S1	100	75	25	78600	12	10,5	8,6
3S2	100	75	25	47600	12	6,3	
3S3	100	75	25	66700	12	8,9	
Adobe + coco fibres							
4S1	100	75	25	67800	12	9,0	11,1
4S2	100	75	25	92400	12	12,3	
4S3	100	75	25	89900	12	12,0	
Adobe + leaves							
5S1	100	75	25	36300	12	4,8	5,7
5S2	100	75	25	51100	12	6,8	
5S3	100	75	25	40100	12	5,3	
Adobe + rope fiber 10cm							
6S1	100	75	25	97600	12	13,0	12,2
6S2	100	75	25	89000	12	11,9	
6S3	100	75	25	89000	12	11,9	
Adobe + rope fiber 40cm							
7S1	100	75	25	91000	12	12,1	10,3

7S2	100	75	25	52700	12	7,0	
7S3	100	75	25	89000	12	11,9	
Adobe + coco fibres + wood chips							
8S	100	75	25	24400	6	3,3	
Large samples							
1L (40cm rope fiber)	160	95	60	58800	15	3,9	2,3
2L (adobe only)	160	95	60	11100	15	0,7	
3L (adobe + coco fibres)	160	95	60	40600	15	2,7	
4L (adobe + straw)	160	95	60	27500	15	1,8	

## 4.2 Estimation of safe design strength per category

In this study, the safe design factor is what each sample is required to be able to withstand. This design factor is defined for a specific application: earthy construction of a parametric designed building for the Zaatari refugee camp in Jordan. The design factor is generally provided in advance and often set by regulatory building codes or policy. For this study, a standard code from Peru is used, as this country has experience with adobe brick constructions and is based on similar conditions as the Zaatari camp, for example, probability of earthquakes. According to the technical construction standard in Peru (Adobe Code E.080) (3), the standard compressive strength of the unit must be minimum 1.2 N/mm<sup>2</sup>.

As shown in chapter 4.1 of this document, all small samples show a higher compressive strength than the minimum standard for adobe brick construction. For the large samples, only the adobe-only mixture do not comply with the minimum standard. The rest of the three different mixtures for the large samples show a higher strength than the minimum to be achieved for construction purposes.

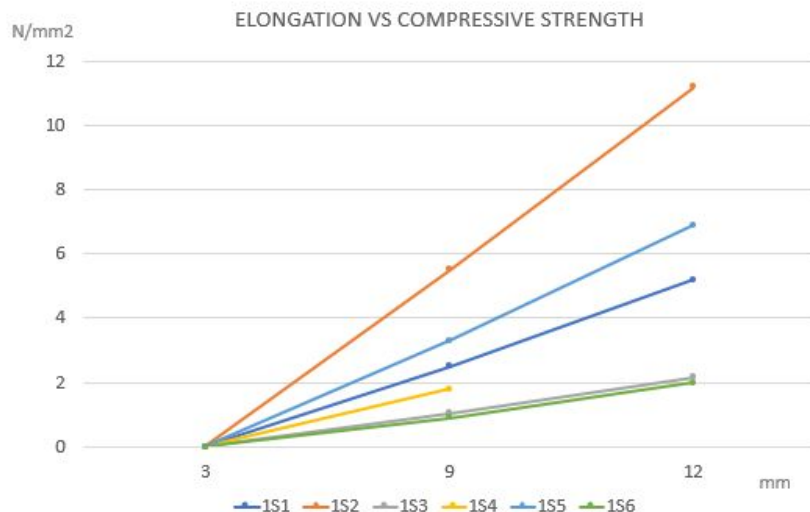
Sample	Max. compressive strength (N/mm <sup>2</sup> )	Average value
<b>Adobe only</b>		
1S1	5.2	4.9
1S2	11.2	
1S3	2.1	
1S4	1.8	
1S5	6.9	
1S6	2.0	
<b>Adobe + wood chips</b>		
2S1	7.6	6.6
2S2	5.1	
2S3	7.0	
<b>Adobe + straw</b>		
3S1	10.5	8.6
3S2	6.3	
3S3	8.9	
<b>Adobe + coco fibres</b>		
4S1	9.0	11.1
4S2	12.3	
4S3	12.0	
<b>Adobe + leaves</b>		
5S1	4.8	5.7
5S2	6.8	
5S3	5.3	
<b>Adobe + rope fiber 10cm</b>		
6S1	13.0	12.2
6S2	11.9	
6S3	11.9	
<b>Adobe + rope fiber 40cm</b>		
7S1	12.1	10.3
7S2	7.0	
7S3	11.9	
<b>Adobe + coco fibres + wood chips</b>		
8S	3.3	
<b>Large samples</b>		
1L (40cm rope fiber)	3.9	2.3
2L (adobe only)	0.7	
3L (adobe + coco fibres)	2.7	
4L (adobe + straw)	1.8	

## 4.3 Cumulative ultimate compressive strength for different compositions and dimensions

In this chapter, the maximum/minimum compressive strength and elongation for each composition and dimensions is shown.

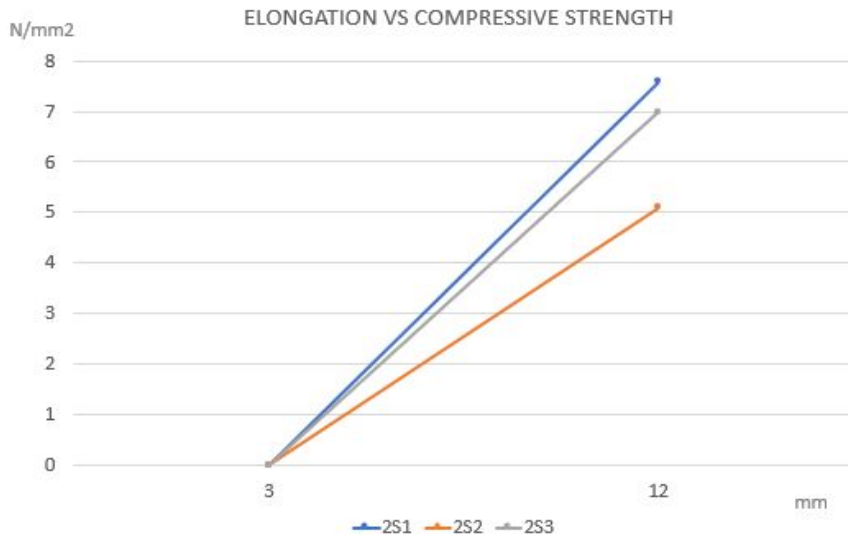
### 4.3.1 Adobe only category:

The following chart shows the different behavior of the same mixture of adobe and small size components. With a maximum elongation of 12 mm, the maximum compressive strength is 11.2 N/mm<sup>2</sup> for sample 1S2. The minimum value is 1.8 N/mm<sup>2</sup> for sample 1S4, which is the only sample that did not reach the minimum elongation limit. The average value within this category is 4.9 N/mm<sup>2</sup>.



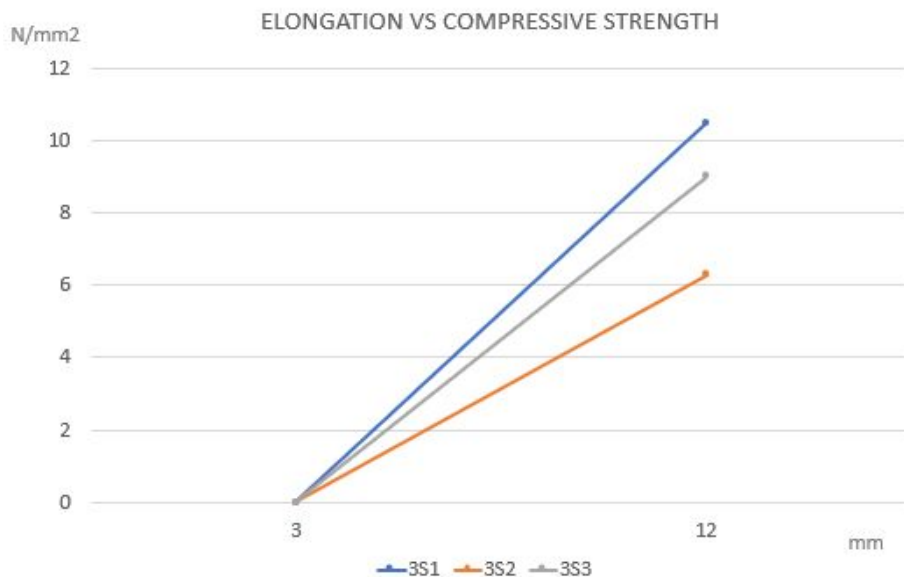
### 4.3.2 Adobe + wood chips category:

The following chart shows the different behavior of the same mixture of adobe + wood chips and small size components. With a maximum elongation of 12 mm, the maximum compressive strength is 7.6 N/mm<sup>2</sup> for sample 2S1. The minimum value is 5.1 N/mm<sup>2</sup> for sample 2S2. The average value within this category is 6.6 N/mm<sup>2</sup>, behaving better than the adobe only category.



#### **4.3.3 Adobe + straw category:**

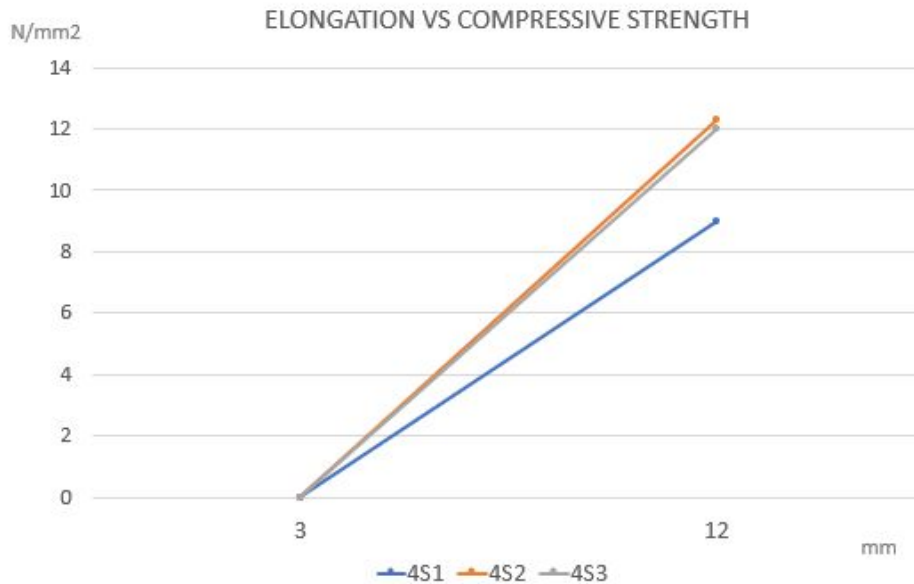
The following chart shows the different behavior of the same mixture of adobe + straw and small size components. With a maximum elongation of 12 mm, the maximum compressive strength is 10.5 N/mm<sup>2</sup> for sample 3S1. The minimum value is 6.3 N/mm<sup>2</sup> for sample 3S2. The average value within this category is 8.6 N/mm<sup>2</sup>, behaving better than the adobe-only and wood chips categories.



#### **4.3.4 Adobe + coco fibers category:**

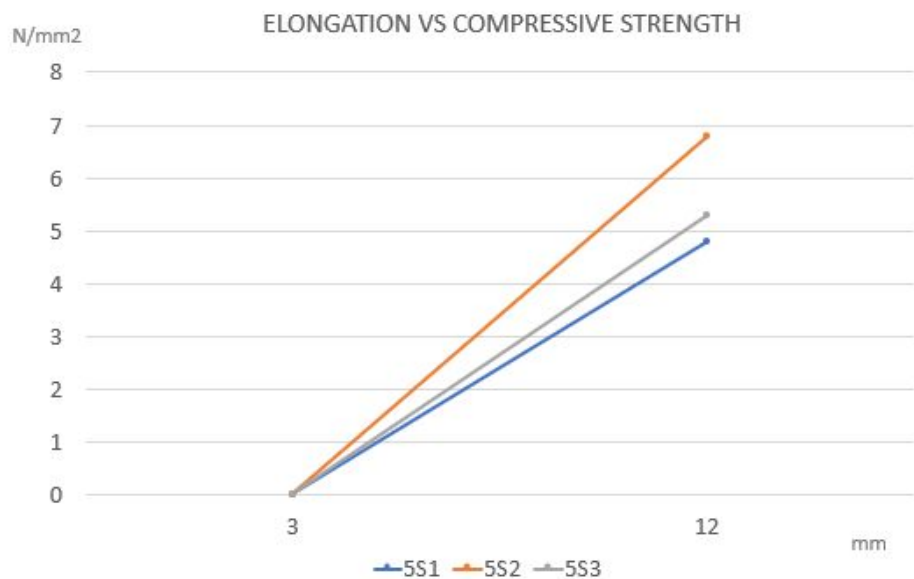
The following chart shows the different behavior of the same mixture of adobe + coco fibers and small size components. With a maximum elongation of 12 mm, the maximum compressive strength is 12.3 N/mm<sup>2</sup> for sample 4S3. The minimum value is 9.0 N/mm<sup>2</sup> for sample 4S1. The average

value within this category is 11.1 N/mm<sup>2</sup>, behaving better than the adobe-only, wood chips and straw categories.



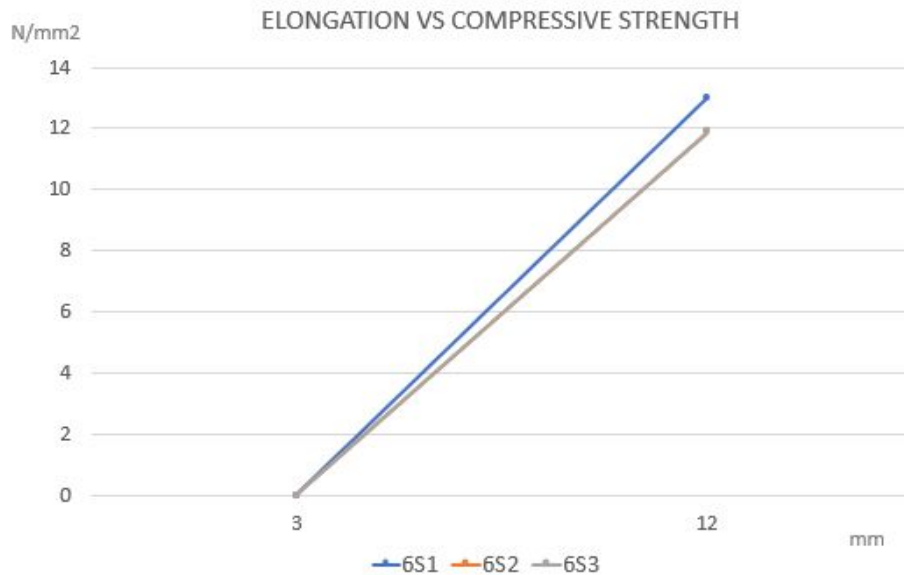
#### **4.3.5 Adobe + leaves category:**

The following chart shows the different behavior of the same mixture of adobe + leaves and small size components. With a maximum elongation of 12 mm, the maximum compressive strength is 6.8 N/mm<sup>2</sup> for sample 5S2. The minimum value is 4.8 N/mm<sup>2</sup> for sample 5S1. The average value within this category is 5.7 N/mm<sup>2</sup>, behaving better than the adobe-only category but worse than the wood chips, straw and coco fibers categories.



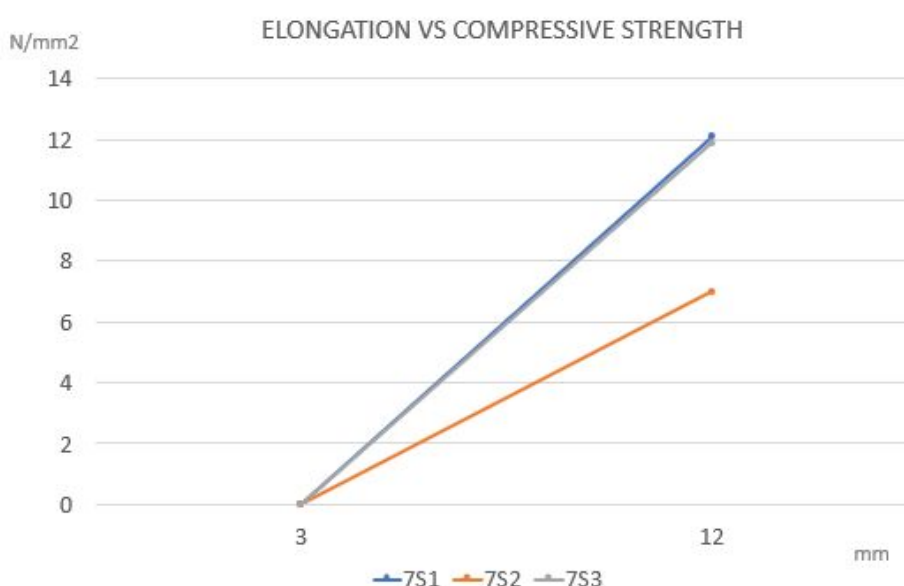
#### **4.3.6 Adobe + rope fiber 10 cm category:**

The following chart shows the different behavior of the same mixture of adobe + rope fiber 10 cm and small size components. With a maximum elongation of 12 mm, the maximum compressive strength is 13.0 N/mm<sup>2</sup> for sample 6S1. The minimum value is 11.9 N/mm<sup>2</sup> for sample 6S2 and 6S3. The average value within this category is 12.2 N/mm<sup>2</sup>, behaving better than the adobe-only, wood chips, straw, leaves and coco fibers categories.



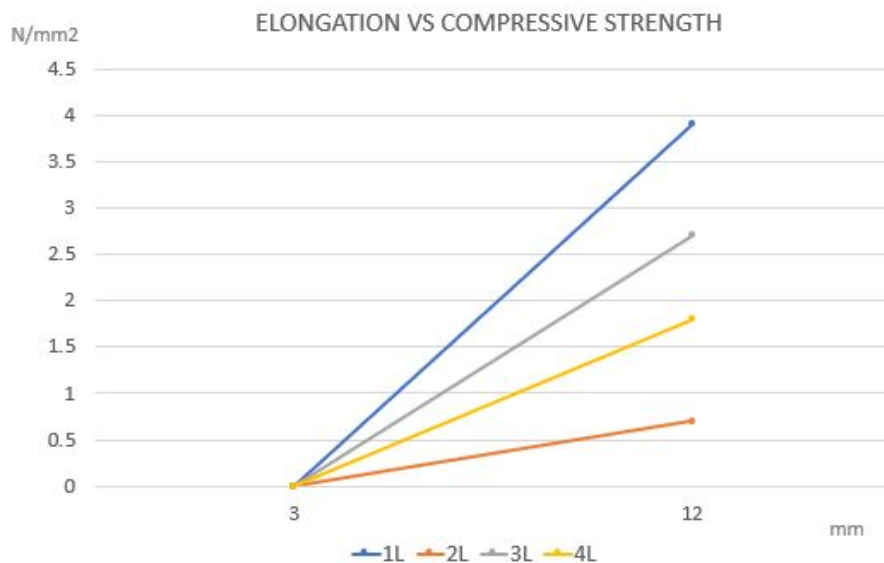
#### **4.3.7 Adobe + rope fiber 40 cm category:**

The following chart shows the different behavior of the same mixture of adobe + rope fiber 40 cm and small size components. With a maximum elongation of 12 mm, the maximum compressive strength is 12.1 N/mm<sup>2</sup> for sample 7S1. The minimum value is 7.0 N/mm<sup>2</sup> for sample 7S2. The average value within this category is 10.3 N/mm<sup>2</sup>, behaving better than the adobe-only, wood chips, straw and leaves categories, but worse than the coco fibers and rope 10 cm categories.



#### **4.3.8 Adobe large samples category:**

The following chart shows the different behavior of different mixtures of adobe and large size components. With a maximum elongation of 12 mm, the maximum compressive strength is 3.9 N/mm<sup>2</sup> for sample 1L. The minimum value is 0.7 N/mm<sup>2</sup> for sample 2L. The average value within this category is 2.3 N/mm<sup>2</sup>, behaving worse than all the rest of samples.



## **5. Discussion of reliability of the data**

### **5.1 Analysis of the data**

In the small adobe brick specimens, taking into consideration the compressive strength, it is evident that certain mixtures had a higher compressive strength in comparison to the others. The adobe only mixture has an average compressive strength of 4.9 N/mm<sup>2</sup>. From the results it is evident that pure adobe bricks need more structural reinforcement to be able to withstand additional forces. While the highest average compressive strength recorded was between Adobe + coco fibers giving 11.1N/mm<sup>2</sup> and Adobe + rope fibers of 10cm with 12.2 N/mm<sup>2</sup>. We believe the high compressive strength in both these materials was due to the coarse (for grip and more surface area for the material to bond with the clay) yet thin nature of both these fibers.

Due to the excellent compressive strength and elongation of the Adobe + rope fiber (10cm) it was decided that this brick would be used further in the specifications of the brick.

## 5.2 Compare with standard/ other source strength values

There are generalised international pressed brick standards such as 295mm x 140mm x 90mm corresponding to the type of block press in use. However, block sizes vary widely according to context and site specificity.(2) The geometry of the test block have a significant influence on the value measured compressive strength. This is evident in the two different sizing of the adobe bricks used for the compression tests in this study.

Since group 7 was the only group with brick samples of adobe+rope fiber (10 cm), there was an unavailability of more data to compare the material properties of the chosen brick in particular. Below, will be a comparison of material properties of plain adobe bricks made by a few other groups and the samples of group 7 all within a similar size range.

Code	Dimensional Properties (mm)			Fmax (N)	dL at Fmax	Average
	L	W	H			
<b>GROUP 7- ADOBE ONLY</b>						
A2	100	75	30	83998.44	11.9737	11.11872667
A4	100	75	30	13672.56	9.4266	
A6	100	75	30	14996.25	11.95588	
<b>GROUP 6 - ADOBE ONLY</b>						
A7	105	75	30	78228.37	14.97	14.98666667
A9	105	75	30	29158.42	15	
A10	105	75	30	87904.19	14.99	
<b>GROUP 5 - ADOBE ONLY</b>						
6	110	80	30	98453.83	14.98	11.63666667
7	110	80	30	35100	9.97	
10	110	80	30	35138.97	9.96	

Table: Comparative adobe only brick samples test results from other groups with same size samples.

The above table compares deflection at maximum stress averages for three samples each from three different groups. Group 6 has a higher value of 14.99 while group 7 and group 5 have a similar deflection at maximum stress of 11.12 and 11.64 accordingly. Given that all samples are of a similar size, cured for the same amount of time in the same conditions, the difference comes down to the slight changes in the adobe mix ratio for each group while weighing manually and the

amount of compression pressure when pressing the brick into its mould, yet again manually. Therefore if large groups of bricks are made manually for the refugee camp in Jordan, it is safe to say that each batch of bricks will have similar differences in deflection at maximum stress due to the variety of adobe mixes, manual compressing of the bricks varying from person to person and also the different weather conditions one each day of curing the brick.

In order to compare the Adobe+rope fiber (10cm)samples,A study done on compressive strength of unfired and compressed clay bricks mixed with sisal or coir fibers sized at 15 x 7.5 x 5 cm was studied and provided the following data (2) :

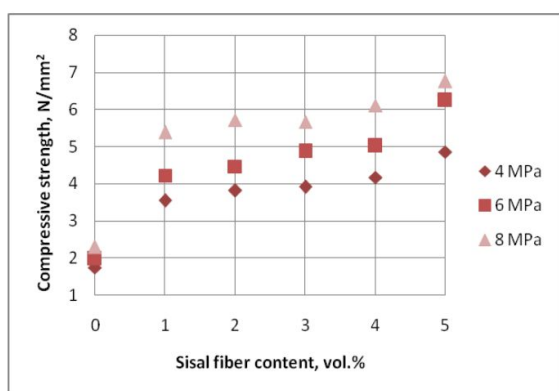


Chart -1: Compressive strength of UCCB reinforced with sisal fiber after 28 days of curing

Although the following information is based on bricks compressed mechanically and cured for 28 days, the different mixtures tested in this study present similar ultimate compression values, in a range of 2.3 N/mm<sup>2</sup> (large samples) to 12.2 N/mm<sup>2</sup> (small samples). Showing higher the fiber content, the higher compressive strength in a brick. This may allow for further studies done using the Adobe+rope fiber(10cm) brick samples. Further tests could be conducted in order to see if adding more

There maybe other influences on the varying results of the adobe compression tests such as the influence of the test procedure, dry density, moisture content and the quality of the adobe itself.

## 6. Conclusions

According to the above information, with regards to the results of ultimate strength per category, it is evident that the average Compressive strength endured by the adobe only bricks were a low 4.9 N/mm<sup>2</sup> compared to the average of Adobe+rope fiber of 12.2 N/mm<sup>2</sup>. Safe design strength per category was defined under earthy construction of a parametrically designed building for site specifically, Jordan. Due to the absence of regulatory building codes for Adobe bricks in Jordan itself, standard codes from Peru was used. Peru has experience with adobe brick constructions and is based on similar conditions as the Zaatri camp. According to the technical construction standard in Peru (Adobe Code E.080) (3), the standard compressive strength of the unit must be minimum 1.2 N/mm<sup>2</sup>.

Given that all small samples tested had the lowest average value of 4.9 N/mm<sup>2</sup>, we presume all small adobe only bricks and adobe+material bricks pass necessary standard and also exceed expectations. Cumulative ultimate compressive strength for the smaller compression adobe bricks were of much higher value comparative to the larger sized adobe bricks. The lowest average being for adobe only of 0.7 N/mm<sup>2</sup> with the highest Adobe+rope fiber 3.9 N/mm<sup>2</sup>. Overall the

large adobe bricks with rope fiber had a much higher compressive strength compared to the large plain Adobe brick with 3.9 N/mm<sup>2</sup> above necessary for standard codes. In terms of mixture with adobe and an external material,

Adobe+rope fiber 10cm had an exceptionally high compressive strength therefore would be the most ideal to use in the construction phase.

## 7. Recommendations.

It is important to keep in mind a few limitations to this test compared to the values/ processes we obtain in real life. Firstly, the **material** we have used in the experiments are of the highest quality clay and purest of water. This may not always be the case due to where the material will be sourced from. When building in Jordaan, we will be limited to earth manually dug out from the site with water that may be infused with other elements.

Secondly, the **process**, we were given the opportunity to use an electric mixer, which allowed for the adobe mix to be of good/equal consistency. This may not always be the case due to the limited availability of resources in a refugee camp. The drying conditions were quite controlled as it was indoors during temperatures of 20°C-13°C throughout the week. This will definitely not be the case on site because the adobe bricks will be drying outside and influenced by the local temperature and weather conditions. Therefore the conditions will influence properties such as the drying time and drying rate, therefore the overall performance of the bricks. Thirdly, **method used for testing**. We have used the A Zwick z100 machine for conducting the above tests. In real time, a load will not be continuously pressed no top of the brick in an even manner over a controlled period of time. They will only fail over time with external influences such as weather wear and tear.

Overall, the brick tests are of good use in a controlled environment to get specific measurements, however will not be the case in real life. It is important to take into consideration the above research. However, also important to keep in mind of how valid they are in real time over a specific time period using slightly different materials. The inability to test the material in its original environment having undergone natural wear and tear would be a limitation to this research process.

## 8. References

- (1) *Mafraq Monthly Climate Averages*. (2019). *WorldWeatherOnline.com*. Retrieved 15 October 2019, from  
<https://www.worldweatheronline.com/mafrag-weather-averages/al-mafraq/jo.aspx>
- (2) *Compressive strength testing of compressed earth blocks*, (2017), Morel, J., Walker, P., reserachgate.net, retrieved 15 October 2019,  
[https://www.researchgate.net/publication/222914532 Compressive strength testing of compressed earth blocks?enrichId=rgreq-98b891ee-c066-4450-b794-0abcd51fca96&enrichSource=Y292ZXJQYWdI OzlyMjkxNDUzMitBUzo5NzY4NjQzMDY4MzEzQUAxNDAwMzAxNjY4NDMz&el=1\\_x\\_2](https://www.researchgate.net/publication/222914532_Compressive_strength_testing_of_compressed_earth_blocks?enrichId=rgreq-98b891ee-c066-4450-b794-0abcd51fca96&enrichSource=Y292ZXJQYWdI OzlyMjkxNDUzMitBUzo5NzY4NjQzMDY4MzEzQUAxNDAwMzAxNjY4NDMz&el=1_x_2)
- (3) Norma Técnica E.080 Design and construction with reinforced earth, (2017), Ministry of Housing, Construction and Sanitation, retrieved 16 October 2019,  
<http://www3.vivienda.gob.pe/dgprvu/docs/TITULO III EDIFICACIONES/III.2%20ESTRUCTURAS/E.080%20ADOBEPDF>
- (4)

## 8. Appendix

Maximum compression strength diagrams for tested brick samples:  
Exported via readings from A Zwick Z 100 machine,

